1-1-2016

Parallel Computing Applications in Large-Scale Power System Operations

Chunheng Wang

Parallel computing applications in large-scale power system operations

By

Chunheng Wang

A Dissertation
Submitted to the Faculty of
Mississippi State University
in Partial Fulfillment of the Requirements
for the Degree of Doctor of Philosophy
in Electrical and Computer Engineering
in the Department of Electrical and Computer Engineering

Mississippi State, Mississippi

August 2016

Parallel computing applications in large-scale power system operations

By

Chunheng Wang

Approved:

Yong Fu
(Major Professor)

Sherif Abdelwahed
(Committee Member)

Masoud Karimi Ghartemani
(Committee Member)

Shantia Yarahmadian
(Committee Member)

James E. Fowler
(Graduate Coordinator)

Jason M. Keith
Dean
Bagley College of Engineering

Name: Chunheng Wang

Date of Graduation: August 12, 2016

Institution: Mississippi State University

Major Field: Electrical and Computer Engineering

Major Professor: Yong Fu

Title of Study: Parallel computing applications in large-scale power system operations

Pages in Study 112

Candidate for Degree of Doctor of Philosophy

Electrical energy is the basic necessity for the economic development of human societies. In recent decades, the electricity industry is undergoing enormous changes, which have evolved into a large-scale and competitive industry. The integration of volatile renewable energy, and the emergence of transmission switching (TS) techniques bring great challenges to the existing power system operations problems, especially security-constrained unit commitment (SCUC) solution engines. In order to deal with the uncertainty of volatile renewable energy, scenario-based stochastic optimization approach has been widely employed to ensure the reliability and economic of power systems, in which each scenario would represent a possible system situation. Meanwhile, the emergence of TS techniques allows the system operators to change the topology of transmission systems in order to improve economic benefits by mitigating transmission congestion. However, with the introduction of extra scenarios and decision variables, the complexity of the SCUC model increases dramatically and more computational efforts are required, which might make the power system operation problems difficult to solve and even intractable. Therefore, an advanced solution technique is urgently needed to

solve both stochastic SCUC problems and TS-based SCUC problems in an effective and fast way.

In this dissertation, a decomposition framework is presented for the optimal operation of the large-scale power system, which decomposes the original large-size power system optimization problem into smaller-size and tractable subproblems, and solves these decomposed subproblems in a parallel manner with the help of high performance computing techniques. Numerical case studies on a modified IEEE 118-bus system and a practical 1168-bus system demonstrate the effectiveness and efficiency of the proposed approach which will offer the power system a secure and economic operation under various uncertainties and contingencies.

DEDICATION

Firstly, I would like to thank my tutor, Dr. Yong Fu, for his understanding and guidance in both the academic study and my personal life. Without his selfless direction and help, it is impossible for me to finish my Ph. D. study.

Second, I would like to thank the faculty, staffs and colleagues in Mississippi State University, especially Dr. Stanislaw Grzybowski, Dr. Sherif Abdelwahed, Dr. Masoud Karimi Ghartemani, Dr. Shantia Yarahmadian, Dr. Jian Shi, Mr. Jeff Ellis, Ms. Ellen Harpole, Dr. Amin Kargarian and Mr. Mojtaba Khanabadi.

Last but most important, I would like to thank for the unconditional support and love from my parents, my wife, and our coming baby. All my life I knew that I am a rich man because I had you. Thank you for everything you have done for me, my dear and lovely family.

TABLE OF CONTENTS

LIST OF TABLES

LIST OF FIGURES

CHAPTER I

INTRODUCTION

1.1 Background

Electric power systems are networks of electrical components used to generate, transfer, and consume electric power. With the expansion of electric power grids, electrical energy is essential to human societies all over the world. In the conventional electricity power industry, the entire power system operation is dominated by vertical integrated utilities. The vertical integrated utilities own the generating sources, transmission networks, and distribution networks. In recent years, the electricity industry is undergoing enormous changes and has evolved into a distributed and competitive industry [1]. The market forces decide the price of electricity and increase the total social welfare.

The Federal Energy Regulatory Commission (FERC) Order No. 888 required the power industry to restructure and unbundle electricity markets. As a result, the conventional power system has been decomposed into three components: generating companies (GENCOs), transmission companies (TRANSCOs), and distribution companies (DISCOs). The independent operational control of each component would promote a competitive market, which would lead to a more economic power system operation. On the other side, the competition would also reduce the reliability of the electricity industry. In order to operate the competitive market while ensuring the reliability of power systems, an independent operational control of the power grid is necessary [2]. Thus, an independent entity, such as the independent system operator (ISO), is introduced to guarantee the independent operation of the grid.

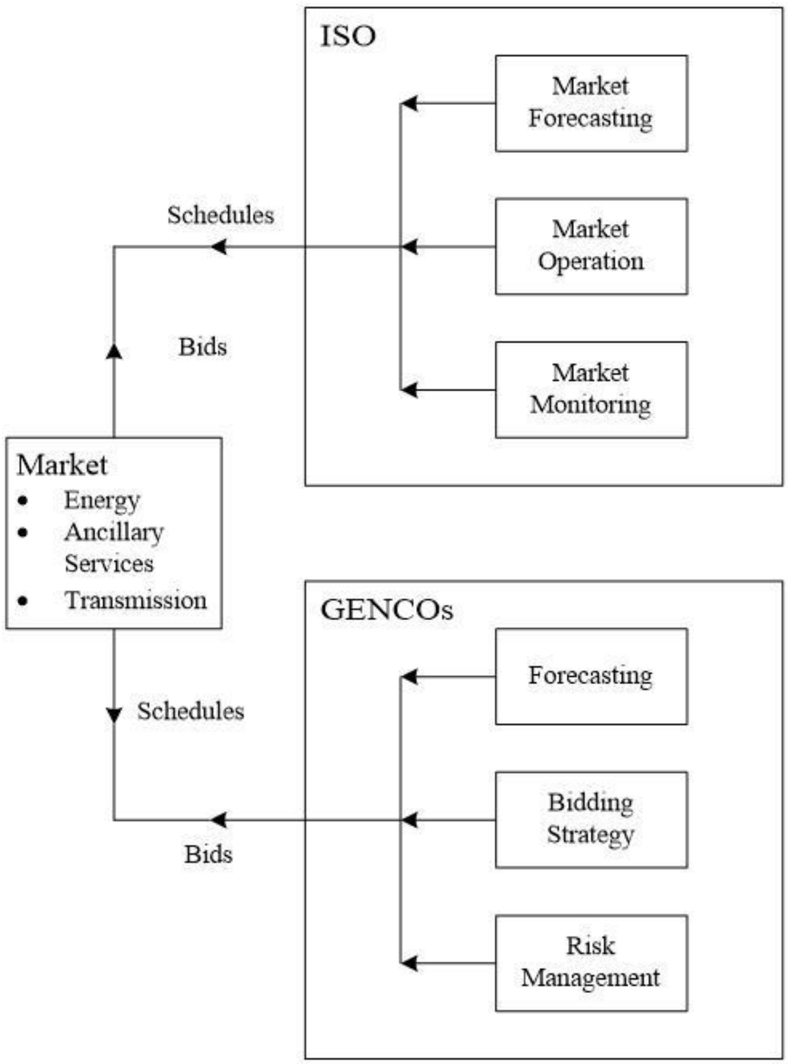

Figure 1.1 Restructured electricity market operation

Restructured power market operation is shown in Figure 1.1. A GENCO operates and maintains existing generating plants. GENCOs can compete to sell energy to customers by submitting competitive bids to the electricity market. They try to maximize their own profit regardless of the system profit and reliability. Then, ISOs schedule generating units in a constrained transmission system to ensure the reliability of the power grid [3].

Security-constrained unit commitment (SCUC) is widely employed by ISOs and regional transmission organizations (RTOs) to schedule a secure and economic power operation in both day-ahead and real-time power markets [4]. SCUC handles the economic unit generation schedule in a power system for serving the load demand with an adequate reserve margin while satisfying temporal and operational limits of generation and transmission facilities. The increasing size and complexity of modern power systems, the integration of volatile renewable energy, and the emergence of transmission switching (TS) techniques bring great challenges to the existing SCUC solution engines. With the increasing size of the power systems, the number of branches and nodes can be very large; for example, a typical size of the transmission network model of Texas consists of 4,500 buses, while the Great Britain model has around 2,000 – 2,500 [5]. In addition, due to the uncertainty of renewable energy and integration of TS techniques, the constraints and control variables of the generating unit commitment problem increase exponentially.

Recently, significant contributions have been made by many researchers to solve large-scale power system operation problems, especially SCUC problems. Most research of the power systems optimization and operation study are focused on the day-ahead market of the transmission system [6].

1.2 Literature review

Unit commitment (UC) refers to the task of deciding an optimal schedule and a production level of each generating unit to meet the required power demand. The traditional UC only considers generating unit constraints but ignores the network constraints; but, the SCUC considers the constraints of both generating units and transmission network, as well as the contingencies of generating units and/or transmission network [7].

From the viewpoint of market operators, SCUC is adopted in the vertically integrated environment to minimize the total operating cost of the power system, or in the deregulated environment to maximize the total social welfare. In this work, the applications of the SCUC in both the vertical integrated environment and deregulated environment are investigated. In the past several decades, various approaches have been developed by our researchers to solve the optimal UC/SCUC problem, including the enumeration, priority listing, dynamic programming, branch-and-bound, Benders decomposition, Lagrangian relaxation (LR), and augmented Lagrangian relaxation (ALR) method.

1.2.1 Exhaustive enumeration method and priority listing method

The exhaustive enumeration method [8, 9] is adopted to solve the UC problem by enumerating all possible combinations of the generating units and then choosing the least expensive operating combinations as the optimal solution. In [10, 11], the priority listing method is employed to arrange the generating units based on the operational cost and then selects the generating units to meet the system load demand. In advance, [12] used the priority listing method to solve the single and multi-area UC problem based on a classical index. [13] proposed an efficient algorithm using the priority listing method with import/export constraints.

1.2.2 Dynamic programming

Some researchers adopted dynamic programming method to solve the UC problem. The dynamic programming can easily add constraints at an hour [14]. However, it is difficult to include the constraints affect over time (e.g. minimum up/down constraints and time-dependent startup cost). Reference [15] discussed the dynamic programming application of UC problem on both the wholly owned and commonly owned units. In [16], the practical applicability of the generating unit commitment by dynamic programming is discussed.

1.2.3 Branch-and-bound method

Branch-and-bound method is another widely adopted mathematics to solve the UC problem. In [17], an integer programming method is developed to solve a practical size scheduling problem based on the branch-and-bound method. [18] proposed an approach to solve UC problem based on branch-and-bound method, which does not require a priority listing of the generating units. In [19], a constraint logic programming based approach is proposed, in which the constraint logic programming and branch-and-bound method are applied to provide a flexible approach to the UC problem.

1.2.4 Benders decomposition method

Benders decomposition [20] is another widely used optimization method for utilities' use. Figure. 2.1 depicts the hierarchy of SCUC problem, which is based on the existing structure in restructured power systems. The Benders decomposition method decompose the original SCUC problem into a master (UC) problem and a network security check subproblem. The initial master problem obtains the optimal generating units solution based on the available market information. Then the network security subproblem checks the violations and returns the Benders cuts to the master problem to reformulate the UC problem. The optimal result would be obtained until all violations are eliminated [21-24]. In [25], a transmission-constrained unit commitment is proposed with utilization of Benders decomposition. In [26], a Benders decomposition based optimization method with consideration of both transmission security and voltage constraints is presented, which employs two separate subproblems to check transmission and voltage violations. [27] proposed a new approach using Benders decomposition to solve the SCUC problem with alternating current (AC) constraints. A Benders decomposition based AC corrective/preventive contingency model is proposed in [28], which includes unit commitment, ac security-constrained optimal power, and load shedding for steady state and contingencies. [29] proposed an efficient fast SCUC for the large-scale power system using Benders decomposition, which presented an operational strategy for fixing and unlocking the generating units.

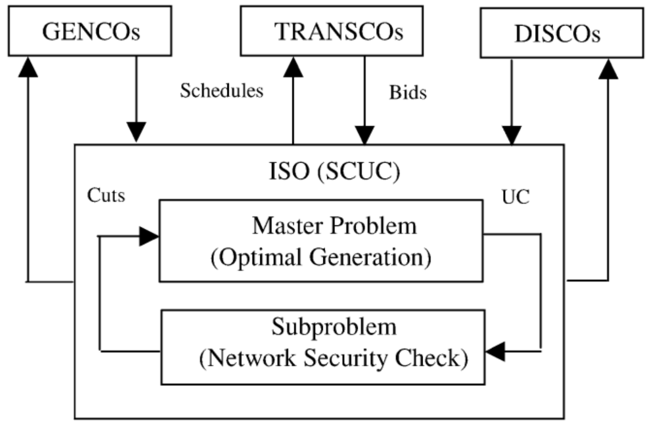

Figure 1.2 Benders decomposition

1.2.5 Lagrangian relaxation method

Lagrangian relaxation based approaches are widely used by some utilities [30, 31] to relax some constraints and decompose the original optimization problem into several independent subproblems. [32] proposed a Lagrangian Relaxation method for UC problem and applied that at Electricite De France. In [33, 34], Lagrangian Relaxation method is used for a large-scale UC problem with different kinds of generating units, including usual thermal units, fuel-constrained thermal units, and pumped storage hydro units. [35] proposed a Lagrangian relaxation based optimization framework to deal with the ramping rate limit in the UC problem. In [36], Lagrangian relaxation method is employed to replace transmission constraints with penalty functions and includes the functions in the objective function.

1.2.6 Augmented Lagrangian relaxation method

In order to improve the performance of the Lagrangian relaxation based optimization method, augmented Lagrangian relaxation method is adopted with the second order penalty term [37, 38]. ALR method is adopted in [39], which presented a transient stability constrained unit commitment (TSCUC) model which achieves the objective of maintaining both transient stability and economical operation. Alternatively, [40] adopted ALR to propose a SCUC solution for the optimal integration of large-scale offshore wind energy into a power grid, which considers a linear static state representation of multi-terminal voltage source converter (VSC)-based high voltage direct current (HVDC) and effectively incorporates this model into SCUC. Reference [41] employed ALR to propose a distributed calculation platform to obtain a global shift factor in interconnected power systems while protecting information privacy of individuals.

1.3 Research motivations

Nowadays, the development of power systems is bringing new challenges into SCUC solutions, such as increasing size of power systems, high penetration of intermittent renewable energy, and the emergence of advanced techniques in the smart grids. To solve these emerging challenges, several advanced solution algorithms are proposed by our researchers, which will introduce a great number of decision variables and constraints.

In order to deal with the uncertainty introduced by the renewable energy, significant contributions have been made by researchers by using scenario-based stochastic optimization approaches, in which each scenario would represent a possible system situation. Typically, the stochastic SCUC problem needs to model a certain number of scenarios, which will dramatically increase the size of the problem in terms of the large number of variables and constraints. In addition, the emergence of TS technique allows the system operators to change the topology of transmission systems in order to improve economic benefits by mitigating transmission congestion, in which the transmission switching lines can be switched ON/OFF. Thus, binary variables are employed for both the states of generating units and switchable transmission lines. This co-optimization problem is a large-scale and computationally complex optimization problem.

As a result, the complexity of the SCUC model will increase dramatically and more computational efforts will be required, which can make the problem difficult to solve and even intractable. Therefore, an advanced solution technique is urgently needed to solve such stochastic SCUC problems and TS-based SCUC problems in an effective and fast way. As one of the major challenges in large-scale power system operation problems comes from its model size, the solution efficiency can be improved if we could reduce the size of solved problems. Thus, in this dissertation, a decomposition framework is presented for the optimal operation of the large-scale power system, which decomposes the original large-size power system optimization problem into smaller-size and tractable subproblems, and solves these subproblems in a parallel manner with the help of high performance computing techniques.

1.4 Contributions

In order to overcome the computational bottleneck of the power system operations problems in the stochastic security-constrained unit commitment problem and co-optimization of the generating unit and transmission switching problem, we propose proper decomposition algorithms and implement the proposed approaches in a parallel computing environment.

1.4.1 Fully decomposed solution module

The proposed approach decomposes the entire SCUC problem into several solution modules, and each major module can be further decomposed into multiple smaller submodules, which make the proposed decomposition structure more favorable to parallelism. As a result, the proposed decomposition approach makes all decomposed problems scalable and tractable, which will theoretically allow us to handle power systems of any size with a large number of scenarios/contingencies assuming enough processors.

1.4.2 Fully parallel solution procedure

As the auxiliary problem principle (APP) method is more desirable to be applied for large-scale power system optimization problems in terms of computational speed and convergence performance [42], this method is applied to coordinate all above solution modules. With the application of APP method, all of decomposed solution submodules can be solved simultaneously, instead of in a sequential process. In other words, one module does not need to wait for the decisions from another module. Consequently, all of the solution modules are solved in a parallel manner, which can fully utilize the high performance computing techniques to improve the computational efficiency.

1.4.3 Handling complicating constraints

To be specific, in the stochastic SCUC study, the solution performance is improved by avoiding the discreteness of unit commitment variables during the coordination procedure and improving the convexity of Lagrangian relaxation function. The existing SCUC decomposition methods [43-47] coordinate unit commitment decisions (binary variables) between base case and scenarios. The classical Lagrangian relaxation method is adopted to satisfy the complicating (non-anticipativity or consistency) constraints with integer variables (unit commitment decisions). In other words, they directly process the integer variables appearing in the complicating constraints. However, the proposed method will create the complicating constraints with only continuous variables (such as the power dispatch of generating units) to indirectly coordinate the unit commitment between base case and scenarios by using the augmented Lagrangian relaxation method (with the second order penalty function in the Lagrangian objective function). These strategies can enhance the solution performance by avoiding the discreteness of unit commitment variables during the coordination procedure and improving the convexity of Lagrangian relaxation function.

1.4.4 Decomposed co-optimization subproblem:

Particularly, in the co-optimization of generating scheduling and transmission switching study, we further investigate how to effectively incorporate the transmission switching problem into the SCUC problem. The proposed approach decomposes the entire TS-based SCUC problem into three major solution modules: the UC module that determines the state of generating units; the OPF module that optimizes the power generation of generating units while satisfying the network security constraints for both base case and credible contingencies; and the individual TS module that only determines the state of switchable transmission lines. Secondly, unlike the existing research [48],[49] that only considered the preventive action in the proposed TS study. The proposed parallel co-optimization approach in this study can allow the contingency dispatch represented by both corrective (post-contingency) and preventive (pre-contingency) dispatch control actions.

1.5 Dissertation organization

The rest of the dissertation is organized as follows. Chapter II introduces the decomposition algorithms and the parallel computing environment. Among these decomposition algorithms, the augmented Lagrangian method and auxiliary problem principle are employed to decompose the original large-scale power system optimization problem into smaller-size and tractable subproblems. In addition, the structure of the parallel computing cluster is introduced.

Chapter III states application of “fully parallel stochastic security-constrained unit commitment”. In this chapter, the proposed decomposition framework is applied into stochastic security-constrained unit commitment problem, which solves the power system optimization problem with consideration of integration of renewable energy and uncertainty of the load demand.

Chapter IV demonstrates the decomposition framework and its application in the “parallel co-optimization of generating unit commitment and transmission switching with post-contingency corrective”. In this chapter, a co-optimization problem is presented and solved with the proposed decomposition framework.

The conclusion and future work are drawn in Chapter VI.

CHAPTER II

PARALLEL ALGORITHMS AND CALCULATION ENVIRONMENT

A decomposition framework is presented for optimal operation of the large-scale power system, which is applied to scenario-based stochastic SCUC problem and TS-based SCUC. In this chapter, the proposed parallel algorithms and the parallel computing environment will be introduced.

2.1 Parallel decomposition algorithms

From the viewpoint of computational complexity, SCUC problem is a large-scale, non-linear, non-convex, mixed-integer optimization problem, which makes the SCUC problem difficult to solve [50]. With the integration of renewable energy and TS technique, the complexity of the SCUC model will increase and more computational efforts will be required, which might make the problem difficult to be solved and even intractable. Therefore, an advanced solution technique is urgently needed to solve such stochastic SCUC problems and TS-based SCUC problems in an effective and fast way.

The development of distributed multi-processor environment potentially greatly increases the computational availability and decreases the communication time consumption. In the past several decades, various approaches based on augmented Lagrangian method have been developed to decompose the original large-scale, non-linear, mixed-integer optimization problem. The basic idea of augmented Lagrangian method is to replace the original problem by an equivalent problem. Consider a convex program with separable structure as shown below:

$$\begin{aligned} &\min \quad F(\mathrm{x})+\mathrm{G}(\mathrm{y}) \\ &\text{s.t.} \\ &\qquad h(\mathrm{x}) \le 0 \\ &\qquad l(\mathrm{y}) \le 0 \\ &\qquad ax+by=0 \end{aligned} \tag{2.1}$$

where, x and y present two sets of variables, F(x) and G(y) are convex, proper, and lower semi-continuous functions. Then the augmented Lagrangian for the problem (2.1) is defined as

$$L_c(x,\pi) = F(x) + \mathrm{G}(\mathrm{y}) + \lambda^T\left(ax+by\right) + \frac{c}{2}\left\|ax+by\right\|^2 \tag{2.2}$$

where λ is defined as the first order Lagrangian multipliers and c is a second order Lagrangian multipliers. During the iterative solution procedure, the first order and second Lagrangian multipliers are updated based on (2.3).

$$\begin{aligned} &\lambda^{k+1} = \lambda^k + c(ax+by) \\ &c^{k+1} = \beta c^k \end{aligned} \tag{2.3}$$

where, coefficient β is set to be equal or larger than one in order to obtain a converged optimal result. Detailed discussions about augmented Lagrangian relaxation techniques and parameter update strategies can be found in [51]. The principal disadvantage of the above Lagrangian (2.2) to the classic Lagrangian relaxation for decomposition methods is the presence of the term $\frac{c}{2}\left\|ax+by\right\|^2$, because of the production of two variables, which destroys the reparability in the (2.2). In order to divide the coupling terms introduced by $\frac{c}{2}\left\|ax+by\right\|^2$, several decomposition methods are proposed, including Alternating

Direction Method of Multipliers (ADMM), Diagonalization Quadratic Approximation (DQA), and APP.

2.1.1 Alternating direction method of multipliers

The basic idea of alternating direction method of multipliers is a relaxation approach, in which, we first minimize the augmented Lagrangian (2.2) with respect to *x* and then with respect to *y*, and finally update the Lagrangian multiplier λ, as shown in (2.3).

$$\begin{aligned} x^{k+1} &= \arg\min\left\{F(x) + \mathrm{G}(\mathrm{y}^k) + \lambda^T\left(ax + by^k\right) + \frac{c}{2}\left\|ax + by^k\right\|^2\right\} \\ y^{k+1} &= \arg\min\left\{F(x^{k+1}) + \mathrm{G}(\mathrm{y}) + \lambda^T\left(ax^{k+1} + by\right) + \frac{c}{2}\left\|ax^{k+1} + by\right\|^2\right\} \\ \lambda^{k+1} &= \lambda^k + c(ax^{k+1} + by^{k+1}) \end{aligned} \tag{2.4}$$

2.1.2 Diagonalization quadratic approximation

Compared with ADMM method, the DQA method adopted Taylor series to divide the coupled term $\frac{c}{2}\left\|ax + by\right\|^2$ in the (2.2). As a result, the augmented Lagrangian (2.2) can be rewritten as:

$$\begin{aligned} L(\mathrm{x}^{k+1}, \mathrm{y}^{k+1}, \lambda) = {} & F(x) + \mathrm{G}(\mathrm{y}) + \lambda^T\left(ax + by\right) \\ & + \frac{c}{2}\left(a^2x^2 + b^2y^2 + 2ab\left(x^k\right)^T y + 2ab\left(y^k\right)^T x - 2ab\left(x^k\right)^T y^k\right) \end{aligned} \tag{2.5}$$

which can be further written as:

$$\begin{aligned} \mathrm{x}^{k+1} &= \arg\min\left\{F(x) + \lambda^T\left(ax\right) + \frac{c}{2}\left(a^2x^2 + 2abx^k y\right)\right\} \\ y^{k+1} &= \arg\min\left\{\mathrm{G}(\mathrm{y}) + \lambda^T\left(by\right) + \frac{c}{2}\left(b^2y^2 + 2abx^k y\right)\right\} \end{aligned} \tag{2.6}$$

The fundamental difference between ADMM and DQA method is the solution structure. In the ADMM method, the optimization of y^{k+1} has to wait for the result of x^{k+1}; on the other hand, in the DQA method, these two optimization problems can be processed in parallel.

2.1.3 Auxiliary problem principle

The APP allows us to substitute the augmentation terms with decoupled terms at iteration *k*. According to the APP theory, a master problem could be replaced by an alternative problem. We consider the so-called master problem (MP) as:

$$Min \quad J(u)+J_1(u) \tag{2.7}$$

where, we assume $J\ (u)$ is a convex, and differentiable function, $J_1(u)$ can be non-convex function. Now let $K(u)$ be another functional with the same assumptions as for $J(u)$ and consider the following function as auxiliary which depends on some specific v and $\varepsilon > 0$:

$$Min \quad G^v(u) = K(u) + \left[\varepsilon J'(v) - K'(v)\right]^T \times u + \varepsilon J_1(u) \tag{2.8}$$

where, $J'(v)$, $K'(v)$ are differential result of $J(v)$ and $K(v)$, and v is the optimal solution of G^v such that:

$$G^v(v) = Min \ \ G^v(u) \tag{2.9}$$

Then, we can get:

$$J(v)+J_1(v) = Min \quad J(u)+J_1(u) \tag{2.10}$$

The proof is based on variational inequality character [52]. This means, if v happens to be a solution of the problem of minimizing G^v (so-called auxiliary problem), then it is also a solution of MP. From the theory above, the equivalent function G^v depends on choice of $K(u)$. With different choices of $K(u)$, we can get different equivalent function G^v to original function $J(u)+J_1(u)$.

Therefore, in order to decompose the coupled term $x \cdot y$ of (2.2), $J(u)$, $J_1(u)$ and $K(u)$ are selected as below:

$$J(u)=\frac{c}{2}\|ax+by\|^2 \tag{2.11}$$

$$J_1(u)=F(x)+\mathrm{G(y)}+\lambda^T\left(ax+by\right) \tag{2.12}$$

$$K(u)=c(a^2x^2+b^2y^2) \tag{2.13}$$

Here, ε is set to 1. Thus, based on the equation we discussed above, we can get:

$$\begin{aligned} G^v &= c(a^2x^2+b^2y^2) \\ &+\left(\begin{bmatrix} ca^2x^{(k-1)}+caby^{(k-1)} \\ cabx^{(k-1)}+cb^2y^{(k-1)} \end{bmatrix}^T - \begin{bmatrix} 2ca^2x^{(k-1)} \\ 2cb^2y^{(k-1)} \end{bmatrix}^T\right)\begin{bmatrix} x \\ y \end{bmatrix} \\ &+F(x)+G(y)+\lambda^T\left(ax+by\right) \\ &= c(a^2x^2+b^2y^2) - c(ax^{(k-1)}-by^{(k-1)})(ax-by) \\ &+F(x)+G(y)+\lambda^T\left(ax+by\right) \end{aligned} \tag{2.14}$$

where, $x^{(k-1)}$, $y^{(k-1)}$ are optimal solutions of x, y from last iteration, which can be considered as constants at each iteration. Consequently, the coupled term x, y is decomposed into two separated terms.

2.1.4 Convergence of the decomposition algorithms

The success of the augmented Lagrangian based algorithms depends on the ability of the algorithm to drive Lagrangian multipliers to the value of multipliers associated with coupling constraints at the optimal solution. The convergence of the augmented Lagrangian method for convex problem has been proved in [51]. However, for a non-convex optimization problem, the non-convexity can be mitigated by quadratic penalty terms in the augmented Lagrangian method as a local convexifier [53].

Although there is no direct proof for the Lagrangian method for mixed-integer programming problem, there are several methodologies that have been proposed to improve the convergence performance. Reference [54] introduced the standard Lagrangian dual problem. Based on this concept, reference [55] employed stabilization techniques [56] to improve the convergence performance of augmented Lagrangian method, in which the primal form of the stabilization allows a controlled violation of the constraints relaxed in a corresponding Lagrangian dual problem. In further, some methods have been proposed by other researchers to improve the convergence performance. In [57], authors proposed an alternating direction method with self-adaptive penalty parameters for monotone variational inequalities, which offers a better convergence performance than original sub-gradient method. In [58], the convergence proof of the DQA method is given, and authors discussed several method to improve the convergence performance, including trust region technique and truncated analytical target cascading. In reference [37], the authors proved the convergence of the APP method with a convex function and discussed several convergence improvement methods.

2.2 Parallel calculation environment

High Performance Computing (HPC) most generally refers to the practice of aggregating computing power in a way that delivers much higher performance than one could get out of a typical desktop computer or workstation in order to solve large problems in science, engineering, or business. Recent years have seen a dramatic increase of the performance of the HPC platforms

HPC platform is referring to a supercomputer with a high-level computational capacity compared to a general-purpose computer. Performance of a supercomputer is measured in floating-point operations per second (FLOPS). Supercomputer was introduced in the 1960s. While in the 1970s, the super computers only had a few processors. Since the appearance of machines with thousands of processors in the 1990s, the massively parallel supercomputers with tens of thousands processors are widely used. The high performance computing center in Mississippi state university provides substantial high performance computing resources for use: Raptor has a peak performance of over 10.6 teraFLOPS; Talon has a peak performance of over 34.4 teraFLOPS; Shadow has a peak performance of 322 teraFLOPS, which was also the 16th most energy efficient supercomputer in the world according to the June 2014 Green500 list [59].

The MathWorks Inc. provides the parallel computing toolbox with MATLAB. Parallel Computing Toolbox can be used to solve computationally and data-intensive problems using MATLAB on multi-core and multiprocessor computers. Parallel processing constructs such as parallel for-loops and code blocks, distributed arrays, parallel numerical algorithms, and message-passing functions, can be used to implement task- and data-parallel algorithms in MATLAB at a high level without programming for specific hardware and network architectures. The parallel computing tools can be ran on a local machine, or on a remote server, as shown in the Figure. 2.1.

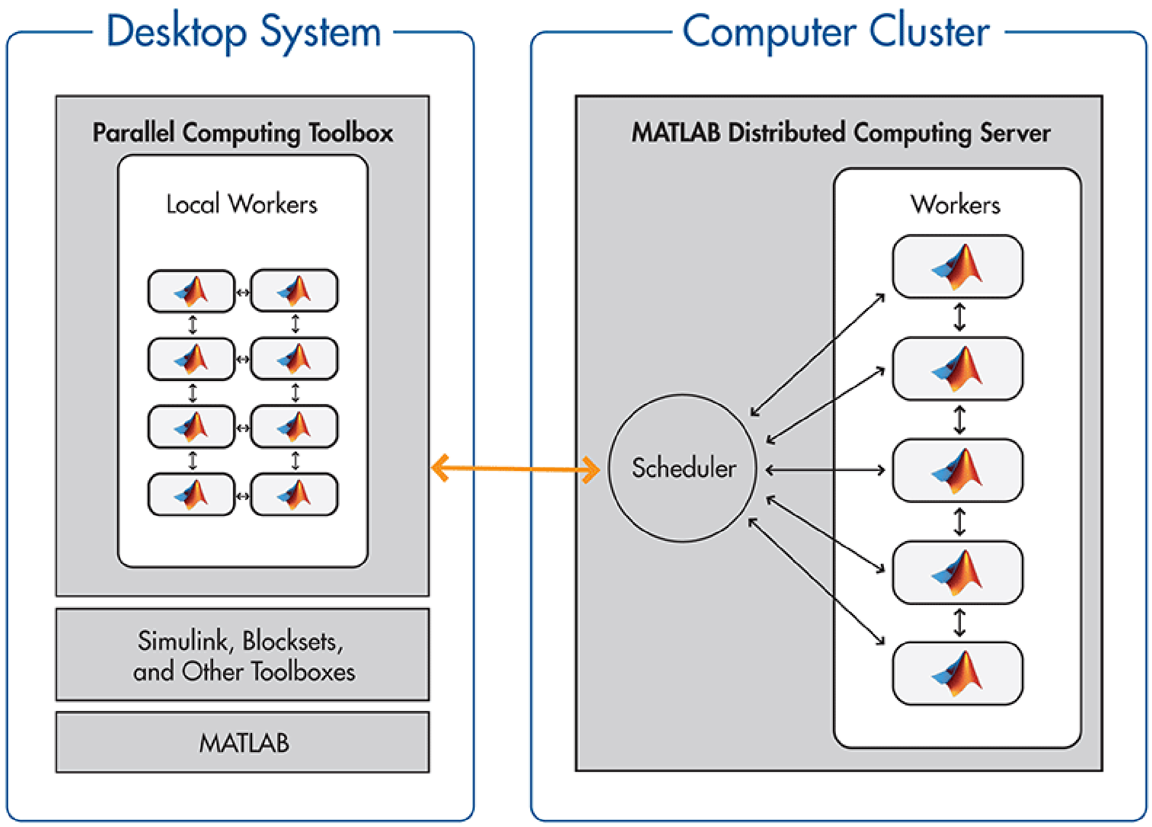

Figure 2.1 Operation structure of parallel computing tools

The development of HPC promotes the application of parallel computing techniques in the power system optimization problems. Parallel computing techniques offer significant potential in critical infrastructure application areas of power and energy systems. [60] presents a review of the research activities developed in recent years in the field of HPC application to power system problems. Parallel computing techniques can significantly improve computational efficiency of power system optimization problem with utilization of multi-processors and multi-threads [61], which is a desirable solution to today's stochastic SCUC problem. However, these improvements cannot be achieved by the architectures of the machines alone, it is equally important to develop suitable mathematical algorithms and proper decomposition technique in order to effectively utilize parallel architectures [62].

By adopting decomposition techniques and parallel computing techniques, magnitude performance improvement can be obtained in the power system optimization problem.

CHAPTER III

FULLY PARALLEL STOCHASTIC SECURITY-CONSTRAINED UNIT COMMITMENT

The increasing size and complexity of modern power systems and the integration of volatile renewable energy bring great challenges to the existing security-constrained unit commitment (SCUC) solution engines. This chapter presents a fully parallel stochastic SCUC approach to obtain an efficient and fast solution for a large-scale power system with wind energy uncertainty. Variables duplication and auxiliary problem principle techniques are adopted to fully decompose the original stochastic optimization problem into three major solution modules: the unit commitment (UC) module solves multiple single UC problems; the optimal power flow (OPF) module handles multiple hourly direct current optimal power flow (DC-OPF) problems; and the bridge module builds a connection between the UC and OPF modules. These three modules are conducted for both base case and scenarios, and can be totally solved in a parallel manner. Numerical case studies on a modified IEEE 118-bus system and a practical 1168-bus system demonstrate the effectiveness and efficiency of the proposed approach which will offer the power system a secure and economic operation under various uncertainties [63].

3.1 Introduction

Nowadays, the development of power systems is bringing new challenges into SCUC solutions, such as increasing size of power systems and high penetration of intermittent renewable energy. A traditional approach is to incorporate system reserve constraints to ensure sufficient generation capacity available in real time to accommodate uncertainties. This is a conservative approach which could over-commit generating units and consequently lead to a very high operating cost of power systems [64]. In order to deal with the uncertainty of load and renewable energy, scenario-based stochastic optimization approaches have been proposed by researchers to solve large-scale power system operation problems with uncertainties, in which each scenario would represent a possible system situation. The benefits and applications of using stochastic programming, instead of deterministic study, to account for the uncertainty in unit commitment are examined in [65]. Typically, the stochastic SCUC problem needs to model a certain number of scenarios, which will dramatically increase the size of the problem in terms of the large number of variables and constraints.

Recently, significant contributions have been made by researchers to solve large-scale power system operation problems with uncertainties using scenario-based stochastic optimization approaches, in which each scenario would represent a possible system situation. The benefits and applications of using stochastic programming, instead of deterministic study, to account for the uncertainty in unit commitment are examined in [65]. Typically, stochastic SCUC problem needs to model a certain number of scenarios, which will dramatically increase the size of the problem in terms of large number of variables and constraints. As a result, the complexity of stochastic SCUC model will increase and more computational efforts will be required, which might make the problem hard to be solved and even intractable. Therefore, an advanced solution technique is urgently needed to solve such stochastic SCUC problems in an effective and fast way.

As one of the major challenges in large-scale power system operation problems comes from its model size, the solution efficiency can be improved if we could reduce the size of solved problems. Using this basic idea, researchers have developed various approaches to decompose the original large-scale optimization problem into several small-size and tractable subproblems [66]. The existing decomposition approaches can be classified into three categories: geographical-structure based decomposition, scenario-structure based decomposition, and functional-structure based decomposition.

According to the geographical structure of power systems, reference [67-70] proposed a distributed method to decompose a large-scale deterministic SCUC problem into several small regional subproblems, and then use an analytical target cascading (ATC) technique to coordinate those subproblems. Reference [71] solved a multi-area power system operation problem in which a stochastic programming model has been studied to consider cross-border trading in the presence of wind power uncertainty.

The second category of decomposition approaches is based on the scenario structure of the problem. Reference [43] adopted a progressive hedging algorithm to decompose the stochastic formulations into multiple single-scenario subproblems. Reference [44] presented a scenario-tree based stochastic SCUC that considers load uncertainty as well as outage of multiple generation and transmission components using scenario reduction technique. References [45-47] solved a two-stage stochastic SCUC, which can solve the second stage subproblems with scenarios in parallel.

According to the functional structure of the problem, the original large-scale optimization problem can be decomposed into two major functions: generation scheduling and network security checking. Benders decomposition based approaches have been widely used to coordinate the master UC problem and the network security checking subproblems using Benders cuts (or violation cuts) [27]. Reference [72] proposed a two-stage SCUC algorithm in which unit commitment decisions are made in the first stage, and the second stage considers security-driven redispatching to mitigate the intermittency and volatility of wind power. Benders decomposition technique is applied to coordinate these two stages by adding cuts from the second stage back to the first stage. An auxiliary problem principle based sequential-parallel solution was proposed in [39] to solve a deterministic SCUC problem. In the work [39], single UC subproblems are interacted with hourly OPF subproblems through Lagrangian penalty functions. Although in this work, either single UC subproblems or hourly OPF subproblems can be solved in parallel, the overall solution procedure is still sequential because the hourly OPF subproblems have to wait for the unit commitment decisions from single UC subproblems. As Amdahl's law dictated [73], an upper bound on the relative speedup achieved on a system with multi-processors is decided by the execution time of the sequentially operated applications. This overall sequential solution procedure of SCUC becomes the bottleneck to improve computing efficiency.

In this dissertation, we concentrate on the modeling of the studied stochastic SCUC problem and the development of the parallel algorithms. The proposed parallel stochastic SCUC approach can decompose the stochastic SCUC problem by generating units and time periods, as well as by scenarios. The major contributions of this work are summarized as follows:

3.1.1 Fully decomposed problem structures

The proposed approach decomposes the entire stochastic SCUC problem into three major solution modules: the UC module determines the state of generating units; the OPF module optimizes the power generation of generating units while satisfying the network security constraints; and the bridge module builds a connection between the UC and OPF modules. Each major module can be further decomposed into multiple smaller submodules. The UC module is composed by multiple single UC submodules. The OPF module includes multiple hourly OPF submodules. Multiple bridge submodules will work as junction points to link single UC and hourly OPF submodules. In addition, all submodules are applied to both base case and scenarios. As a result, the proposed decomposition approach makes all decomposed problems scalable and tractable, which will theoretically allow us to handle power systems of any size with a large number of scenarios assuming enough processors.

3.1.2 Handling of complicating constraints

The existing SCUC decomposition methods [43-47] coordinate unit commitment decisions (binary variables) between base case and scenarios. The classical Lagrangian relaxation method is adopted to satisfy the complicating (non-anticipativity or consistency) constraints with integer variables (unit commitment decisions). In other words, they directly process the integer variables appearing in the complicating constraints. However, the proposed method will create the complicating constraints with only continuous variables (such as the power dispatch of generating units) to indirectly coordinate the unit commitment between base case and scenarios by using the augmented Lagrangian relaxation method (with the second order penalty function in the Lagrangian objective function). These strategies can enhance the solution performance by avoiding the discreteness of unit commitment variables during the coordination procedure and improving the convexity of Lagrangian relaxation function.

3.1.3 Fully parallel solution procedure

As the APP method is more desirable to be applied for large-scale power system optimization problems in terms of computational speed and convergence performance [42], this method is applied to coordinate all above solution modules. With the application of APP method, all of the single UC, hourly OPF and bridge/TS modules for both base case and scenarios/contingencies can be solved simultaneously, instead of in a sequential process. In other words, the OPF module does not need to wait for the unit commitment decision from the UC module, and the study on scenarios/contingencies does not need to be based on the solution of base case. Consequently, all of the solution modules are solved in a parallel manner, which can fully utilize the parallel computing techniques to improve the computational efficiency. Also, the parallelization of the proposed algorithm is implemented on a distributed computing cluster which is composed by up to 8 computers.

3.2 Formulations

Scenario-based stochastic SCUC model is widely used by power system operators to deal with increasing uncertainties in power systems, especially from intermittent renewable energy. Mathematically, the stochastic SCUC problem can be formulated as a mixed integer programming (MIP) based two-stage stochastic programming problem. This MIP problem makes the unit commitment decision in the first stage and considers security-driven redispatching with uncertainty in the second stage. Without loss of generality, a set of general MIP formula of the two-stage stochastic SCUC is represented by (4.1) that minimizes the total expected operating cost, while satisfying both unit and system operational constraints for all given scenarios over the studied time horizon.

$$
\begin{aligned}
&\underset{x}{Min} \quad cx + \underset{y^0,\ldots,y^S}{Min} \sum_{s=0}^{NS} \rho^s dy^s \\
&S.t. \quad Ax \le b \\
&\qquad M^s x + N^s y^s \le h^s \quad \forall s
\end{aligned}
\tag{3.1}
$$

where the binary variables x are the first-stage variables, which represent the status of generating units (e.g. ON/OFF); the second-stage decision variables, such as the power dispatch of generating units in both base case (indicated by superscript 0) and scenarios (indicated by superscript s), can be represented by the continuous variables y^0 and y^s, respectively; the cost coefficients c and d are for the corresponding binary x and continuous y variables; and the parameters ρ^s are the probability of base case ($s=0$) and scenarios ($s \ne 0$) and subject to $\rho^0 + \sum_{s=1}^{NS} \rho^s = 1$. In order to clearly introduce the proposed decomposition strategy in the chapter, we reformulate the optimization problem (3.1) by (3.2) – (3.9),

$$
Min \quad cx + \rho^0 dy^0 + \sum_{s=1}^{NS} \rho^s dy^s \tag{3.2}
$$

$$s.t.\quad Ax \le b \tag{3.3}$$

$$E^0 x + F^0 y^0 \le d^0 \tag{3.4}$$

$$H^0 y^0 \le e^0 \tag{3.5}$$

$$y_{\min} x \le y^0 \le y_{\max} x \tag{3.6}$$

$$E^s x + F^s y^s \le d^s \quad \forall s \ne 0 \tag{3.7}$$

$$H^s y^s \le e^s \quad \forall s \ne 0 \tag{3.8}$$

$$y_{\min} x \le y^s \le y_{\max} x \quad \forall s \ne 0 \tag{3.9}$$

The objective function (3.2) minimizes the total expected operating cost. The constraint (3.3) is relevant to only binary variables x, like minimum On/Off time limits of generating units. The constraint (3.4) is for base case, which include both unit state x and continuous power dispatch y^0, such as the ramping limits of generating units. The constraint (3.5) is for only continuous power dispatch variables y^0 in base case, such as the power balance constraints, reserve requirements and the power flow limits with/without the consideration of contingencies. The specific constraint (3.6) represents the generation capacity limits $[y_{\min} x \quad y_{\max} x]$ that depend on the state x of generating units. Similar to above constraints (3.4)-(3.6), the constraints (3.7)-(3.9) are for different scenarios which represent uncertainties in load demands and wind generations in this chapter.

In this stochastic SCUC problem, the objective function (3.2) is decomposable without any coupling terms. The set of constraints (3.3)-(3.9) can be categorized using two strategies. One strategy is to divide the constraints by scenarios, which categorize constraints (3.3)-(3.9) into base case constraints (3.3)–(3.6) and scenario case constraints (3.7)–(3.9). The other strategy is to divide the constraints by its function, which categorizes constraints (3.3)-(3.9) into a MIP based UC model (including (3.3), (3.4), (3.6), (3.7) and (3.9)) and a linear programming (LP) based OPF model (including (3.5) and (3.8)) with only continuous variables y^0 and y^s. This chapter combines both strategies to divide all the constraints into four groups: the MIP based UC model for base case (3.3), (3.4) and (3.6); the MIP based UC model for scenario (3.7) and (3.9); the LP based OPF model for base case (3.5); and the LP based OPF model for scenario (3.8). However, all these four groups of constraints are coupled by complicating variables x, y^0 and y^s. For examples: the status x of generating units should be the same for both base case and scenarios; and the power dispatch variables y^0 and y^s appear in both the UC and OPF models. Such complicating variables are making the entire optimization problem indecomposable and probably intractable. Therefore, a new decomposition strategy and solution method is proposed in the following sections.

3.3 Decomposition strategy

In order to eliminate those complicating variables and fully decompose the original stochastic SCUC problem into scalable subproblems, the following four major steps will be conducted:

- *Step 1:* Replace complicating variables with complicating constraints using variables duplication technique.
- *Step 2*: Relax complicating constraints using augmented Lagrangian relaxation method.

- *Step 3*: Decompose coupling terms in the Lagrangian objective function using APP method.
- *Step 4*: Formulate independent solution modules.

3.3.1 Replace complicating variables

In order to replace complicating variables with complicating constraints, several groups of variables are introduced as duplications of the existing variables. The problem (3.2)-(3.9) can be rewritten as shown in (3.10) – (3.23).

$$Min \quad cx^0 + \rho^0 dy_{uc}^0 + \sum_s \rho^s dy_{uc}^s \tag{3.10}$$

$$s.t. \; Ax^0 \leq b \tag{3.11}$$

$$Ex^0 + Fy_{uc}^0 \leq d \tag{3.12}$$

$$Hy_{opf}^0 \leq e \tag{3.13}$$

$$y_{\min} x^0 \leq y_{uc}^0 \leq y_{\max} x^0 \tag{3.14}$$

$$Ex^s + Fy_{uc}^s \leq d \tag{3.15}$$

$$Hy_{opf}^s \leq e \tag{3.16}$$

$$y_{\min} x^s \leq y_{uc}^s \leq y_{\max} x^s \tag{3.17}$$

$$y_{\min} x^s \leq y_{uc}^{0,s} \leq y_{\max} x^s \tag{3.18}$$

$$y_{uc}^0 = y_{brdg}^0 \tag{3.19}$$

$$y_{opf}^0 = y_{brdg}^0 \tag{3.20}$$

$$y_{uc}^{0,s} = y_{brdg}^0 \tag{3.21}$$

$$y_{uc}^{s} = y_{brdg}^{s} \tag{3.22}$$

$$y_{opf}^{s} = y_{brdg}^{s} \tag{3.23}$$

where x^0 and x^s, as duplications of the original binary variables *x*, are introduced for both base case and scenarios, respectively. Duplications of y^0 for UC and OPF constraints in base case are noted as y_{uc}^{0} and y_{opf}^{0}, respectively. Similarly, duplications of y^s for UC and OPF constraints in scenario cases are noted as y_{uc}^{s} and y_{opf}^{s}, respectively. In addition, one more group of duplications of y^0, variables $y_{uc}^{0,s}$ are introduced into the generation capacity limits (3.18) for scenarios to represent the power dispatch from base case.

In order to guarantee an equal value to above duplications of complicating variables x, y^0 or y^s,

- Bridge variables y_{brdg}^{0} are introduced to ensure that the duplications of complicating variables y^0 have the same value ($y_{uc}^{0} = y_{opf}^{0} = y_{uc}^{0,s}$ from the constraints (3.19)-(3.21));
- Bridge variables y_{brdg}^{s} are added to make sure that the duplications of complicating variables y^s have the same value ($y_{uc}^{s} = y_{opf}^{s}$ based on the constraints (3.22)-(3.23));

- From the constraints (3.19) and (3.21), we get $y_{uc}^{0} = y_{uc}^{0,s}$. And, these two continuous variables y_{uc}^{0}, $y_{uc}^{0,s}$ are restricted by corresponding generation capacity limits (3.14) and (3.18). If both y_{uc}^{0} and $y_{uc}^{0,s}$ are equal to zero (no generation), we can get the state of generating units $x^{0} = 0$ and $x^{s} = 0$. However, if both y_{uc}^{0} and $y_{uc}^{0,s}$ are within their lower ($y_{\min}$) and upper ($y_{\max}$) bounds, we must have $x^{0} = 1$ and $x^{s} = 1$. Therefore, a group of constraints (3.14), (3.18), (3.19) and (3.21) will together ensure that the duplications of complicating variables x are equal ($x^{0} = x^{s}$), which physically means the state of generating units keep the same for both base case and scenarios.

Now, the problem constraints can be grouped into the following six types, including four types (Types 1-4) of separable constraints and two types of complicating constraints:

- Type 1: UC-base constraints: UC constraints for base case include the constraints (3.11), (3.12) and (3.14) with the duplication variables x^{0} and y_{uc}^{0};

- Type 2: UC-scenario constraints: UC constraints for scenarios include the constraints (3.15), (3.17), and (3.18) with the duplication variables x^{s}, y_{uc}^{s} and $y_{uc}^{0,s}$.

- Type 3: OPF-base constraints: OPF constraints for base case include the constraints (3.13) with the duplication variables y_{opf}^{0}.

- Type 4: OPF-scenario constraints: OPF constraints for scenarios include the constraints (3.16) with the duplication variables y_{opf}^{s}.

- Type 5: Complicating constraints for base case: the constraints (3.19)-(3.21) link the duplication variables y_{uc}^{0}, y_{opf}^{0}, $y_{uc}^{0,s}$ using bridge variables y_{brdg}^{0}. Such complicating constraints are coupling above Types 1-3 constraints.
- Type 6: Complicating constraints for scenarios: the constraints (3.22) and (3.23) link the duplication variables y_{uc}^{s} and y_{opf}^{s} using bridge variables y_{brdg}^{s}. Such constraints are coupling above Type 2 and Type 4 constraints.

So far, all the complicating variables x, y^{0} and y^{s} in the original problem (3.2)-(3.9) are replaced by the complicating constraints (3.19)-(3.23), which will be further decomposed using the augmented Lagrangian method as discussed in the following subsection.

3.3.2 Relax complicating constraints

In this subsection, augmented Lagrangian relaxation method is adopted to decompose complicating constraints (3.19) - (3.23) by adding the first-order and the second-order penalty functions into the objective function (3.10). Accordingly, the objective function of corresponding Lagrangian relaxation problem is written as,

$$
\begin{aligned}
&Min \quad L = cx^0 + \rho^0 dy_{uc}^0 + \sum_s \rho^s d y_{uc}^s \\
&+\lambda_{uc}^0\left(y_{uc}^0 - y_{brdg}^0\right) + \frac{c_{uc}^0}{2}\left\|y_{uc}^0 - y_{brdg}^0\right\|^2 \\
&+\lambda_{opf}^0\left(y_{opf}^0 - y_{brdg}^0\right) + \frac{c_{opf}^0}{2}\left\|y_{opf}^0 - y_{brdg}^0\right\|^2 \\
&+\sum_s\left(\lambda_{uc}^{0,s}\left(y_{uc}^{0,s} - y_{brdg}^0\right) + \frac{c_{uc}^{0,s}}{2}\left\|y_{uc}^{0,s} - y_{brdg}^0\right\|^2\right) \\
&+\sum_s\left(\lambda_{uc}^{s}\left(y_{uc}^{s} - y_{brdg}^s\right) + \frac{c_{uc}^{s}}{2}\left\|y_{uc}^{s} - y_{brdg}^s\right\|^2\right) \\
&+\sum_s\left(\lambda_{opf}^{s}\left(y_{opf}^{s} - y_{brdg}^s\right) + \frac{c_{opf}^{s}}{2}\left\|y_{opf}^{s} - y_{brdg}^s\right\|^2\right)
\end{aligned} \tag{3.24}
$$

where λ and c are the penalty multipliers associated with the first-order and the second-order terms, respectively. The penalty multipliers will be updated during the iterative solution process. After relaxing complicating constraints by penalty multipliers, the remaining constraints (3.11)-(3.18) become separable and decomposable. However, the Lagrangian relaxation function (3.24) is still unable to be decomposed because of the coupling terms (the product of variables) introduced by the second order penalty function in (3.24).

3.3.3 Decompose objective function

In order to remove coupling terms from the objective function (3.24), an APP method [37] is applied in this step to replace (3.24) with its auxiliary problem (3.25), in which the coupling terms are substituted by independent terms with the help of iterative results from the previous iterations.

$$
\begin{aligned}
& Min\ cx^0 + \rho^0 dy_{uc}^0 + \sum_s \rho^s dy_{uc}^s \\
& + \begin{bmatrix} \lambda_{uc}^0 \left(y_{uc}^0 - y_{brdg}^0 \right) + c_{uc}^0 \left((y_{uc}^0)^2 + (y_{brdg}^0)^2 \right) \\ -c_{uc}^0 \left(y_{uc}^{0,(k-1)} + y_{brdg}^{0,(k-1)} \right) \left(y_{uc}^0 + y_{brdg}^0 \right) \end{bmatrix} \\
& + \begin{bmatrix} \lambda_{opf}^0 \left(y_{opf}^0 - y_{brdg}^0 \right) + c_{opf}^0 \left((y_{opf}^0)^2 + (y_{brdg}^0)^2 \right) \\ -c_{opf}^0 \left(y_{opf}^{0,(k-1)} + y_{brdg}^{0,(k-1)} \right) \left(y_{opf}^0 + y_{brdg}^0 \right) \end{bmatrix} \\
& + \sum_s \begin{bmatrix} \lambda_{uc}^{0,s} \left(y_{uc}^{0,s} - y \right) + c_{uc}^{0,s} \left((y_{uc}^{0,s})^2 + (y_{brdg}^0)^2 \right) \\ -c_{uc}^{0,s} \left(y_{uc}^{0,s,(k-1)} + y_{brdg}^{0,(k-1)} \right) \left(y_{uc}^{0,s} + y_{brdg}^0 \right) \end{bmatrix} \\
& + \sum_s \begin{bmatrix} \lambda_{uc}^s \left(y_{uc}^s - y_{brdg}^s \right) + c_{uc}^s \left((y_{uc}^s)^2 + (y_{brdg}^s)^2 \right) \\ -c_{uc}^s \left(y_{uc}^{s,(k-1)} + y_{brdg}^{s,(k-1)} \right) \left(y_{uc}^s + y_{brdg}^s \right) \end{bmatrix} \\
& + \sum_s \begin{bmatrix} \lambda_{opf}^s \left(y_{opf}^s - y_{brdg}^s \right) + c_{opf}^s \left((y_{opf}^s)^2 + (y_{brdg}^s)^2 \right) \\ -c_{opf}^s \left(y_{opf}^{s,(k-1)} + y_{brdg}^{s,(k-1)} \right) \left(y_{opf}^s + y_{brdg}^s \right) \end{bmatrix}
\end{aligned}
\tag{3.25}
$$

where $y^{(k-1)}$ are the results obtained from the previous iteration *k*-1, which can be considered as constants in the current iteration *k*. As a result, decoupled auxiliary objective functions can be obtained by reorganizing this auxiliary problem (3.25), which is relevant to different groups of variables, and will be presented in the next subsection.

3.3.4 Formulate independent solution modules

By associating decoupled objective functions with their corresponding constraints groups, the original stochastic SCUC problem can be divided into the following six independent solution modules, including the UC-base module, the UC-scenario module, the OPF-base module, the OPF-scenario module, the bridge-base module and the bridge-scenario module. The relationship and variables/data exchange between modules are shown in Figure 3.1.

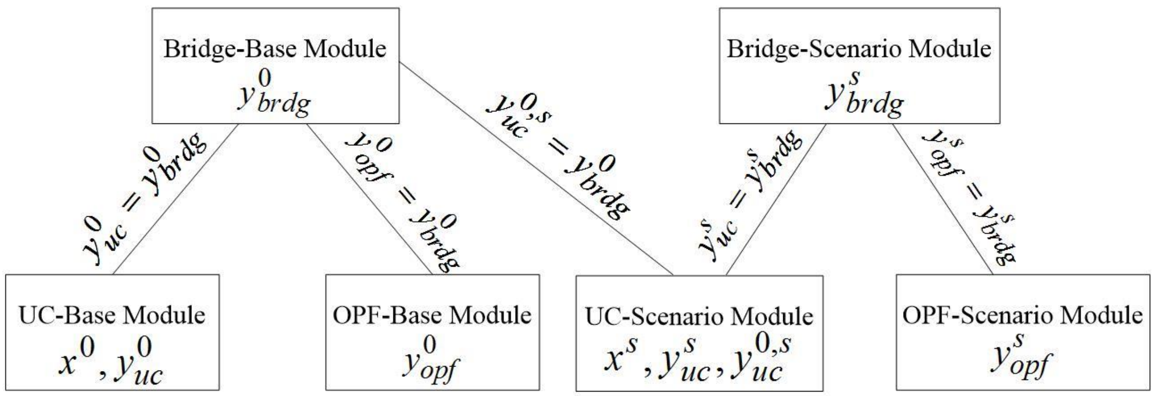

Figure 3.1 The relationship and variables exchange between solution modules

3.3.4.1 UC-base module

The UC-base module is composed by the objective function (3.26) and constraints (3.11), (3.12) and (3.14), with variables x^0 and y^0_{uc}.

$$\begin{aligned} &Min\ cx^0 + c^0_{uc}(y^0_{uc})^2 \\ &\quad + \left(\rho^0 d + \lambda^0_{uc} - c^0_{uc}(y^{0,(k-1)}_{uc} + y^{0,(k-1)}_{brdg})\right) y^0_{uc} \end{aligned} \tag{3.26}$$

Note that constraints in the UC-base module can be separated for individual generating units, and there is no coupling terms between the generating units in the objective function as well. Thus, the UC-base module can be further decomposed into multiple single UC-base submodules.

3.3.4.2 UC-scenario module

The UC-scenario module includes the objective function (3.27) and constraints (3.15), (3.17), (3.22) and (3.23), with variables x^s, y_{uc}^s and $y_{uc}^{0,s}$. Similar to the UC-base module, for each scenario, the UC-scenario module can be further decomposed into multiple single UC-scenario submodules.

$$\begin{aligned} Min \quad & \sum_s \rho^s d y_{uc}^s \\ & + \sum_s \left[c_{uc}^s (y_{uc}^s)^2 + \left(\lambda_{uc}^s - c_{uc}^s y_{uc}^{s,(k-1)} - c_{uc}^s y_{brdg}^{s,(k-1)} \right) y_{uc}^s \right] \\ & + \sum_s \left[c_{uc}^{0,s} (y_{uc}^{0,s})^2 + \left(\lambda_{uc}^{0,s} - c_{uc}^{0,s} (y_{uc}^{0,s,(k-1)} + y_{brdg}^{0,(k-1)}) \right) y_{uc}^{0,s} \right] \end{aligned} \tag{3.27}$$

3.3.4.3 OPF-base module

The OPF-base module is adopted to optimize decomposed objective functions under network constraints in base case. This module consists of the objective function (3.28) and constraint (3.13), with variables y_{opf}^0. As all the constraints in the OPF-base module can be separated for single period study, this module can be further divided into multiple single-hour OPF-base submodules.

$$\begin{aligned} Min \quad & c_{opf}^0 (y_{opf}^0)^2 \\ & + \left(\lambda_{opf}^0 - c_{opf}^0 (y_{opf}^{0,(k-1)} + y_{brdg}^{0,(k-1)}) \right) y_{opf}^0 \end{aligned} \tag{3.28}$$

3.3.4.4 OPF-scenario module

The OPF-scenario module has the objective function (3.29) and constraint (3.16), with variables y_{opf}^{s}. Similar to the OPF-base module, for each scenario, the OPF-scenario module can be further decomposed into multiple single-hour OPF-scenario submodules.

$$Min \quad \sum_{s} \begin{bmatrix} c_{opf}^{s}(y_{opf}^{s})^{2} \\ +\left(\lambda_{opf}^{s} - c_{opf}^{s}(y_{opf}^{s,(k-1)} + y_{brdg}^{s,(k-1)})\right) y_{opf}^{s} \end{bmatrix} \tag{3.29}$$

3.3.4.5 Bridge-base module

The bridge-base module is introduced here as an unconstrained optimization problem (3.30) with variable y_{brdg}^{0}, which is used to collaborate the UC-base, the OPF-base and the UC-scenario modules, as shown in Figure.3.1.

$$\begin{aligned} Min \quad & \left(c_{uc}^{0} + c_{opf}^{0} + \sum_{s} c_{uc}^{0,s}\right)(y_{brdg}^{0})^{2} \\ & + \begin{bmatrix} -\lambda_{uc}^{0} - c_{uc}^{0}\left(y_{uc}^{0,(k-1)} + y_{brdg}^{0,(k-1)}\right) \\ -\lambda_{opf}^{0} - c_{opf}^{0}\left(y_{opf}^{0,(k-1)} + y_{brdg}^{0,(k-1)}\right) \\ -\sum_{s} \lambda_{uc}^{0,s} - \sum_{s} c_{uc}^{0,s}\left(y_{uc}^{0,s,(k-1)} + y_{brdg}^{0,(k-1)}\right) \end{bmatrix} y_{brdg}^{0} \end{aligned} \tag{3.30}$$

In (3.30), the solution of the k^{th} iteration in bridge-base is impacted by the iterative result of the (k-1)th iteration from itself and other modules like the UC-base, OPF-base, and UC-scenario modules for all scenarios. Obviously, this objective function can be decomposed into multiple submodules in terms of generating units, studied periods and scenarios.

3.3.4.6 Bridge-scenario module

Similarly, the bridge-scenario module is introduced to connect the UC-scenario and OPF-scenario modules, as shown in Figure.3.1. The bridge-scenario module is also an unconstrained optimization problem (3.31) with variable y_{brdg}^{s}. This module can be further decomposed into multiple submodules in terms of generating units, studied periods and scenarios.

$$
\begin{aligned}
Min \quad & \sum_{s}\left(c_{uc}^{s}+c_{opf}^{s}\right)(y_{brdg}^{s})^{2} \\
& +\sum_{s}\begin{bmatrix} -\lambda_{uc}^{s}-c_{uc}^{s}\left(y_{uc}^{s,(k-1)}+y_{brdg}^{s,(k-1)}\right) \\ -\lambda_{opf}^{s}-c_{opf}^{s}\left(y_{opf}^{s,(k-1)}+y_{brdg}^{s,(k-1)}\right) \end{bmatrix} y_{brdg}^{s}
\end{aligned}
\tag{3.31}
$$

Finally, a fully decomposed structure of the studied stochastic SCUC problem is illustrated in Figure.3.2. By adopting the proposed decomposition strategy, the original large-scale stochastic SCUC problem is decomposed into numbers of small-size submodules which can be simultaneously solved. Commercial MIP solvers can be used to solve submodules with a piecewise linearized objective function and a set of linear equality and inequality constraints.

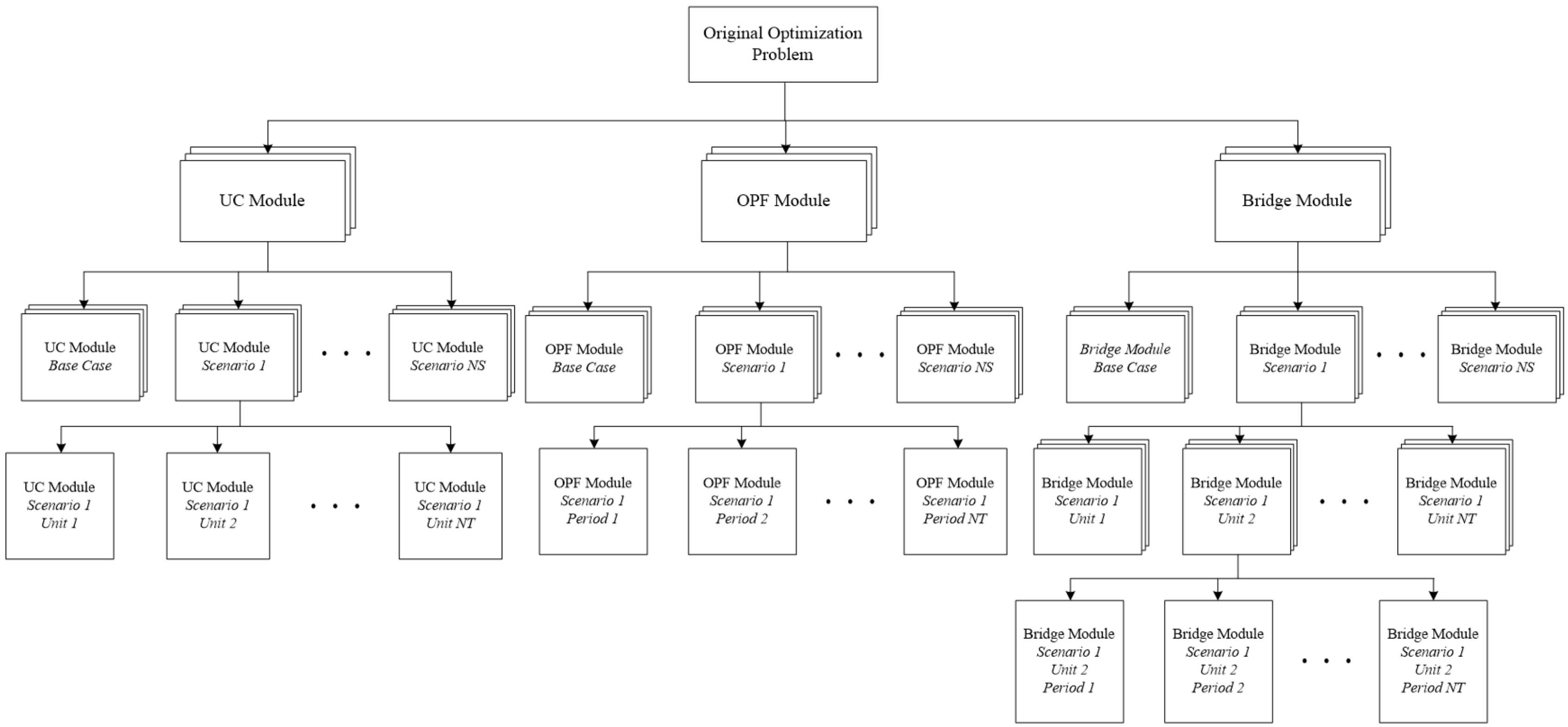

Figure 3.2 Decomposition structure of fully decomposed submodules

3.4 Solution procedure

According to the discussions above, two levels of decomposition are adopted in the chapter. Augmented Lagrangian relaxation method is used in the first level to decompose complicating constraints, while the APP technique is employed in the second level to decouple the Lagrangian relaxation function. Thus, the proposed parallel solution procedure includes two loops: an outer loop and an inner loop. The outer loop collaborates UC, OPF and bridge modules by updating penalty multipliers, while the inner loop ensures the accuracy of APP approximation. Figure. 3.34 shows the proposed parallel solution procedure which is discussed below:

- Step 1: Set the iteration index, r=0 for the inner loop and k=0 for the outer loop, and choose initial values for all the variables $\bar{z}^0$ (including y^0, y^s, y_{uc}^0, y_{opf}^0, $y_{uc}^{0,s}$, y_{uc}^s and y_{opf}^s) and Lagrangian multipliers λ and c.

- Step 2: Set the inner loop iteration index r=r+1, solve UC, OPF and bridge modules in parallel, and obtain optimal results $\bar{z}^{k,r}$ of the current inner iteration r.

- Step 3: Check the inner loop convergence using (3.32) where ε_1 is the convergence threshold for the mismatch of duplicated variables within inner loops. If it is satisfied, set $\bar{z}^k = \bar{z}^{k,r}$, and go to Step 4. Otherwise, go back to Step 2.

$$\left\| \bar{z}^{k,r} - \bar{z}^{k,r-1} \right\| \le \varepsilon_1 \tag{3.32}$$

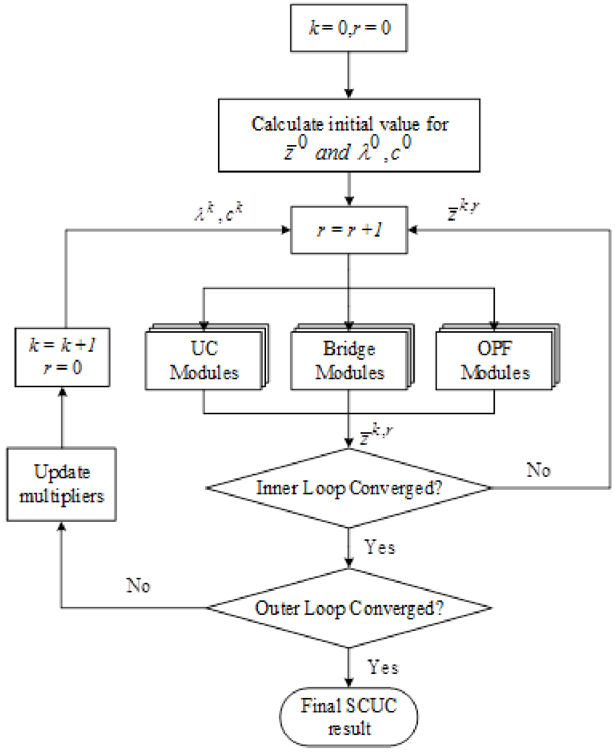

Figure 3.3 Flowchart of the proposed parallel SCUC approach

- Step 4: Check the following stopping criteria including necessary-consistency conditions (3.33) and (3.34) where ε_2 is the convergence threshold for the mismatch of duplicated variables within outer loops and ε_3 is the convergence threshold for the mismatch between each couple of complicating variables; and sufficiency condition (3.35) where ε_4 is the convergence threshold for the cost difference between two successive iterations [74]. If all of them are satisfied, then stop and the optimal value $\bar{z}^*$ is obtained; otherwise, go to Step 5.

Necessary-consistency conditions:

$$\left\| \bar{z}^{k} - \bar{z}^{k-1} \right\| \le \varepsilon_2 \tag{3.33}$$

$$\left\{\begin{array}{l}\left\|y_{uc}^{0,k}-y_{bdg}^{0,k}\right\|,\left\|y_{opf}^{0,k}-y_{bdg}^{0,k}\right\|,\left\|y_{uc}^{0,s,k}-y_{bdg}^{0,k}\right\| \\ \left\|y_{uc}^{s,k}-y_{bdg}^{s,k}\right\|,\left\|y_{opf}^{s,k}-y_{bdg}^{s,k}\right\|\end{array}\right\} \leq \varepsilon_3 \qquad (3.34)$$

Sufficiency condition:

$$\left\|\frac{L(\bar{z}^{k})-L(\bar{z}^{k-1})}{L(\bar{z}^{k})}\right\| \leq \varepsilon_4 \qquad (3.35)$$

where $L(\bar{z}^{k})$ is the optimal result of (3.24) at the outer loop iteration *k*.

- Step 5: Update Lagrangian multipliers using (3.36) and (3.37), set $k = k+1$ and $r=0$, and go to Step 2.

$$\begin{aligned}
\lambda_{uc}^{0,k+1} &= \lambda_{uc}^{0,k} + c_{uc}^{0,k}(y_{uc}^{0,k} - y_{bdg}^{0,k}) \\
\lambda_{opf}^{0,k+1} &= \lambda_{opf}^{0,k} + c_{opf}^{0,k}(y_{opf}^{0,k} - y_{bdg}^{0,k}) \\
\lambda_{uc}^{0,s,k+1} &= \lambda_{uc}^{0,s,k} + c_{uc}^{0,s,k}(y_{uc}^{0,s,k} - y_{bdg}^{0,k}) \\
\lambda_{uc}^{s,k+1} &= \lambda_{uc}^{s,k} + c_{uc}^{s,k}(y_{uc}^{s,k} - y_{bdg}^{s,k}) \\
\lambda_{opf}^{s,k+1} &= \lambda_{opf}^{s,k} + c_{opf}^{s,k}(y_{opf}^{s,k} - y_{bdg}^{s,k})
\end{aligned} \qquad (3.36)$$

$$c^{k+1} = \beta c^{k} \qquad (3.37)$$

where *c* is the second order penalty multiplier (including c_{uc}^{0}, c_{opf}^{0} ,c_{uc}^{s},c_{uc}^{s}, and $c_{uc}^{0,s}$) and the coefficient β is set to be equal or larger than one in order to obtain a converged optimal result. The success of the proposed Lagrangian relaxation based method depends on the ability of the algorithm to drive Lagrangian multipliers to the value of multipliers associated with complicating constraints at the optimal solution. With the combination of convergence criteria (3.32)-(3.35) and multipliers updating process (3.36)-(3.37), it has been proven to converge to the optimal solution of the original optimization problem when the problem is convex [37]. Although there is a convergence proof of the APP algorithm for convex optimization problems, there is no direct proof for a non-convex MIP problem, which is modeled in this chapter. However, for this non-convex optimization problem, the non-convexity can be mitigated by the augmented Lagrangian method. Quadratic penalty terms are added to the Lagrangian objective function as a local convexifier to improve the convexity of the problem [53]. In addition, according to our experiments/testing experiences, we would like to mention that the effectiveness of the used APP algorithm on the studied non-convex stochastic SCUC problem is satisfactory and acceptable, which can be supported by the following case studies.

3.5 Numerical study

The proposed decomposition framework has been tested on the scenario-based stochastic SCUC problem. In this chapter, a modified IEEE 118-bus power system and a practical 1168-bus power system are used to illustrate the computational efficiency and convergence performance of the proposed parallel approach for solving the stochastic SCUC problem with consideration of wind generating units.

As a key input to the scenario-based stochastic SCUC study, the possible realization of the system uncertainties can be simulated by various scenario generation and selection methods[75]. For the scenarios generation, different probability distribution functions have been adopted by researchers to generate a group of scenarios representing the load and wind generation uncertainties, such as hyperbolic distribution function [76], normal distribution function [77], and truncated normal distribution function [78, 79]. In this chapter, the forecasts of the load and wind generation are represented by the truncated normal distribution function with 99.95% confidence interval and they are in the range of $[\mu - 3.5\sigma, \mu + 3.5\sigma]$. In this study, the mean μ is the hourly power forecast, and the standard deviation σ is 5% of the mean. In our study, the wind power generation profiles for base case are obtained and scaled based on the actual wind generation data [80].

For the scenario selection, normally, the scenario reduction technique is used to reduce the size of scenarios and create a proper scenario tree that will be studied by the stochastic SCUC problem. Several scenario reduction algorithms have been adopted by researchers, which include the fast backward method, the fast backward/forward method, and the fast backward/backward method [81, 82]. As these scenario reduction algorithms have different computational performance and accuracy, the selection of an algorithm would depend on the size of the problem and the required accuracy. For example, the fast backward method provides the best computational performance but the worst accuracy, while the fast forward method could provide a more accurate result with longer computational time [79]. Since the main purpose of this chapter is to handle as many scenarios as possible using the proposed parallel algorithm, the scenario reduction technique is not adopted in our study. However, as an input study, it can be easily integrated with our work.

The specific parameters are set as the same in all case studies. The penalty multipliers are set as $\lambda^0 = 0$, $c^0 = 0.05$ for all penalty functions, and updating parameters for the second order multipliers is $\beta = 1.01$. The convergence thresholds are set as $\varepsilon_1 = 0.2MW$ (3.32), $\varepsilon_2 = 0.1MW$ (3.33), $\varepsilon_3 = 0.1MW$ (3.34), and $\varepsilon_4 = 0.01\%$ (3.35).

3.5.1 Modified IEEE 118-bus power system

A modified IEEE 118-bus system [27] consisting of 54 generating units, 10 wind units, 186 branches, 91 demand sides, 5 critical transmission line contingencies and up to 30 scenarios is studied. The following three cases are solved using ILOG CPLEX 12.5's MIP solver on a 3.4 GHz personal computer with 8G memory:

- Case 1: Deterministic case
- Case 2: Stochastic case with one scenario
- Case 3: Stochastic case with up to 30 scenarios

3.5.1.1 Deterministic case

A deterministic SCUC problem is studied using the proposed method. Because of no consideration of load and wind uncertainties in this case, there are only three major modules cooperating with each other in parallel, which are the UC-base, OPF-base and bridge-base modules. A converged result is obtained after 157 iterations. In order to compare the proposed parallel method with the conventional centralized method (a single MIP model with all variables and constraints together), their total operating cost and calculation time are listed in Table 3.1. The total operating cost of the system is $1,585,539, which is very close to the conventional centralized SCUC solution of $1,585,065. However, as the testing case is small, the calculation speed of the centralized solution is faster than our method on a single PC.

Table 3.1 Operating cost and computation time in case A.

Items	Centralized	Parallel	% Change
Total Cost ($)	$1,585,065	$1,585,539	+0.03%
Time (seconds)	39.58	235.56	+495.15%

3.5.1.2 Stochastic case with one scenario

A stochastic case with one scenario is studied in this case. In this stochastic study, there are a total of 18,624 variables (x^0 , x^s , y_{uc}^0 , y_{opf}^0 , $y_{uc}^{0,s}$, y_{uc}^s and y_{opf}^s) and 139,248 constraints (including 6,480 complicating constraints (3.19)-(3.23)). Six major modules are implemented to obtain a converged result after 211 iterations. Table 3.2 shows the total operating cost and computation time of both centralized and parallel solutions. As we can see, the CPU time consumption of the proposed parallel solution is still higher than the centralized one, while its total operating cost is very close to the centralized solution (only 0.07% increase).

Table 3.2 Operating cost and computation time in case A.2

Items	**Centralized**	**Parallel**	**% Change**
Total Cost ($)	$ 1,584,882	$ 1,585,938	+0.07%
Time (seconds)	66.1	760.7	+1150.14%

3.5.1.3 Stochastic case with up to 30 scenarios

In order to further examine the impact of increasing number of scenarios, case studies with more scenarios (up to 30) are studied in this case. Because of the size of the optimization problem and the limitation of computing hardware, only up to 5 scenarios can be tested by the centralized method. The comparison of the total operating cost and computational time between the centralized method and the proposed parallel method are listed in Table 3.3, in which with the increase of number of scenarios, the CPU time consumption of the centralized method increases from 39.58 seconds (base case) to 960.16 seconds (5 scenarios). However, using the proposed parallel algorithm, we can obtain the results for all cases having up to 30 scenarios. As an example, Table 3.4 lists the size of submodules for a case with 30 scenarios using the proposed parallel solution. All submodules are scalable and tractable. From Table 3.3, we can see that with the increase of number of scenarios, the CPU time consumption of the proposed parallel method increases from 235.56 seconds to 21,210.6 seconds (around 5.892 hours). Considering a significant increase in the number of variables (from 8,016 to 326,256), constraints (from 67,032 to 2,233,512), and complicating constraints (from 2,592 to 41,472), the increase in calculation time is reasonable and acceptable for such a complicated optimization problem running on a single PC. Note that more iterations might be needed to obtain an optimal solution for the cases with more scenarios and it results in increase of total calculation time.

Table 3.3 Results of stochastic SCUC with up to 30 Scenarios in case A.3

# of scen	Centralized		Parallel		
	Time (sec.)	Total Cost ($)	Time (sec.)	Total Cost ($)	# of Iter
0	39.58	$1,585,065	235.6	$1,585,540	157
1	66.14	$1,584,882	760.7	$1,585,939	211
2	230.89	$1,585,185	1,237.7	$1,586,395	208
3	390.19	$1,584,120	3,757.5	$1,586,638	228
4	632.36	$1,585,296	5,350.7	$1,586,797	264
5	960.16	$1,591,332	5,618.2	$1,592,664	288
10	N/A	N/A	6,712.5	$1,590,585	382
15	N/A	N/A	9,187.0	$1,605,158	438
20	N/A	N/A	11,639.9	$1,610,329	520
25	N/A	N/A	14,533.0	$1,616,201	515
30	N/A	N/A	21,210.6	$1,621,116	557

Table 3.4 Size of submodules for 30 Scenarios in case A.3

Module	Number of submodules	Number of variables	Number of Constraints
UC base	54	96	192
UC scenario	1620	144	288
OPF base	24	64	2361
OPF scenario	720	64	2361
Bridge base	1,296	1	0
Bridge scenario	38,880	1	0

3.5.2 A practical 1168-bus power system

In this case, a practical 1168-bus power system with 169 thermal units, 10 wind units, 1474 branches, 568 demand sides, 10 critical transmission line contingencies and up to 20 scenarios is studied to illustrate the computational performance of the proposed parallel algorithm for solving a large-scale stochastic SCUC problem. The following two cases are solved using ILOG CPLEX 12.5's MIP solver on a 3.4 GHz personal computer with 8G memory:

- Case 1: Deterministic case
- Case 2: Stochastic case with up to 20 scenarios

3.5.2.1 Deterministic case

In this case, we studied a deterministic case with 24,576 variables and 819,336 constraints. Using the proposed parallel method, a converged result is obtained after 282 iterations. The total operating cost and calculation time of the proposed algorithm are $3,332,264 and 514.4 seconds on a single PC, respectively. The comparison with the centralized solution ($3,313,296 with 573.2 seconds) listed in Table 3.5 supports that the accuracy of the proposed parallel solution can be guaranteed while its calculation time is 10.26% less than the centralized one.

Table 3.5 Operating cost and computation time in case B.1

Items	Centralized	Parallel	% Change
Total Cost ($)	$3,313,296	$ 3,332,264	+0.57%
Time (Seconds)	573.2	514.4	-10.26%

In order to further illustrate the convergence performance of the proposed algorithm, the power mismatch Δy^0 between the generation outputs obtained from the UC-base and OPF-base modules, $\Delta y^0 = (y_{opf}^0 - y_{uc}^0)$, are shown in Figure. 3.4. The total number of power mismatches is 4,056 (169 units ×24 hours). From Figure.3.45 (a), at the first iteration, the power mismatch is very huge (the largest one is 294.45 MW) because all the generating units in the UC-base module are uncommitted in order to minimize their operating cost, while some of generating units in the OPF-base module must be committed and supply certain amount of power to satisfy the system constraints such as power balances. As shown in Figure.3.4 (b), after 50 iterations, the worst power mismatch has been dramatically reduced to 54.00 MW, and 2,893 out of 4,056 power mismatches are below the predefined convergence threshold (0.1MW). At the 282th iteration, as shown in Figure.3.4(c), all the power mismatches converged within their thresholds (0.1MW), and the largest power mismatch is 0.0748MW, while the majority of those mismatches have nearly no error at convergence.

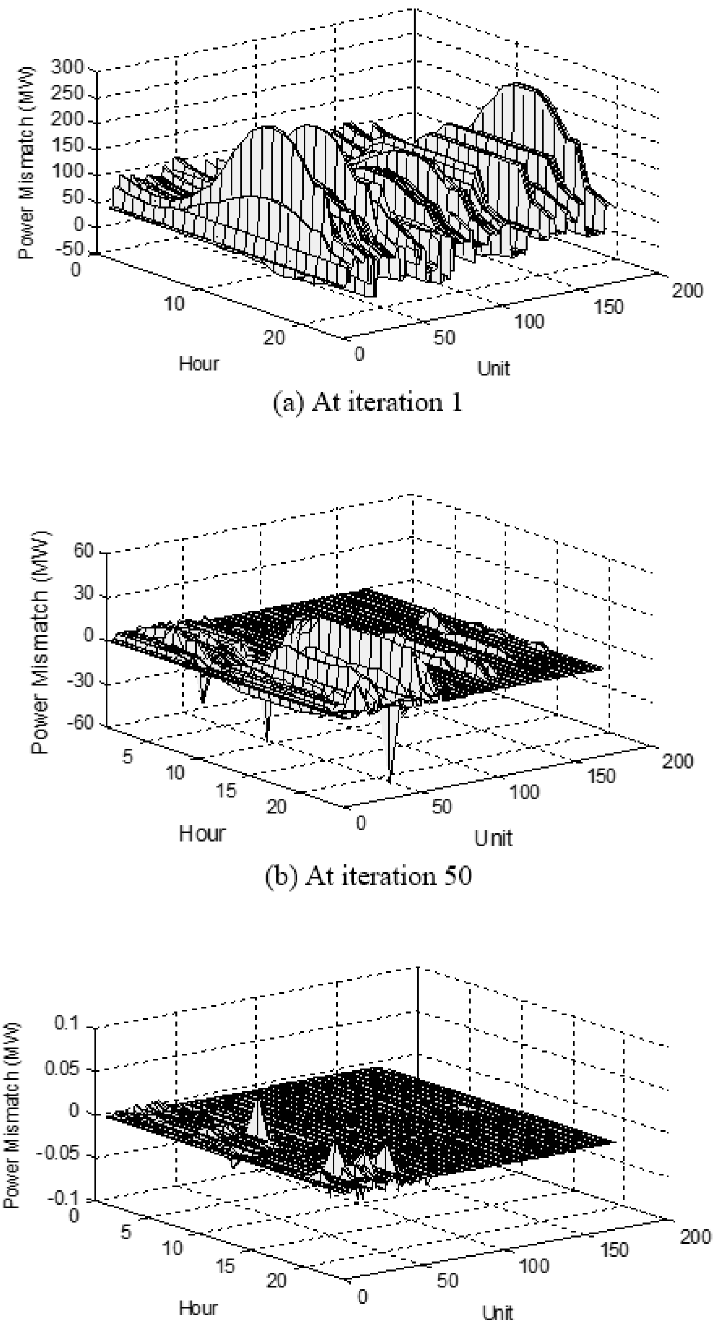

(a) At iteration 1

(b) At iteration 50

(c) At iteration 282

Figure 3.4 The power mismatches between the UC-base and OPF-base modules over iterations

3.5.2.2 Stochastic case with up to 20 scenarios

In this case, a stochastic SCUC problem with up to 20 scenarios is studied. Basically, it is really difficult to get an optimal and even a near-optimal centralized solution within a limited calculation time. However, the proposed parallel method makes it possible and doable to solve such large-scale optimization problems on a single PC. As an example, the case with 20 scenarios includes 678,336 variables and 17,530,536 constraints (including 251,472 complicating constraints (3.19)-(3.23)). After using the proposed parallel method, we list the size of submodules in Table 3.6. Table 3.7 summarizes the detailed computational results for the proposed parallel solution. For the case with 20 scenarios, an optimal result is obtained after 530 iterations with an operating cost of $3,660,700 and a CPU time of 13.889 hours. Figure 3.5 shows the convergence performance of the proposed method. In these four cases, most complicating constraints can quickly converge after 200 iterations. For example, in the test case with 20 scenarios, 221,717 out of 251,472 (87.95% within threshold) are converged at 200 iterations, and 330 more iterations are needed to find the final converged result (100% within threshold).

Table 3.6 Size of Submodules for 20 scenarios in Case B.2

Module	Number of submodules	Number of variables	Number of Constraints
UC base	169	96	192
UC scenario	3380	144	288
OPF base	24	179	32,787
OPF scenario	480	179	32,787
Bridge base	4,056	1	0
Bridge scenario	81,120	1	0

Table 3.7 Operating cost and computation time in case B.2

# of Scen.	# of Iter	Time (hours)	Total Cost ($)
5	372	3.636	$3,370,900
10	471	7.026	$3,468,400
15	462	8.031	$3,562,200
20	530	13.889	$3,660,700

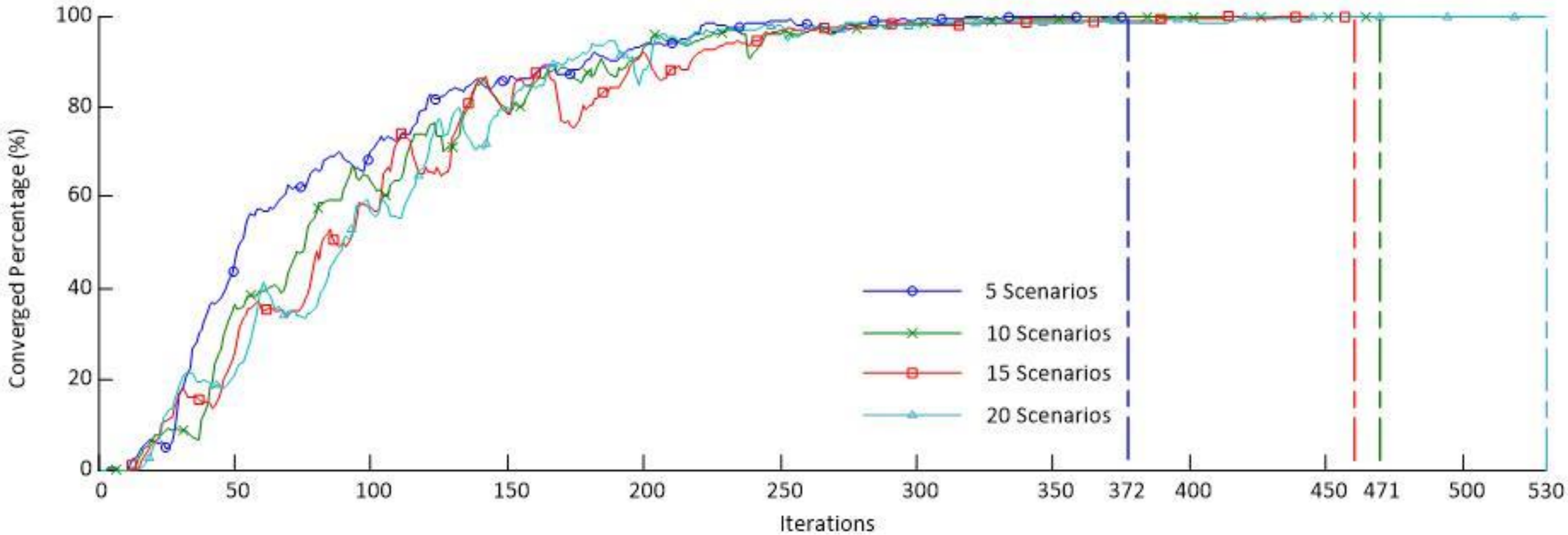

Figure 3.5 Percentage of satisfied complicating constraints

3.5.3 Parallel implementation

To further justify the effectiveness of the proposed parallel algorithm, the two largest cases in Case Studies A and B are tested on a computing cluster that is composed by up to 8 computers with a quad-core 2.8GHz Intel Core processor, 8GB of RAM and 8MB of cache per node: one for the IEEE118-bus power system with 30 scenarios and the other for the 1168-bus power system with 20 scenarios.

For this parallel implementation, all of the single UC and hourly OPF submodules for both the base case and the scenarios are evenly distributed among multiple processors. However, all the bridge submodules are assigned to the head node of the cluster because they all can be solved very quickly by one processor (e.g. less than 1 second per iteration in our tests).

The performance of the parallel implementation has been evaluated using from 1 to 8 nodes of the cluster. First of all, the obtained results are exactly the same as that presented in Case Studies A and B. Figure 3.6- 3.8 show the processing time, the speedup and the efficiency curves with the increasing number of processors, respectively. The processing time of the parallel computing includes the computational time (e.g. the time for the data processing and CPLEX solver), and the communication time (e.g. the time for the job submit and data return) between the head node and computing nodes. The speedup is a ratio of the processing time on a single processor to the processing time using multiple processors. The efficiency is defined as the speedup divided by its number of processors. The following observations can be obtained from Figure. 3.6-3.8:

- The processing time is significantly reduced as the number of processors increases (e.g. the processing time for the case of the 1168-bus power system with

20 scenarios is reduced from 21.96 hours on a single processor to 2.90 hours using 8 processors).

- The speed up curves are almost linear, which indicates that the proposed parallel algorithm is scalable.
- The parallel implementation illustrates an excellent efficiency for both cases; around 94%-99% efficiency using multiple processors.

Therefore, the above observations showed that the processing time can be further reduced when more computer processors are available.

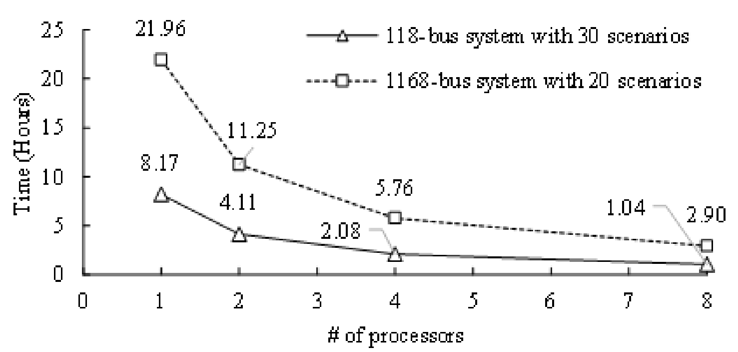

Figure 3.6 Processing time vs. the number of processors

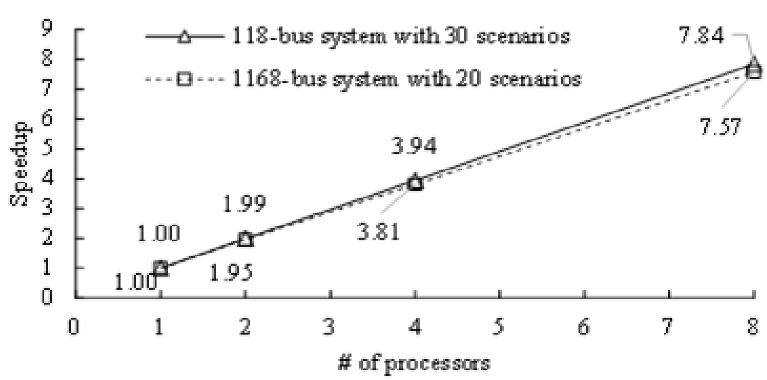

Figure 3.7 Speedup vs. the number of processors

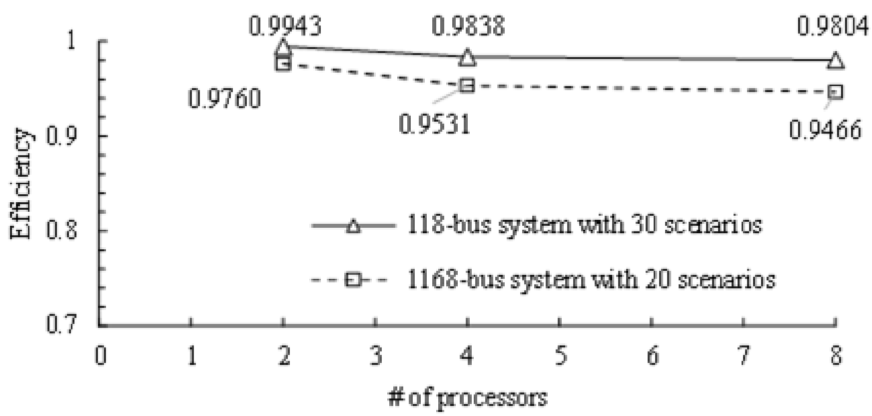

Figure 3.8 Efficiency vs. the number of processors

CHAPTER IV

PARALLEL CO-OPTIMIZATION OF GENERATING UNIT COMMITMENT AND TRANSMISSION SWITCHING WITH POST-CONTINGENCY CORRECTIVE ACTION

Transmission switching is an efficient way to improve the network controllability, which is also adopted to increase the economic benefits of power systems by mitigating the network congestion. The co-optimization of the generating unit commitment and transmission switching is a large-scale and computationally complex optimization problem, which is hard to solve by traditional centralized and/or master-slave based decomposition approaches. This chapter presents a parallel co-optimization approach to obtain an efficient and fast solution for a power system operation with post-contingency corrective actions. Augmented Lagrangian method and auxiliary problem principle are adopted to decompose the original co-optimization problem into three major solution modules: the unit commitment (UC) module, the optimal power flow (OPF) module and the transmission switching (TS) module. These three major function modules make the decision for different optimization problems: the UC module determines the generating unit statues (ON/OFF) and power output level based on the generation constraints; the OPF module decides the power output of each generating units based on the transmission network constraints; the TS module selects the transmission line statues (ON/OFF) in order to mitigate the congestion on the transmission network. In addition, UC module can be further decomposed by generating units, OPF and TS module can be further decomposed by time periods. These three modules can be solved simultaneously, which makes the proposed method favorable for parallelization to consequently improve the computational efficiency. Numerical cases are tested on a distributed computing cluster with 16 computers to justify the effectiveness and efficiency of the proposed approach.

Numerical cases are tested on a distributed computing cluster with 16 computers to justify the effectiveness and efficiency of the proposed approach.

4.1 Introduction

Transmission switching (TS) has been discussed in the past few years as an effective way to increase the controllability of power system operations. From a conventional viewpoint, the network topology was considered static during the normal system operation. Therefore, transmission switching was usually used as corrective actions for system security reasons [83] (e.g. line overloading [84], [85] and voltage stability [86], [87]). Significant contributions have been made by our researchers to improve the system controllability using transmission switching. In order to mitigate the line overloading during contingencies, reference [84] applied a current injection to simulate the change of the transmission topology. In [85], a fast algorithm was developed for selecting and ranking possible circuits for corrective control by network switching to relieve line overloading. In addition to line overloading mitigation, reference [86], [87] proposed methodologies for corrective controls to improve voltage stability during contingencies.

Transmission switching can also improve the economic efficiency of power system operations by mitigating the network congestion, which was introduced in [88].

Inspired by this idea, dispatching transmission lines was extended to re-configure the transmission network topology by switching a set of branches off, which increases the economic benefit in the generation dispatching problem. Reference [89] formulated a mixed integer programming (MIP) problem to find the optimal generation dispatch and transmission topology by employing binary variables to represent the states of switchable transmission lines. Reference [48, 90-92] further analyzed the N-1 reliable DC optimal generation dispatch with transmission switching. Also, [93] proposed a Benders-based optimization framework to solve the TS-based generation dispatch problem with consideration of voltage stability and N-1 reliability test.

In addition to TS-based generation dispatch problem, a co-optimization problem of generating unit commitment and transmission switching was developed in [49]. In this study, authors employed binary variables for both the states of generating units and switchable transmission lines, which leads to a large-scale and computationally complex TS-based SCUC problem. In order to reduce the computational burden, a heuristic decomposition approach was employed in this study, which solved for the transmission switching variables with fixed unit commitment variables, and then solved for the new unit commitment variables with the fixed transmission switching variables, iteratively. In order to improve the computational efficiency of the TS-based SCUC co-optimization, [94] leveraged Benders method to decompose this large-scale TS-based SCUC co-optimization problem into two MIP problems: a unit commitment master problem solves generation scheduling problem; in turn, a TS subproblem handles optimal power flow problem and transmission switching decisions together. Because of the mathematical nature of the TS subproblem with binary variables, this MIP subproblem cannot always generate effective Benders cuts that guarantee a converged solution of the studied TS-based SCUC problem. Furthermore, the overall solution procedure of the above papers [49] and [94] is sequential because the TS problem has to wait for the unit commitment decisions from the UC problem. Because the computationally complex MIP-based problems and the overall sequential solution procedure become the bottlenecks to improve computational efficiency, therefore, a more efficient approach with fully decomposed structure and parallel solution procedure is needed to solve this large-scale TS-based SCUC co-optimization problem.

We further investigate how to effectively incorporate the transmission switching problem into the parallel SCUC. The proposed approach decomposes the entire TS-based SCUC problem into three major solution modules: the UC module that determines the state of generating units; the OPF module that optimizes the power generation of generating units while satisfying the network security constraints for both base case and credible contingencies; and the individual TS module that only determines the state of switchable transmission lines. Moreover, each major module is further decomposed into multiple smaller submodules: the UC module can be decomposed by unit into multiple single UC submodules; the OPF module can be divided by period into multiple hourly OPF for both base case and contingencies; and the TS module can be divided into multiple submodules in terms of switchable transmission lines and studied periods; Secondly, unlike the existing research [48],[49] that only considered the preventive action in the proposed TS study. The proposed parallel co-optimization approach in this study can allow the contingency dispatch represented by both corrective (post-contingency) and preventive (pre-contingency) dispatch control actions; Finally, the proposed parallel solution procedure can fully utilize the parallel computing techniques to improve the computational efficiency, which can be illustrated on our distributed computing cluster composed by 16 computers with a quad-core 3.4GHz Intel Core processor, 16GB of RAM and 8MB of cache per computer.

4.1 Formulations

The TS-based SCUC co-optimization problem can be formulated as a mixed integer programming (MIP) problem. Its objective function is to minimize the total operating cost of the power system, while satisfying the physical constraints of the system. This optimization problem subjects to four groups of constraints: unit commitment constraints group (UC constraints), network security constraints group (OPF constraints) for both base case and contingencies, transmission switching constraints group (TS constraints), and complicating constraints group which is used to link the above three constraints groups. In the following subsections, the variables used in different constraints groups are noted with their corresponding superscript and subscript. The variables in the UC, OPF and TS constraints groups are noted by superscript *uc, opf* and *ts*, respectively; the variables and parameters in the base case and contingency case are noted by subscript *0* and *c*, respectively; and the variables of switchable and non-switchable lines are noted by subscript *S* and *NS.*

4.1.1 Objective function

The objective function of the studied problem is to minimize the total operating cost (4.1),

$$Min \quad F(I, P_0) \tag{4.1}$$

where the binary variables I are the unit commitment decision variables (e.g. On/Off); the power dispatches of generating units in base case are represented by the continuous variables P_0; and the function $F(\cdot)$ represents the generation cost plus startup/shutdown cost of the generating units. The operating cost of the post-contingency generation re-dispatch is not included in the objective function since the feasibility of surviving a contingency, rather than the economic interest, has high priority during the contingency.

4.1.2 Unit commitment constraints

The UC constraints group represents the unit commitment constraints of the generating units under the normal and contingency operating conditions, which include physical generation constraints in the base case (4.2) – (4.4), and the contingency cases (4.5), and the permissible adjustment constraint between base case and contingency cases (4.6).

$$P_{\min} I \le P_0^{uc} \le P_{\max} I \tag{4.2}$$

$$A_0 I \le b_0 \tag{4.3}$$

$$E_0 I + F_0 P_0^{uc} \le h_0 \tag{4.4}$$

$$P_{\min} I \le P_c^{uc} \le P_{\max} I \tag{4.5}$$

$$\left| P_c^{uc} - P_0^{uc} \right| \le \Delta_c \tag{4.6}$$

Constraint (4.2) limits the output of generating units within their capacity, which depends on the states of the generating units. Constraint (4.3) represents a set of constraints which are only relative with commitment variables I (e.g. min ON/OFF limit of generating units). Constraint (4.4) stands for a set of constraints which are related to both power output and commitment variables (e.g. ramping up/down constraints). Constraint (4.5) represents the generation capability limit for the contingency cases. Constraint (4.6) ensures that a generating unit is capable to transfer from its base case operating point to a new operating point when a contingency occurs (corrective action). By setting permissible adjustment limits Δ_c to zero, constraint (4.6) stands for the preventive N-1 security requirement.

4.1.3 Optimal power flow constraints

The OPF constraints group represents the network security, which is composed by the following two groups of constraints: OPF-base and OPF-contingency constraints groups:

4.1.3.1 OPF-base constraints

The OPF-base constraints (4.7)-(4.13) represent the network security constraints in the normal operation.

$$\theta_{\min} \le \theta_0 \le \theta_{\max} \tag{4.7}$$

$$0 \le P_0^{opf} \le P_{\max} \tag{4.8}$$

$$K_0^P P_0^{opf} + K_{0,NS}^L PL_{0,NS}^{opf} + K_{0,S}^L PL_{0,S}^{opf} - K_0^D D = 0 \tag{4.9}$$

$$-PL_{NS}^{\max} \le PL_{0,NS}^{opf} \le PL_{NS}^{\max} \tag{4.10}$$

$$-PL_S^{\max} \le PL_{0,S}^{opf} \le PL_S^{\max} \tag{4.11}$$

$$PL_{0,NS}^{opf} = \left(X_{0,NS}\right)^{-1} \left(K_{0,NS}^L\right)^T \theta_0 \tag{4.12}$$

$$\overline{PL}_{0,S}^{opf} = \left(X_{0,S}\right)^{-1} \left(K_{0,S}^L\right)^T \theta_0 \tag{4.13}$$

where K_0^P, $K_{0,NS}^L$, $K_{0,S}^L$ and K_0^D are incidence matrices for generator to bus, non-switchable line to bus, switchable line to bus, and the load demand to bus, respectively; variables $PL_{0,NS}^{opf}$ and $PL_{0,S}^{opf}$ stand for the "*Actual*" power flow on the non-switchable lines and switchable lines, respectively; $X_{0,NS}$ and $X_{0,S}$ are the line reactance matrix of non-switchable lines and switchable lines, respectively; variable $\overline{PL_{0,S}^{opf}}$ in (4.13) is introduced to define a "*Fictitious*" value for the power flow on a switchable line, which is calculated by the voltage angles of the switchable line's ending points. Constraint (4.7) limits the voltage angle of each bus; constraint (4.8) is unit's generation output limit (noticing the lower bound of the generating unit output is relaxed); constraint (4.9) ensures the Kirchhoff current law at each node in the normal operating case; power flow limits of non-switchable and switchable lines are enforced by constraints (4.10) and (4.11), respectively; constraint (4.12) stands for power flow equations for non-switchable lines; and constraint (4.13) is used to get a "*Fictitious*" power flow value for switchable lines. To be noticed, the equality/inequality relationship between the "*Actual*" power flow $PL_{0,S}^{opf}$ and the "*Fictitious*" power flow $\overline{PL_{0,S}^{opf}}$ for switchable lines is decided by the TS module, which is discussed in the subsection II.D.

4.1.3.2 OPF-contingency constraints

The OPF-contingency constraints group includes the network security constraints in the contingency operation (4.14)–(4.20), in which all parameters, variables, equalities and inequalities are similar to that in the OPF-base constraints group (4.7)-(4.13).

$$\theta_{\min} \le \theta_c \le \theta_{\max} \tag{4.14}$$

$$0 \le P_c^{opf} \le P_{\max} \tag{4.15}$$

$$K_c^P P_c^{opf} + K_{c,NS}^L PL_{c,NS}^{opf} + K_{c,\mathrm{S}}^L PL_{c,S}^{opf} - K_c^D D = 0 \tag{4.16}$$

$$-PL_{NS}^{\max} \le PL_{c,NS}^{opf} \le PL_{NS}^{\max} \tag{4.17}$$

$$-PL_S^{\max} \le PL_{c,S}^{opf} \le PL_S^{\max} \tag{4.18}$$

$$PL_{c,NS}^{opf} = \left(X_{c,NS}\right)^{-1} \left(K_{c,NS}^L\right)^T \theta_c \tag{4.19}$$

$$\overline{PL}_{c,S}^{opf} = \left(X_{c,S}\right)^{-1} \left(K_{c,S}^L\right)^T \theta_c \tag{4.20}$$

4.1.4 Transmission switching constraints

The transmission switching constraints group limits the state of the switchable lines, including base case constraints (4.21), (4.22), and contingency case constraints (4.23), (4.24).

$$-Z \cdot PL_{\max} \le PL_{0,S}^{ts} \le Z \cdot PL_{\max} \tag{4.21}$$

$$-(1-Z)M_0 \le \overline{PL}_{0,S}^{ts} - PL_{0,S}^{ts} \le (1-Z)M_0 \tag{4.22}$$

$$ZPL_{\max} \le PL_{c,S}^{ts} \le ZPL_{\max} \tag{4.23}$$

$$-(1-Z)M_c \le \overline{PL}_{c,S}^{ts} - PL_{c,S}^{ts} \le (1-Z)M_c \tag{4.24}$$

where variable Z represents the state of the switching lines; variables $PL_{0,S}^{ts}$ and $\overline{PL}_{0,S}^{ts}$ stand for the "*Actual*" power flow and the "*Fictitious*" power flow in the TS module, respectively; M_0 and M_c, in (4.22) and (4.24), are often called the "big M" values for base case and contingency cases, respectively. Constraints (4.21) and (4.22) stand for the physical constraints in the normal operating condition. Constraint (4.21) limits the

"*Actual*" power flow of the switchable lines, which depends on the state of the lines. In addition, the relationship between "*Fictitious*" power flow $\overline{PL}_0^{ts}$ and "*Actual*" power flow PL_0^{ts} are defined by (4.22). As a result of these two constraints in the base case, when one switchable line is operating/closed, the binary variable Z is equal to one, and the "*Actual*" power flow of a switchable transmission line $PL_{0,S}^{ts}$ is equal to its "*Fictitious*" value $\overline{PL}_{0,S}^{ts}$, in other words, its power flow meets Kirchhoff voltage law; otherwise, Z is equal to zero, and the "*Actual*" power flow $PL_{0,S}^{ts}$ is equal to zero, which has no matter with the "*Fictitious*" value $\overline{PL}_{0,S}^{ts}$ that is relaxed. Similarly, constraints (4.23) and (4.24) are employed to represent the physical constraints of transmission switching under contingency conditions.

4.1.5 Complicating constraints

In order to secure the equal value of the complicating variables in the above constraints groups (including P_0^{uc} and P_0^{opf}, P_c^{uc} and P_c^{opf}, $PL_{0,S}^{opf}$ and $PL_{0,S}^{ts}$, $\overline{PL}_{0,S}^{opf}$ and $\overline{PL}_{0,S}^{ts}$, $PL_{c,S}^{opf}$ and $PL_{c,S}^{ts}$, $\overline{PL}_{c,S}^{opf}$ and $\overline{PL}_{c,S}^{ts}$), the complicating constraints (4.25)–(4.27) are introduced as follows,

$$P_0^{uc} = P_0^{opf},\ P_c^{uc} = P_c^{opf} \tag{4.25}$$

$$PL_{0,S}^{opf} = PL_{0,S}^{ts},\ \overline{PL}_{0,S}^{opf} = \overline{PL}_{0,S}^{ts} \tag{4.26}$$

$$PL_{c,S}^{opf} = PL_{c,S}^{ts},\ \overline{PL}_{c,S}^{opf} = \overline{PL}_{c,S}^{ts} \tag{4.27}$$

Constraint (4.25) ensures the equality of the complicating variables between UC and OPF module for base case and contingency cases. Constraints (4.26)–(4.27) are the complicating constraints between OPF and TS modules, which ensure the physical relationship between the "*Actual*" power flow ($PL_{0,S}^{opf}$, $PL_{0,S}^{ts}$, $PL_{c,S}^{opf}$, and $PL_{c,S}^{ts}$) and the "*Fictitious*" power flow ($\overline{PL}_{0,S}^{ts}$, $\overline{PL}_{0,S}^{opf}$, $\overline{PL}_{c,S}^{ts}$, and $\overline{PL}_{c,S}^{opf}$) in the base case and contingency cases. For example, in the base case, the physical relationship between the "*Actual*" power flow ($PL_{0,S}^{opf}$ and $PL_{0,S}^{ts}$) and the "*Fictitious*" power flow ($\overline{PL}_{0,S}^{ts}$ and $\overline{PL}_{0,S}^{opf}$) for a switchable line is ensured by a combination of constraints (4.13), (4.21), (4.22), and (4.26). When a switchable line is operating/closed, Z is equal to one in the TS module. Because of constraints (4.21) and (4.22) in the TS module, the "*Actual*" power flow of a switchable transmission line $PL_{0,S}^{ts}$ is equal to its "*Fictitious*" value $\overline{PL}_{0,S}^{ts}$; with the help of constraints (4.13) and (4.26), we can get

$$PL_{0,S}^{opf} = PL_{0,S}^{ts} = \overline{PL}_{0,S}^{ts} = \overline{PL}_{0,S}^{opf} = \left(X_{0,S}\right)^{-1}\left(K_{0,S}^{L}\right)^{T}\theta_0 \tag{4.28}$$

On the other hand, when a switchable line is disconnected/opened, Z is equal to zero. As a result of constraints (4.21) and (4.22) in the TS module, the "*Actual*" power flow $PL_{0,S}^{ts}$ is equal to zero, which is no matter with the "*Fictitious*" power flow $\overline{PL}_{0,S}^{ts}$. In addition, based on the constraint (4.26), we can get the "*Actual*" power flow from both OPF and TS modules are equal, $PL_{0,S}^{opf} = PL_{0,S}^{ts} = 0$. Similarly, the corresponding physical relationship in the contingency cases are ensured by constraints (4.20), (4.23), (4.24) and (4.27).

4.2 Parallel decomposition and solution strategies

In this section, a decomposition strategy is presented to decompose the original TS-based SCUC co-optimization problem into three independent solution modules solved in a parallel manner: UC module, OPF module and TS module.

4.2.1 Relax complicating constraints

In this section, augmented Lagrangian relaxation method is adopted to decompose coupling constraints (4.25)-(4.27) by adding the first-order and the second-order penalty functions into the objective function (4.1). Accordingly, the objective function of corresponding Lagrangian relaxation problem is written as,

$$
\begin{aligned}
Min \quad & F(I, P_0^{uc}) + \lambda_0^P (P_0^{uc} - P_0^{opf}) + \frac{c_0^P}{2} \left\| P_0^{uc} - P_0^{opf} \right\|^2 \\
& + \lambda_0^{PL} (PL_{0,S}^{opf} - PL_{0,S}^{ts}) + \frac{c_0^{PL}}{2} \left\| PL_{0,S}^{opf} - PL_{0,S}^{ts} \right\|^2 \\
& + \lambda_0^{\overline{PL}} (\overline{PL}_{0,S}^{opf} - \overline{PL}_{0,S}^{ts}) + \frac{c_0^{\overline{PL}}}{2} \left\| \overline{PL}_{0,S}^{opf} - \overline{PL}_{0,S}^{ts} \right\|^2 \\
& + \sum_c \left(\lambda_c^P (P_c^{uc} - P_c^{opf}) + \frac{c_c^P}{2} \left\| P_c^{uc} - P_c^{opf} \right\|^2 \right) \\
& + \sum_c \left(\lambda_c^{PL} (PL_{c,S}^{opf} - PL_{c,S}^{ts}) + \frac{c_c^{PL}}{2} \left\| PL_{c,S}^{opf} - PL_{c,S}^{ts} \right\|^2 \right) \\
& + \sum_c \left(\lambda_c^{\overline{PL}} (\overline{PL}_{c,S}^{opf} - \overline{PL}_{c,S}^{ts}) + \frac{c_c^{\overline{PL}}}{2} \left\| \overline{PL}_{c,S}^{opf} - \overline{PL}_{c,S}^{ts} \right\|^2 \right)
\end{aligned}
\tag{4.29}
$$

where the first term is the operating cost and the other terms are the penalty functions of relaxed coupling constraints (4.25)-(4.27). λ (including λ_0^P, λ_0^{PL}, $\lambda_0^{\overline{PL}}$, λ_c^P, λ_c^{PL}, and $\lambda_c^{\overline{PL}}$) and c (including c_0^P, c_0^{PL}, $c_0^{\overline{PL}}$, c_c^P, c_c^{PL}, and $c_c^{\overline{PL}}$) are the first-order and second-order Lagrangian multipliers associated with coupling constraints, respectively.

4.2.2 Decompose objective function

After relaxing coupling constraints by penalty multipliers, the remaining constraints (4.2)-(4.24) become separable and decomposable. To remove coupling terms (the product of variables) from the objective function, APP method [74] is applied to replace (4.29) with its auxiliary problem (4.30) (see Appendix for the detailed derivation), in which the coupling terms are substituted by independent terms with the help of iterative results from the previous iteration *k-1*.

$$
\begin{aligned}
Min \quad & F(I, P_0^{uc}) + \begin{bmatrix} \lambda_0^P (P_0^{uc} - P_0^{opf}) + c_0^P \left((P_0^{uc})^2 + (P_0^{opf})^2 \right) \\ -c_0^P (P_0^{uc,(k-1)} + P_0^{opf,(k-1)})(P_0^{uc} + P_0^{opf}) \end{bmatrix} \\
& + \begin{bmatrix} \lambda_0^{PL} (PL_{0,S}^{opf} - PL_{0,S}^{ts}) + c_0^{PL} \left((PL_{0,S}^{opf})^2 + (PL_{0,S}^{ts})^2 \right) \\ -c_0^{PL} (PL_{0,S}^{opf,(k-1)} + PL_{0,S}^{ts,(k-1)})(PL_{0,S}^{opf} + PL_{0,S}^{ts}) \end{bmatrix} \\
& + \begin{bmatrix} \lambda_0^{\overline{PL}} (\overline{PL}_{0,S}^{opf} - \overline{PL}_{0,S}^{ts}) + c_0^{\overline{PL}} \left((\overline{PL}_{0,S}^{opf})^2 + (\overline{PL}_{0,S}^{ts})^2 \right) \\ -c_0^{\overline{PL}} (\overline{PL}_{0,S}^{opf,(k-1)} + \overline{PL}_{0,S}^{ts,(k-1)})(\overline{PL}_{0,S}^{opf} + \overline{PL}_{0,S}^{ts}) \end{bmatrix} \\
& + \sum_c \begin{bmatrix} \lambda_c^P (P_c^{uc} - P_c^{opf}) + c_c^P \left((P_c^{uc})^2 + (P_c^{opf})^2 \right) \\ -c_c^P (P_c^{uc,(k-1)} + P_c^{opf,(k-1)})(P_c^{uc} + P_c^{opf}) \end{bmatrix} \\
& + \sum_c \begin{bmatrix} \lambda_c^{PL} (PL_{c,S}^{opf} - PL_{c,S}^{ts}) + c_c^{PL} \left((PL_{c,S}^{opf})^2 + (PL_{c,S}^{ts})^2 \right) \\ -c_c^{PL} (PL_{c,S}^{opf,(k-1)} + PL_{c,S}^{ts,(k-1)})(PL_{c,S}^{opf} + PL_{c,S}^{ts}) \end{bmatrix} \\
& + \sum_c \begin{bmatrix} \lambda_c^{\overline{PL}} (\overline{PL}_{c,S}^{opf} - \overline{PL}_{c,S}^{ts}) + c_c^{\overline{PL}} \left((\overline{PL}_{c,S}^{opf})^2 + (\overline{PL}_{c,S}^{ts})^2 \right) \\ -c_c^{\overline{PL}} (\overline{PL}_{c,S}^{opf,(k-1)} + \overline{PL}_{c,S}^{ts,(k-1)})(\overline{PL}_{c,S}^{opf} + \overline{PL}_{c,S}^{ts}) \end{bmatrix}
\end{aligned} \tag{4.30}
$$

4.2.3 Formulate independent solution modules

By associating decoupled objective functions (4.30) with their individual constraints groups, the original TS-based SCUC co-optimization problem is divided into submodules as shown in the Figure 4.1.

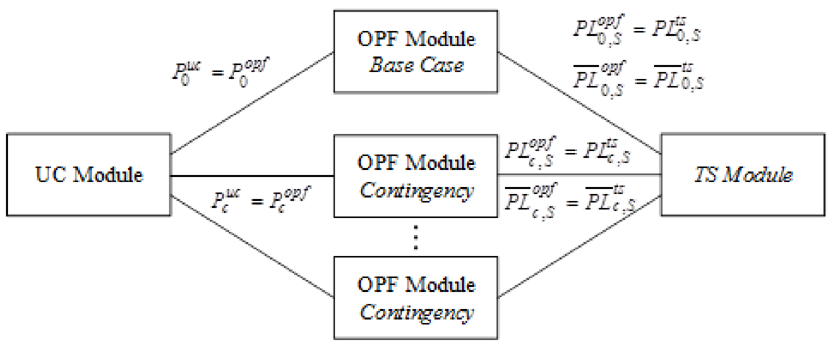

Figure 4.1 Decomposed Modules of TS-based SCUC

4.2.3.1 UC module

The UC module is a mixed integer quadratic programming (MIQP) problem, which determines the state and dispatch of generating units. This module is composed by the objective function (4.31), and unit commitment constraints group (4.2)-(4.6). Apparently, the UC module can be further decomposed into multiple single UC submodules, since there are no coupling relationships among generating units in this UC module.

$$\begin{aligned} Min \quad & F(I, P_0^{uc}) + \left(c_0^P + \sum_c c_{0,c}^P \right)(P_0^{uc})^2 + \sum_c c_c^P (P_c^{uc})^2 \\ & + \left(\lambda_0^P - c_0^P (P_0^{uc,(k-1)} + P_0^{opf,(k-1)}) \right) P_0^{uc} \\ & + \sum_c \left[\left(\lambda_c^P - c_c^P (P_c^{uc,(k-1)} + P_c^{opf,(k-1)}) \right) P_c^{uc} \right] \end{aligned} \tag{4.31}$$

4.2.3.2 OPF modules

The OPF module is a quadratic programming problem without any mixed integer variables, including OPF-base module and OPF-contingency module to optimize the decomposed objective functions under network security constraints in the normal operation and the possible contingency states, respectively.

4.2.3.2.1 OPF-base module

The OPF-base module is composed by the objective function (4.32) and OPF-base constraints group (4.7)-(4.13). As all the constraints in the OPF module can be separated for single period study, this module can be further divided into multiple single-hour OPF submodules.

$$
\begin{aligned}
Min \quad & c_0^P (P_0^{opf})^2 + c_{0,S}^{PL} (PL_{0,S}^{opf})^2 + c_{0,S}^{\overline{PL}} (\overline{PL}_{0,S}^{opf})^2 \\
& + \left(-\lambda_0^P - c_0^P (P_0^{uc,(k-1)} + P_0^{opf,(k-1)}) \right) P_0^{opf} \\
& + \left(\lambda_{0,S}^{PL} - c_{0,S}^{PL} (PL_{0,S}^{opf,(k-1)} + PL_{0,S}^{ts,(k-1)}) \right) PL_{0,S}^{opf} \\
& + \left(\lambda_{0,S}^{\overline{PL}} - c_{0,S}^{\overline{PL}} (\overline{PL}_{0,S}^{opf,(k-1)} + \overline{PL}_{0,S}^{ts,(k-1)}) \right) \overline{PL}_{0,S}^{opf}
\end{aligned}
\tag{4.32}
$$

4.2.3.2.2 OPF-contingency module

Similarly, the OPF-contingency module optimizes decomposed objective functions under possible contingency states. This module is composed by the objective function (4.33) and OPF-contingency constraints group (4.14)-(4.20), which can be further divided into multiple single-hour OPF submodules.

$$
Min \sum_c \begin{bmatrix}
c_c^P (P_c^{opf})^2 + c_{c,S}^{PL} (PL_{c,S}^{opf})^2 + c_{c,S}^{\overline{PL}} (\overline{PL}_{c,S}^{opf})^2 \\
+ \left(-\lambda_c^P - c_c^P (P_c^{uc,(k-1)} + P_c^{opf,(k-1)}) \right) P_c^{opf} \\
+ \left(\lambda_{c,S}^{PL} - c_{c,S}^{PL} (PL_{c,S}^{opf,(k-1)} + PL_{c,S}^{ts,(k-1)}) \right) PL_{c,S}^{opf} \\
+ \left(\lambda_{c,S}^{\overline{PL}} - c_{c,S}^{\overline{PL}} (\overline{PL}_{c,S}^{opf,(k-1)} + \overline{PL}_{c,S}^{ts,(k-1)}) \right) \overline{PL}_{c,S}^{opf}
\end{bmatrix}
\tag{4.33}
$$

4.2.3.3 TS module

The TS module, a mixed integer quadratic programming (MIQP) problem, decides the state of switchable transmission lines. This module consists of the objective function (4.34) and TS constraint group (4.21)-(4.24). The TS module can be further separated into multiple single line single period TS submodules, which will make it more favorable to be adopted in the parallel computing implementation.

$$
\begin{aligned}
Min \quad & \left(c_{0,S}^{PL} + \sum_{c} c_{0,c,S}^{PL}\right)(PL_{0,S}^{ts})^2 + c_{0,S}^{\overline{PL}}(\overline{PL}_{0,S}^{ts})^2 \\
& + \left(-\lambda_{0,S}^{PL} - c_{0,S}^{PL}(PL_{0,S}^{opf,(k-1)} + PL_{0,S}^{ts,(k-1)})\right) PL_{0,S}^{ts} \\
& + \left(-\lambda_{0,S}^{\overline{PL}} - c_{0,S}^{\overline{PL}}(\overline{PL}_{0,S}^{opf,(k-1)} + \overline{PL}_{0,S}^{ts,(k-1)})\right) \overline{PL}_{0,S}^{ts} \\
& + \sum_{c} \begin{bmatrix} c_{c,S}^{PL}(PL_{c,S}^{ts})^2 + c_{c,S}^{\overline{PL}}(\overline{PL}_{c,S}^{ts})^2 \\ + \left(-\lambda_{c,S}^{PL} - c_{c,S}^{PL}(PL_{c,S}^{opf,(k-1)} + PL_{c,S}^{ts,(k-1)})\right) PL_{c,S}^{ts} \\ + \left(-\lambda_{c,S}^{\overline{PL}} - c_{c,S}^{\overline{PL}}(\overline{PL}_{c,S}^{opf,(k-1)} + \overline{PL}_{c,S}^{ts,(k-1)})\right) \overline{PL}_{c,S}^{ts} \end{bmatrix}
\end{aligned}
\tag{4.34}
$$

Finally, a fully decomposed structure of the studied TS-based SCUC co-optimization problem is illustrated in Figure 4.2. By adopting the proposed decomposition strategy, the original large-scale TS-based SCUC problem is divided into numbers of small-size submodules that can be simultaneously solved by using ILOG CPLEX 12.6's solvers.

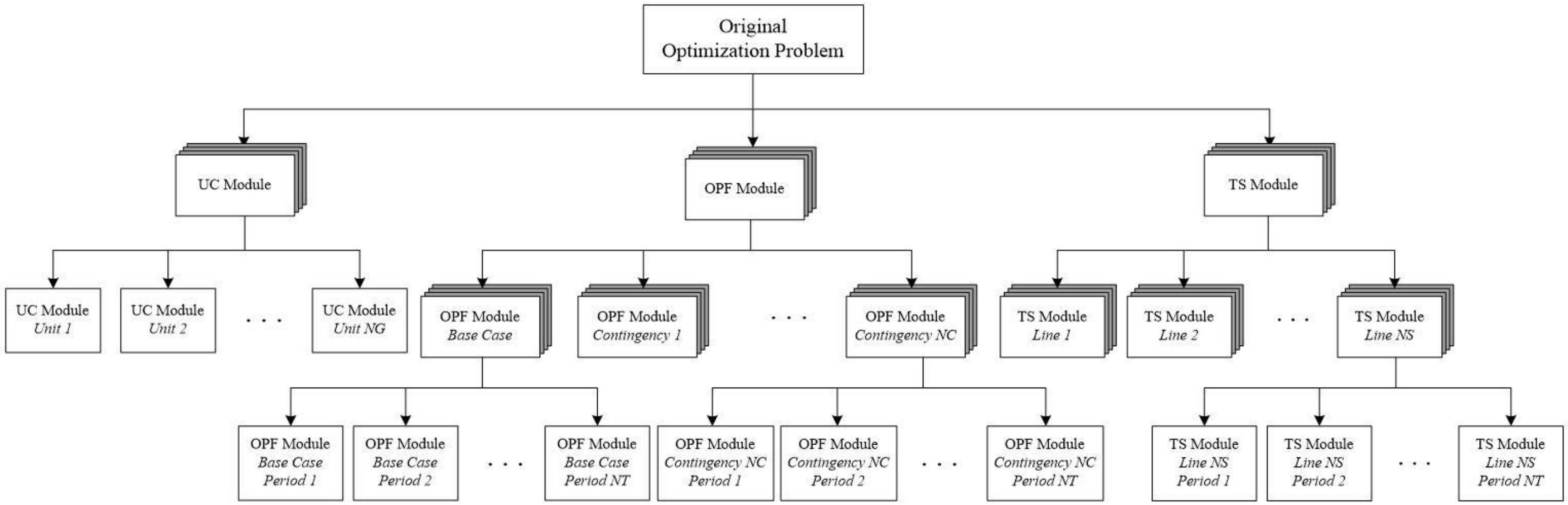

Figure 4.2 Decomposition Structure

4.3 Parallel solution procedure

A parallel solution procedure, as shown in Figure 4.3, is discussed as below:

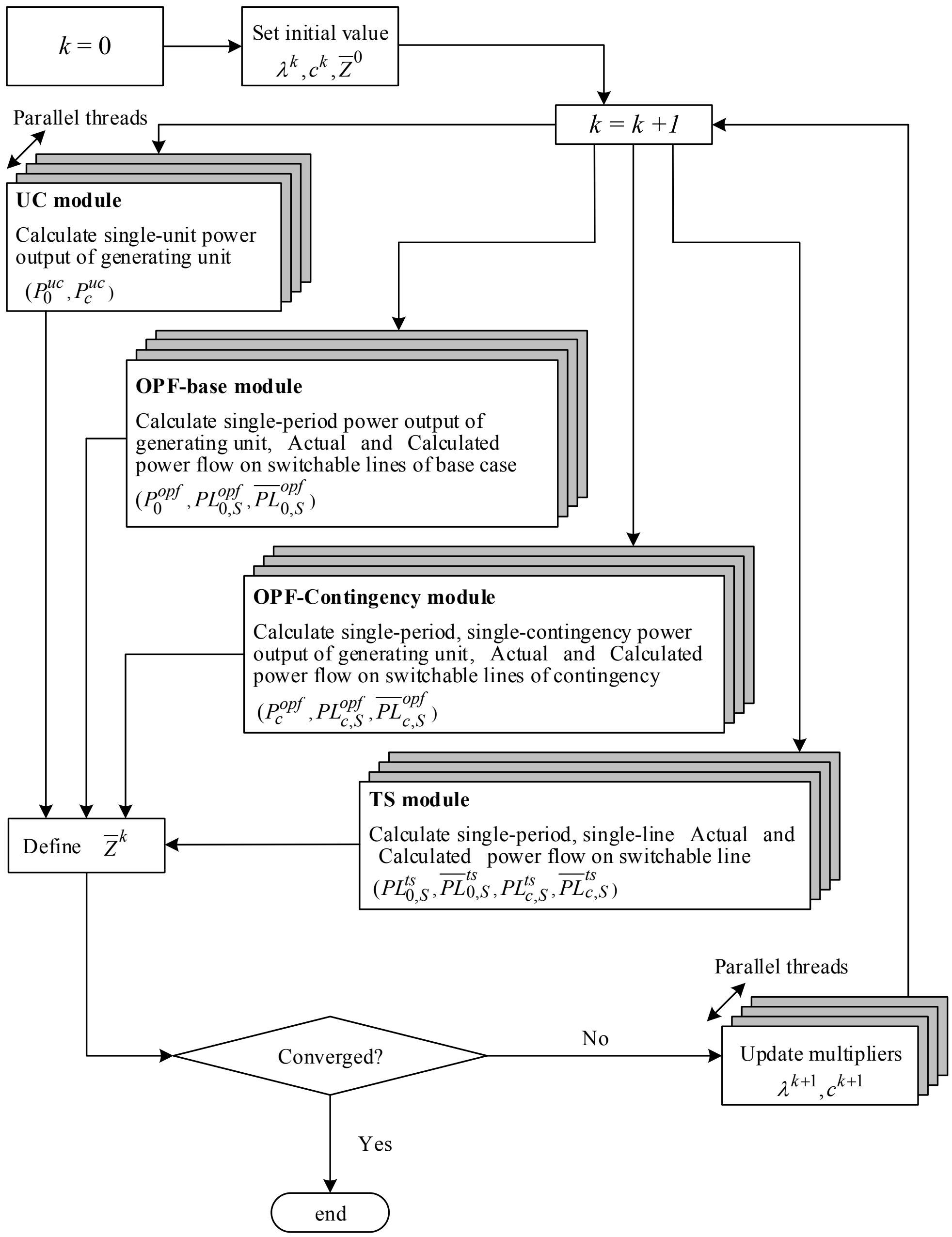

Figure 4.3 Solution flow chart

- <u>*Step 1*</u>: Set the iteration index *k=1*, and choose initial values for all the variables $\bar{z}^0$ (including P_0^{uc} , P_c^{uc} , P_0^{opf} , $PL_{0,S}^{opf}$, $\overline{PL}_{0,S}^{opf}$, P_c^{opf} , $PL_{c,S}^{opf}$, $\overline{PL}_{c,S}^{opf}$, $PL_{0,S}^{ts}$, $\overline{PL}_{0,S}^{ts}$, $PL_{c,S}^{ts}$, and $\overline{PL}_{c,S}^{ts}$), the Lagrangian multipliers λ and c .

- <u>*Step 2*</u>: Solve single unit UC submodules, single period OPF-base submodules, single period single contingency OPF-contingency submodule, and single line single period TS submodules in parallel. Collect optimal results from each individual submodule, to obtain $\bar{z}^k$ for the current iteration *k*.

- <u>*Step 3*</u>: Check the following stopping criteria (4.35)-(4.37), where ε_1 is the convergence threshold for the mismatch of complicating variables between outer loops; ε_2 is the convergence threshold for the mismatch between each couple of complicating variables; and ε_3 is the convergence threshold for the cost difference between two successive iterations (where $L(\cdot)$ is the optimal result of (4.29)). If all of them are satisfied, then stop and set the optimal value $\bar{z}^*$ equal to $\bar{z}^k$ and stop; otherwise, go to Step 4.

$$\left\| \bar{z}^k - \bar{z}^{k-1} \right\| \le \varepsilon_1 \tag{4.35}$$

$$\left\{ \begin{array}{l} \left\| P_0^{uc,k} - P_0^{opf,k} \right\|, \left\| PL_{0,S}^{opf,k} - PL_{0,S}^{ts,k} \right\|, \\ \left\| \overline{PL}_{0,S}^{opf,k} - \overline{PL}_{0,S}^{ts,k} \right\|, \left\| P_c^{uc,k} - P_c^{opf,k} \right\|, \\ \left\| PL_{c,S}^{opf,k} - PL_{c,S}^{ts,k} \right\|, \left\| \overline{PL}_{c,S}^{opf,k} - \overline{PL}_{c,S}^{ts,k} \right\| \end{array} \right\} \le \varepsilon_2 \tag{4.36}$$

$$\left| \frac{L(\bar{z}^k) - L(\bar{z}^{k-1})}{L(\bar{z}^k)} \right| \le \varepsilon_3 \tag{4.37}$$

- <u>Step 4</u>: Update Lagrangian multipliers using (4.38) and (4.39), set $k = k+1$, and go to Step 2.

$$\begin{aligned}
\lambda_0^{P,k+1} &= \lambda_0^{P,k} + c_0^{P,k}(P_0^{uc,k} - P_0^{opf,k}) \\
\lambda_0^{PL,k+1} &= \lambda_0^{PL,k} + c_0^{PL,k}(PL_0^{uc,k} - PL_0^{opf,k}) \\
\lambda_0^{\overline{PL},k+1} &= \lambda_0^{\overline{PL},k} + c_0^{\overline{PL},k}(\overline{PL_0}^{uc,k} - \overline{PL_0}^{opf,k}) \\
\lambda_c^{P,k+1} &= \lambda_c^{P,k} + c_c^{P,k}(P_c^{uc,k} - P_c^{opf,k}) \\
\lambda_c^{PL,k+1} &= \lambda_c^{PL,k} + c_c^{PL,k}(PL_c^{uc,k} - PL_c^{opf,k}) \\
\lambda_c^{\overline{PL},k+1} &= \lambda_c^{\overline{PL},k} + c_c^{\overline{PL},k}(\overline{PL_c}^{uc,k} - \overline{PL_c}^{opf,k})
\end{aligned} \tag{4.38}$$

$$\begin{aligned}
c_0^{P,k+1} &= \beta c_0^{P,k} \\
c_0^{PL,k+1} &= \beta c_0^{PL,k} \\
c_0^{\overline{PL},k+1} &= \beta c_0^{\overline{PL},k} \\
c_c^{P,k+1} &= \beta c_c^{P,k} \\
c_c^{PL,k+1} &= \beta c_c^{PL,k} \\
c_c^{\overline{PL},k+1} &= \beta c_c^{\overline{PL},k}
\end{aligned} \tag{4.39}$$

where the coefficient β is set to be equal or larger than one in order to obtain a converged optimal result. The success of the proposed Lagrangian relaxation based method depends on the ability of the algorithm to drive Lagrangian multipliers to the value of multipliers associated with complicating constraints at the optimal solution. With the combination of convergence criteria (4.35)-(4.37) and multipliers updating process (4.38)-(4.39), it has been proven to converge to the optimal solution of the original optimization problem when the problem is convex. Although there is a convergence proof of the APP algorithm for convex optimization problems[37], there is no direct proof for a non-convex MIP problem, which is modeled in this chapter. However, for this non-convex optimization problem, the non-convexity can be mitigated by the augmented Lagrangian method. Quadratic penalty terms are added to the Lagrangian objective function as a local convexifier to improve the convexity of the problem [53]. In addition, according to our experiments/testing experiences, we would like to mention that the effectiveness of the used APP algorithm on the studied non-convex stochastic SCUC problem is satisfactory and acceptable, which can be supported by the following case studies.

4.4 Numerical study

In order to illustrate the performance of the proposed parallel approach, a modified IEEE 118-bus power system [28] consisting of 54 generating units, 186 branches, 91 demand sides, 10 switchable transmission lines (e.g. line 1, 8, 21, 22, 36, 37, 39, 128, 153, and 181) and up to 20 contingencies is studied in this section. The specific parameters and convergence thresholds are set as the same in all case studies, in which the penalty multipliers are set as $\lambda^0 = 0$, $c^0 = 0.01$ for all penalty functions, the updating parameters for the second order multipliers is $\beta = 1.01$, and the convergence thresholds are set as $\varepsilon_1 = 0.2MW$ (4.35), $\varepsilon_2 = 0.2MW$ (4.36), and $\varepsilon_3 = 0.01\%$ (4.37). In addition, the proposed algorithm is implemented on a parallel computing cluster with 16 computing nodes with a quad-core 3.4GHz Intel Core Processor, 16GB of RAM and 8MB of cache per node to test the computational efficiency.

4.4.1 Case A: Single-hour case without contingency

In this case, a single hour TS-based SCUC without any contingency is adopted to demonstrate the convergence performance of complicating constraints (4.25)-(4.27). The converged result is obtained in 125 iterations with the operating cost of $91,674.5, which is same as the centralized result $91,674.5. Because of the absence of contingencies, there are three modules cooperating with each other in this case study, which are UC module, OPF-base module, and TS module. These three modules coordinate with each other by 74 complicating constraints, including 54 complicating constraints (4.25) coordinating the UC module and the OPF-base module for the power outputs of the generating units, and 20 complicating constraints (4.26) coordinating the OPF-base module and the TS module for both the "*Actual*" and "*Fictitious*" power flows on the switchable transmission lines.

To focus on the transmission line switching study, the switchable transmission line 37 and line 21 are selected to show the convergence performance of the complicating constraint (4.26) in Figure 4.4. In the convergence curves of the switchable transmission line 37, as shown in Figure 4.4 (a), the state of this switchable transmission line is always connected during the iterative procedure. Although there are a disturbance occurring at the 79th iteration, all the values of "*Actual*" and "*Fictitious*" power flow in the OPF-base module and the TS module ($PL_{0,S}^{opf}$, $PL_{0,S}^{ts}$, $\overline{PL}_{0,S}^{ts}$ and $\overline{PL}_{0,S}^{opf}$) try to follow each due to the penalties, and finally converge at -120.04MW. In the convergence curve of "*Actual*" and "*Fictitious*" power flows of line 21, as shown in Figure 4.4 (b), the line 21 is initially connected in the first 71 iterations. As a result of the constraints (4.13), (4.21), (4.22) and (4.26), the values of "*Actual*" and "*Fictitious*" power flows in the OPF-base module and the TS module ($PL_{0,S}^{opf}$, $PL_{0,S}^{ts}$, $\overline{PL}_{0,S}^{opf}$ and $\overline{PL}_{0,S}^{ts}$) are very close to each other at around -180MW. However, according to the updated penalty functions, the state of this switchable line changes at 72th iteration, the value of its "*Actual*" power flow in the TS module, $PL_{0,S}^{ts}$ becomes to zero immediately due to the constraint (4.21). After oscillation in the following several iterations, the “Actual” power flow $PL_{0,S}^{opf}$ in the OPF-base module is also converged to zero. However, because of the constraint (4.22) when the line is disconnected, the value of its “Fictitious” power flow $\overline{PL}_{0,S}^{ts}$ and $\overline{PL}_{0,S}^{opf}$ are relaxed, and get converged after several iterations at a new value of -468.80MW. In addition, the convergence curve of switchable transmission line 22 is shown in Figure 4.4 (c). Initially, this switchable transmission line is disconnected after first several iterations. At 55th iteration, the “*Actual*” and “*Calculated*” power flow in the OPF-base module ($PL_{0,S}^{opf}$ and $\overline{PL}_{0,S}^{opf}$) are almost converged at zero, and which in the TS module ($PL_{0,S}^{ts}$ and $\overline{PL}_{0,S}^{ts}$) the “*Calculated*” power flow are -78.33MW. However, as a result of updated penalty parameter, the mismatch between “*Actual*” power flow $PL_{0,S}^{opf}$ and $PL_{0,S}^{ts}$ increases after the 55th iteration, and finally the state of this line changes to “connected” at the 74th and 75th iterations. As a result, the “*Calculated*” power flow $\overline{PL}_{0,S}^{opf}$ and $\overline{PL}_{0,S}^{ts}$ are equal to each other due to the constraint (4.22); consequently, the “*Actual*” power flow $PL_{0,S}^{opf}$ and $PL_{0,S}^{ts}$ change dramatically according to the updated penalty functions. However, after that, the state changes back to “disconnected” at 77th iteration, which lead to another convergence after several iterations.

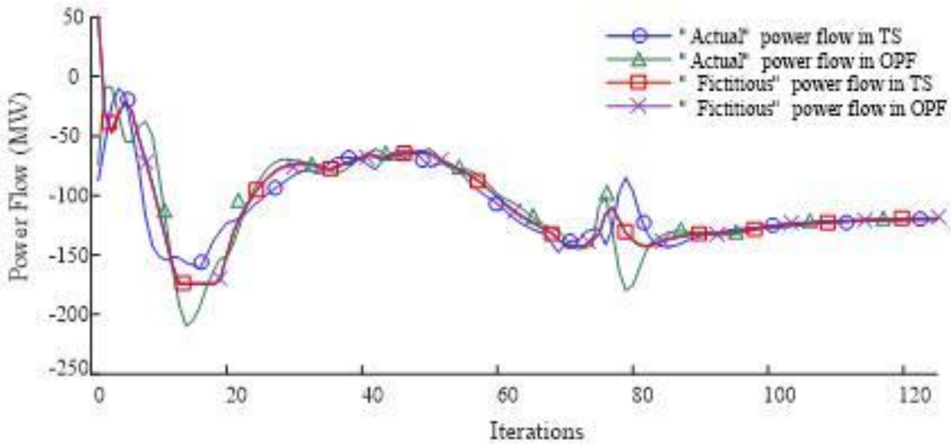

(a) In switchable transmission line 37

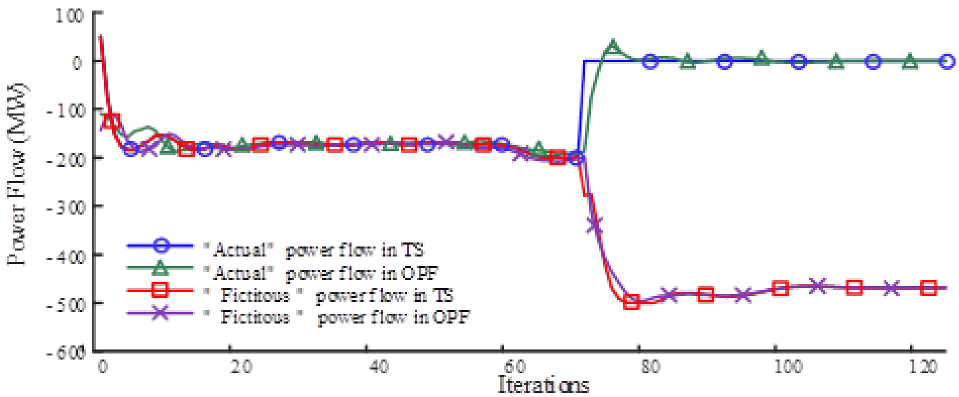

(b) In switchable transmission line 21

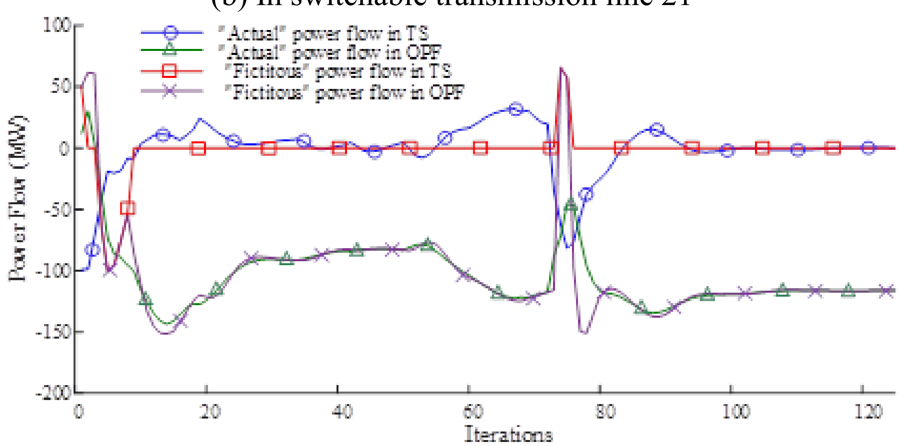

(c) In switchable transmission line 22

Figure 4.4 Convergence performance of "*Actual*" and "*Fictitious*" power flows

4.4.2 Case B: Contingency case with up to 20 contingencies

In order to further examine the performance of the proposed approach with contingencies, a 24-hour case with up to 20 contingencies is studied. The comparisons of the total operating cost and the computational time between the proposed parallel method on 16 computing nodes and the centralized method are listed in Table 4.1. As we can see, a converged parallel result ($1,705,801) for the base case is obtained after 353 iterations, which is very close to the result ($1,703,492) of conventional centralized MIP model (only 0.14% more). Noticing that this testing case is too small to benefit from parallelization in terms of the calculation time, but is used to verify the solution quality by comparing a proven centralized result to our parallel method. With the increase of number of contingencies, the CPU time consumption of the centralized method is 4,682.5 seconds for 5 contingencies (because of the size of this co-optimization problem and the limitation of computing hardware, only up to 5 contingencies can be tested by the centralized method). However, using the proposed parallel method, we can obtain the results for all the cases having up to 20 contingencies. As an example, before the decomposition, the original TS-based SCUC problem with 20 contingencies is composed by 197,904 variables (including 1,536 binary variables and 196,368 continuous variables) and 684,144 constraints (including 37,296 complicating constraints). By adopting the proposed decomposition method, the original co-optimization problem is divided into UC module, OPF-base/OPF-Contingency module, and TS module. Furthermore, these three major modules are decomposed into 54 single UC submodules (with 552 variables and 2,112 constraints per submodule), 24 single hour OPF-base submodules (with 314 variables and 1,020 constraints per submodule), 480 single hour OPF-contingency submodules (with 313 variables and 1,017 constraints per submodule), and 240 single hour and single line TS submodules (with 43 variables and 84 constraints per submodule), respectively. All scalable submodules can be solved within a less computational time (e.g. around 0.0048-0.12 seconds). Table 4.2 shows the subproblem distributions among 16 computing nodes, in which the average computational time of each CPU is very close to each other.

Figure 4.5 further shows the convergence performance of the proposed method for the cases with 0, 5, 10, 15 and 20 contingencies. For example, in the test case with 20 contingencies, 35,188 out of 37,296 (94.35% within threshold) are converged at 200 iterations (as shown in the zoomed figure of Figure 4.5), and 157 more iterations are needed to find the final converged result (100% within threshold).

Table 4.1 Results of multi-hour case with up to 20 Contingencies in Case B

# of Ctgc.	**Centralized**		**Parallel (16 CPUs)**		
	Time (sec.)	**Cost ($)**	**Time (sec.)**	**Cost ($)**	**# of Iter**
0	45.8	1,703,492	1,001.1	1,705,801	353
5	4,682.5	1,713,140	1,403.2	1,722,074	395
10	N/A	N/A	1,689.5	1,728,229	388
15	N/A	N/A	1,851.6	1,732,421	356
20	N/A	N/A	2,165.1	1,739,823	357

Table 4.2 Subproblem distribution among CPUs in case B

CPU NO.	Single UC subproblem	Single hour OPF-base subproblem	Single hour single contingency OPF-ctgc subproblem	Single hour single line TS subproblem	Cplex Time per iteration
1 - 6	4	1	19	14	0.6429
7 - 8	3	1	19	38	0.6434
9 - 16	3	2	41	10	0.6433

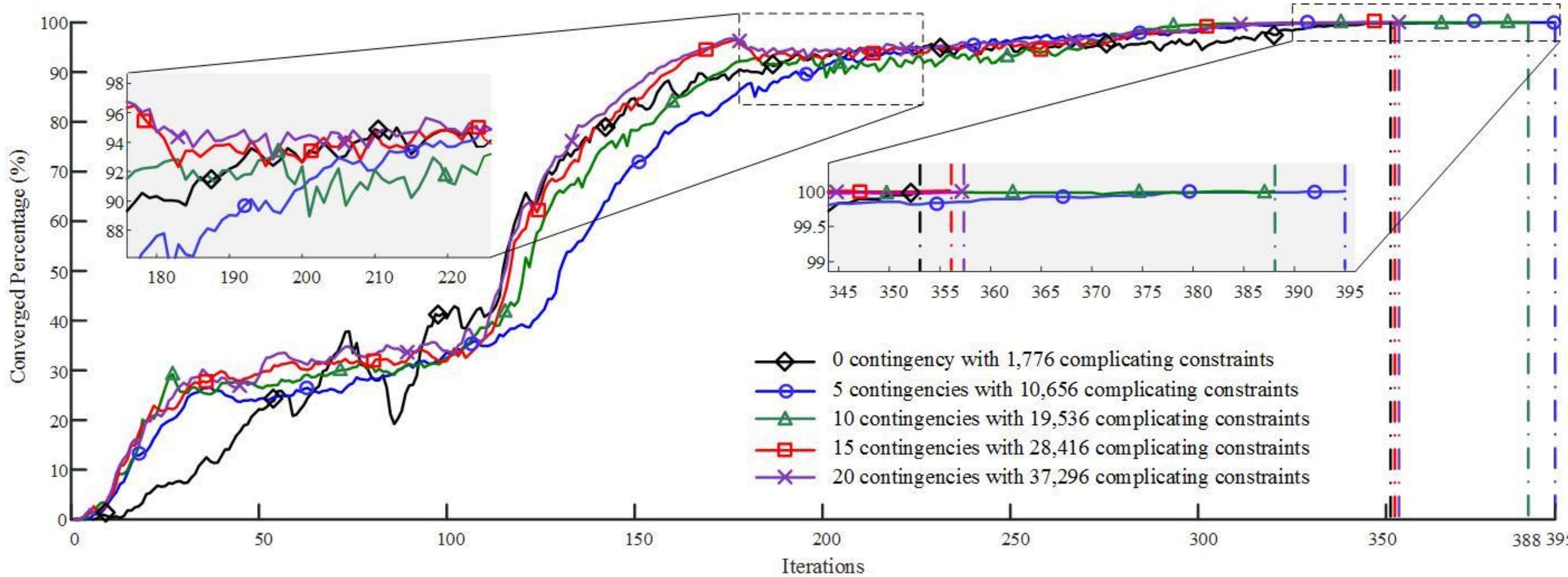

Figure 4.5 Percentage of satisfied complicating constraints

CHAPTER V

CONCLUSION AND FUTURE WORK

5.1 Conclusions

In this dissertation, several decomposition methods are developed to model and solve the modern power system operations problem. The proposed methods are implemented and justified in the high performance environment.

In Chapter 2, the mathematical decomposition methods and high performance environment have been introduced. In this chapter, we introduced the concepts, theories and applications of various optimization algorithm, including augmented Lagrangian method, alternating direction method of multipliers, diagonalization quadratic approximation method, and auxiliary problem principle. The convergence issues of these optimization algorithms have been discussed.

In Chapter 3, a fully parallel stochastic SCUC approach was presented, which can be utilized to quickly implement a generation scheduling of a large-scale power system with uncertainties. The test cases on a modified IEEE 118-bus system and a practical 1168-bus system showed the effectiveness of the proposed approach. With the application of variables duplication and APP techniques, the original stochastic SCUC problem was divided into multiple single UC modules and hourly OPF modules, which are connected by bridge modules. All of the decomposed modules can be simultaneously solved to improve the computational efficiency. Another salient benefit of the proposed decomposition structure is that the number of variables and constraints in each submodule are constant and independent from the number of scenarios. In other words, the complexity of submodules would not increase with a larger number of scenarios, which makes the proposed approach very promising to deal with a large-scale power system with uncertainties. In general, the computational burden of stochastic approaches depends on the number of scenarios considered by the study. The capability of handling scenarios relies on the calculation efforts of solution methods, the availability of computing resource, and the requirements of the solution quality (such as the optimality and the computing time). For a particular power system, a study can be conducted to evaluate the quality of the solution to the number of scenarios, and consequently it can help in choosing a proper number of scenarios that can be handled in the system to avoid unnecessary computation burden.

In Chapter 4, we presented a parallel approach to solve a TS-based SCUC co-optimization problem that minimizes the operating cost of a power system by scheduling generating units and switchable transmission lines with consideration of post-contingency corrective actions. By technically introducing the concept of "*Actual*" and "*Fictitious*" power flows on the switchable line, we successfully separate the transmission line switched-On/Off decision-making from the network-based OPF problem, which dramatically reduce the computational complexity of the OPF problem with TS. With the application of augmented Lagrangian method and auxiliary problem principle, the original TS-based SCUC co-optimization problem is decomposed into several scalable and tractable solution modules, including single unit UC modules, hourly OPF modules, and single line single hour TS modules. All of these divided solution modules can be solved simultaneously to improve the computational efficiency. The test cases showed the effectiveness and efficiency of the proposed approach with parallel implementation on a multi-processor computing cluster. Moreover, the proposed parallel approach will offer the power system a secure and economical efficient operation with more controllability.

5.2 Future works

Based on the proposed decomposition framework and numerical case study result, further research will be conducted as listed below:

The SCUC algorithm proposed in Chapter 3 is formulated based on the DC optimal power flow model. It can be further improved to solve the SCUC problem with AC optimal power flow model, which could provide a more accurate evaluation of the power flow network. In this case, the energy loss and the transient/voltage stability issues can be considered. The TS-based SCUC algorithm proposed in Chapter 4 is formulated to schedule the generating units and states of the switching lines. This study can be further extended to be applied on the mid-term maintenance schedule and the long-term transmission planning problem.

In addition, more function modules of the proposed decomposition framework can be integrated into the decomposition framework. With the development of modern power systems, many innovative techniques have been introduced and implemented in the existing power grids, such as demand response, energy storage system, electric vehicle[95], etc. Many solution approaches and applications have been proposed by our researchers to solve the corresponding power system operation problems. Consequently, extra variables and constraints are included in the existing SCUC solution engines. As a result, the computational burden of the SCUC problem will increase dramatically. In the future, the proposed decomposition framework can be developed to solve more complex power systems with many these advanced techniques, as shown in the figure below.

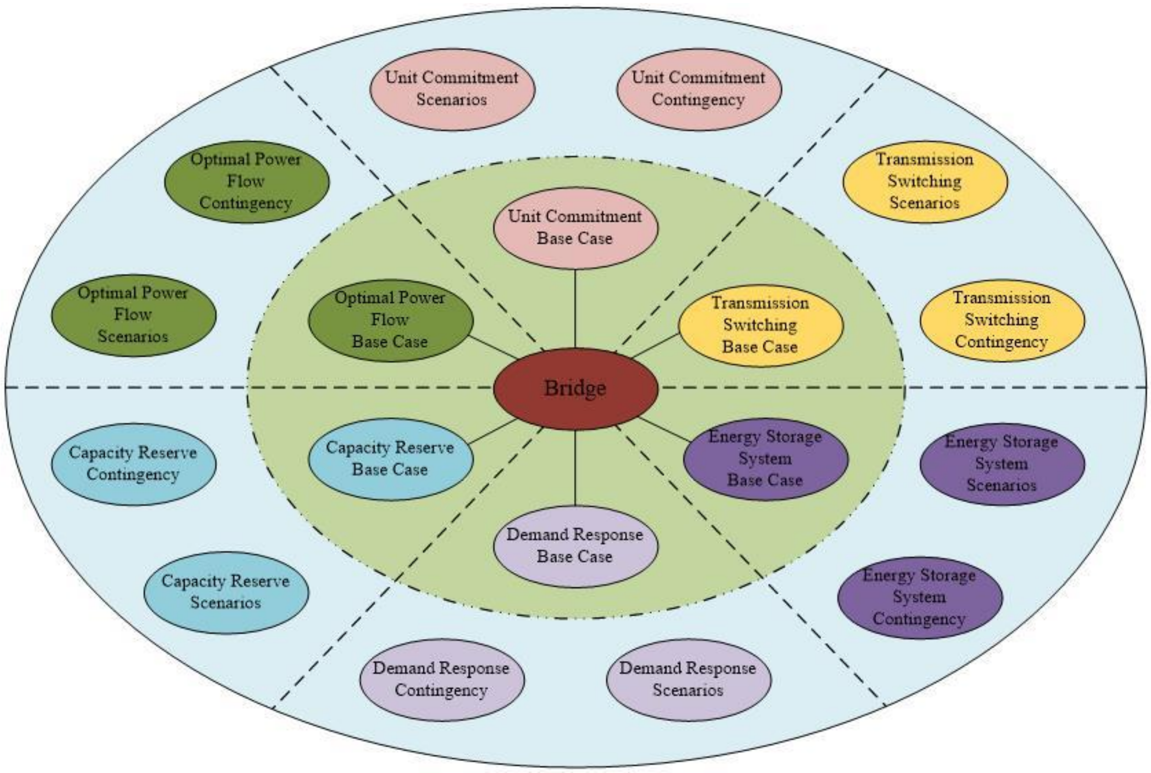

Figure 5.1 Structure with more function modules

REFERENCES

1. Grainger, J.J. and W.D. Stevenson, *Power system analysis*. Vol. 31. 1994: McGraw-Hill New York.

2. Saadat, H., *Power system analysis*. 1999: WCB/McGraw-Hill.

3. Shahidehpour, M., H. Yamin, and Z. Li, *Market operations in electric power systems : forecasting, scheduling, and risk management*. 2002, New York: Institute of Electrical and Electronics Engineers, Wiley-Interscience. xiv, 531 p.

4. Wood, A.J. and B.F. Wollenberg, *Power generation, operation, and control*. 2nd ed. 1996, New York: J. Wiley & Sons. xv, 569 p.

5. Sheble, G.B. and G.N. Fahd, *Unit commitment literature synopsis.* Power Systems, IEEE Transactions on, 1994. **9**(1): p. 128-135.

6. Momoh, J.A., *Electric power system applications of optimization*. 2008: CRC Press.

7. Sen, S. and D. Kothari, *Optimal thermal generating unit commitment: a review.* International Journal of Electrical Power & Energy Systems, 1998. **20**(7): p. 443-451.

8. Kerr, R., J. Scheidt, and J. Wiley, *Unit commitment.* Power Apparatus and Systems, IEEE Transactions on, 1966(5): p. 417-421.

9. Hara, K., M. Kimura, and N. Honda, *A method for planning economic unit commitment and maintenance of thermal power systems.* IEEE Transactions on Power Apparatus and Systems, 1966. **5**(PAS-85): p. 427-436.

10. Burns, R. and C. Gibson. *Optimization of priority lists for a unit commitment program*. in *IEEE TRANSACTIONS ON POWER APPARATUS AND SYSTEMS*. 1975. IEEE-INST ELECTRICAL ELECTRONICS ENGINEERS INC 345 E 47TH ST, NEW YORK, NY 10017-2394.

11. Lee, F.N., *Short-term thermal unit commitment-a new method.* Power Systems, IEEE Transactions on, 1988. **3**(2): p. 421-428.

12. Lee, F.N., *The application of commitment utilization factor (CUF) to thermal unit commitment.* Power Systems, IEEE Transactions on, 1991. **6**(2): p. 691-698.

13. Shoults, R.R., et al., *A practical approach to unit commitment, economic dispatch and savings allocation for multiple-area pool operation with import/export constraints.* Power Apparatus and Systems, IEEE Transactions on, 1980(2): p. 625-635.

14. Lee, F.N., J. Huang, and R. Adapa, *Multi-area unit commitment via sequential method and a DC power flow network model.* IEEE Transactions on Power Systems, 1994. **9**(1): p. 279-287.

15. Kusic, G. and H. Putnam, *Dispatch and unit commitment including commonly owned units*. 1985, University of Pittsburgh, Department of Electrical Engineering, Pittsburgh, PA.

16. Lowery, P., *Generating unit commitment by dynamic programming.* IEEE Transactions on Power Apparatus and Systems, 1966. **5**(PAS-85): p. 422-426.

17. Dillon, T.S., et al., *Integer programming approach to the problem of optimal unit commitment with probabilistic reserve determination.* IEEE Transactions on Power Apparatus and Systems, 1978. **6**(PAS-97): p. 2154-2166.

18. Lauer, G., et al., *Solution of large-scale optimal unit commitment problems.* Power Apparatus and Systems, IEEE Transactions on, 1982(1): p. 79-86.

19. Huang, K.-Y., H.-T. Yang, and C.-L. Huang. *A new thermal unit commitment approach using constraint logic programming*. in *Power Industry Computer Applications., 1997. 20th International Conference on*. 1997. IEEE.

20. Shahidehopour, M. and Y. Fu, *Benders decomposition: applying Benders decomposition to power systems.* Power and Energy Magazine, IEEE, 2005. **3**(2): p. 20-21.

21. Deeb, N. and S. Shahidehpour, *Cross decomposition for multi-area optimal reactive power planning.* Power Systems, IEEE Transactions on, 1993. **8**(4): p. 1539-1544.

22. Deeb, N. and S. Shahidehpour. *Decomposition approach for minimising real power losses in power systems*. in *IEE Proceedings C (Generation, Transmission and Distribution)*. 1991. IET.

23. Shahidehpour, S. and V. Ramesh, *Nonlinear programming algorithms and decomposition strategies for OPF.* IEEE/PES tutorial on optimal power flow, 1996.

24. Alguacil, N. and A. Conejo, *Multiperiod optimal power flow using Benders decomposition.* Power Systems, IEEE Transactions on, 2000. **15**(1): p. 196-201.

25. Ma, H., S. Shahidehpour, and M. Marwali. *Transmission constrained unit commitment based on Benders decomposition*. in *American Control Conference, 1997. Proceedings of the 1997*. 1997. IEEE.

26. Ma, H. and S. Shahidehpour, *Unit commitment with transmission security and voltage constraints.* Power Systems, IEEE Transactions on, 1999. **14**(2): p. 757-764.

27. Fu, Y., M. Shahidehpour, and Z. Li, *Security-constrained unit commitment with AC constraints.* Power Systems, IEEE Transactions on, 2005. **20**(2): p. 1001-1013.

28. Fu, Y., M. Shahidehpour, and Z. Li, *AC contingency dispatch based on security-constrained unit commitment.* Power Systems, IEEE Transactions on, 2006. **21**(2): p. 897-908.

29. Fu, Y. and M. Shahidehpour, *Fast SCUC for large-scale power systems.* Power Systems, IEEE Transactions on, 2007. **22**(4): p. 2144-2151.

30. Cohen, A.I. and S. Wan, *A method for solving the fuel constrained unit commitment problem.* Power Systems, IEEE Transactions on, 1987. **2**(3): p. 608-614.

31. Tong, S. and S. Shahidehpour. *Combination of Lagrangian-relaxation and linear-programming approaches for fuel-constrained unit-commitment problems*. in *IEE Proceedings C (Generation, Transmission and Distribution)*. 1989. IET.

32. Merlin, A. and P. Sandrin, *A new method for unit commitment at Electricité de France.* IEEE Trans. Power Appar. Syst., 1983. **102**(5).

33. Aoki, K., et al., *Unit commitment in a large-scale power system including fuel constrained thermal and pumped-storage hydro.* Power Systems, IEEE Transactions on, 1987. **2**(4): p. 1077-1084.

34. Aoki, K., et al., *Optimal long-term unit commitment in large scale systems including fuel constrained thermal and pumped-storage hydro.* Power Systems, IEEE Transactions on, 1989. **4**(3): p. 1065-1073.

35. Wang, C. and S. Shahidehpour, *Ramp-rate limits in unit commitment and economic dispatch incorporating rotor fatigue effect.* Power Systems, IEEE Transactions on, 1994. **9**(3): p. 1539-1545.

36. Tseng, C.-L., et al. *A transmission-constrained unit commitment method*. in *System Sciences, 1998., Proceedings of the Thirty-First Hawaii International Conference on*. 1998. IEEE.

37. Powell, M.J., *" A method for non-linear constraints in minimization problems"*. 1967: UKAEA.

38. Hestenes, M.R., *Multiplier and gradient methods.* Journal of optimization theory and applications, 1969. **4**(5): p. 303-320.

39. Jiang, Q., B. Zhou, and M. Zhang, *Parallel augment Lagrangian relaxation method for transient stability constrained unit commitment.* Power Systems, IEEE Transactions on, 2013. **28**(2): p. 1140-1148.

40. Fu, Y., et al., *Integration of Large-Scale Offshore Wind Energy via VSC-HVDC in Day-Ahead Scheduling.* IEEE Transactions on Sustainable Energy, 2016. **7**(2): p. 535-545.

41. Wang, C. and Y. Fu, *A Distributed Calculation of Global Shift Factor Considering Information Privacy.* IEEE Transactions on Power Systems, 2015. **PP**(99): p. 1-1.

42. Kim, B.H. and R. Baldick, *A comparison of distributed optimal power flow algorithms.* Power Systems, IEEE Transactions on, 2000. **15**(2): p. 599-604.

43. Takriti, S., J.R. Birge, and E. Long, *A stochastic model for the unit commitment problem.* Power Systems, IEEE Transactions on, 1996. **11**(3): p. 1497-1508.

44. Wu, L., M. Shahidehpour, and T. Li, *Stochastic security-constrained unit commitment.* Power Systems, IEEE Transactions on, 2007. **22**(2): p. 800-811.

45. Papavasiliou, A. and S.S. Oren. *Applying high performance computing to multi-area stochastic unit commitment for renewable penetration*. in *Proc. FERC Technical Conf.: Increasing Real-Time and Day-Ahead Market Efficiency Through Improved Software*. 2012.

46. Papavasiliou, A. and S.S. Oren, *Multiarea stochastic unit commitment for high wind penetration in a transmission constrained network.* Operations Research, 2013. **61**(3): p. 578-592.

47. Papavasiliou, A., S.S. Oren, and R.P. O'Neill, *Reserve requirements for wind power integration: A scenario-based stochastic programming framework.* Power Systems, IEEE Transactions on, 2011. **26**(4): p. 2197-2206.

48. Hedman, K.W., et al., *Optimal transmission switching with contingency analysis.* Power Systems, IEEE Transactions on, 2009. **24**(3): p. 1577-1586.

49. Hedman, K.W., et al., *Co-optimization of generation unit commitment and transmission switching with N-1 reliability.* Power Systems, IEEE Transactions on, 2010. **25**(2): p. 1052-1063.

50. Conejo, A.J., et al., *Decomposition techniques in mathematical programming: engineering and science applications*. 2006: Springer Science & Business Media.

51. Bertsekas, D.P., *Nonlinear programming*. 1995, Belmont, Mass.: Athena Scientific. x, 646 p.

52. Ekeland, I. and R. Temam, *Convex analysis and variational problems*. Classics in applied mathematics. 1999, Philadelphia: Society for Industrial and Applied Mathematics. xiv, 402 p.

53. Tosserams, S., et al. *Augmented lagrangian relaxation for analytical target cascading*. in *In 6th World Congress on Structural and Multidisciplinary Optimization, May 30–June 3*. 2005. Citeseer.

54. Geoffrion, A.M., *Lagrangean relaxation for integer programming*, in *Approaches to integer programming*. 1974, Springer. p. 82-114.

55. Boland, N.L. and A.C. Eberhard, *On the augmented Lagrangian dual for integer programming.* Mathematical Programming, 2015. **150**(2): p. 491-509.

56. Du Merle, O., et al., *Stabilized column generation.* Discrete Mathematics, 1999. **194**(1): p. 229-237.

57. He, B., H. Yang, and S. Wang, *Alternating direction method with self-adaptive penalty parameters for monotone variational inequalities.* Journal of Optimization Theory and applications, 2000. **106**(2): p. 337-356.

58. Li, Y., Z. Lu, and J.J. Michalek, *Diagonal quadratic approximation for parallelization of analytical target cascading.* Journal of Mechanical Design, 2008. **130**(5): p. 051402.

59. *High Performance Computing at the HPCC*. Available from: https://www.hpc.msstate.edu/computing/hpc.php.

60. Falcão, D.M., *High performance computing in power system applications*, in *Vector and Parallel Processing—VECPAR'96*. 1997, Springer. p. 1-23.

61. Green, R.C., L. Wang, and M. Alam. *High performance computing for electric power systems: Applications and trends*. in *Power and Energy Society General Meeting, 2011 IEEE*. 2011. IEEE.

62. Amgai, R., et al. *Research trends in high performance computing application on large scale power system operation*. in *Grand Challenges in Modeling & Simulation*. 2012.

63. Wang, C. and Y. Fu, *Fully Parallel Stochastic Security-Constrained Unit Commitment.* IEEE Transactions on Power Systems, 2015. **PP**(99): p. 1-11.

64. Carpentier, P., et al., *Stochastic optimization of unit commitment: a new decomposition framework.* Power Systems, IEEE Transactions on, 1996. **11**(2): p. 1067-1073.

65. Wang, J., M. Shahidehpour, and Z. Li, *Contingency-constrained reserve requirements in joint energy and ancillary services auction.* Power Systems, IEEE Transactions on, 2009. **24**(3): p. 1457-1468.

66. Fu, Y., Z. Li, and L. Wu, *Modeling and solution of the large-scale security-constrained unit commitment.* Power Systems, IEEE Transactions on, 2013. **28**(4): p. 3524-3533.

67. Kargarian, A. and Y. Fu, *System of systems based security-constrained unit commitment incorporating active distribution grids.* Power Systems, IEEE Transactions on, 2014. **29**(5): p. 2489-2498.

68. Kargarian, A., et al. *A system of systems engineering approach for unit commitment in multi-area power markets*. in *PES General Meeting| Conference & Exposition, 2014 IEEE*. 2014. IEEE.

69. Kargarian Marvasti, A., et al., *Optimal operation of active distribution grids: A system of systems framework.* Smart Grid, IEEE Transactions on, 2014. **5**(3): p. 1228-1237.

70. Kargarian, A., Y. Fu, and Z. Li, *Distributed Security-Constrained Unit Commitment for Large-Scale Power Systems.* IEEE Transactions on Power Systems, 2015. **30**(4): p. 1925-1936.

71. Ahmadi-Khatir, A., A.J. Conejo, and R. Cherkaoui, *Multi-area unit scheduling and reserve allocation under wind power uncertainty.* Power Systems, IEEE Transactions on, 2014. **29**(4): p. 1701-1710.

72. Wang, J., M. Shahidehpour, and Z. Li, *Security-constrained unit commitment with volatile wind power generation.* Power Systems, IEEE Transactions on, 2008. **23**(3): p. 1319-1327.

73. Censor, Y. and S.A. Zenios, *Parallel optimization: Theory, algorithms, and applications*. 1997: Oxford University Press.

74. Cohen, G., *Optimization by decomposition and coordination: a unified approach.* Automatic Control, IEEE Transactions on, 1978. **23**(2): p. 222-232.

75. Zhang, G.L., W, , *Stochastic Unit Commitment based on ARIMA Scenario Generation and Reduction.* T&D Conference and Exposition, 2016.

76. Hodge, B.-M., et al. *A comparison of wind power and load forecasting error distributions*. in *2012 World Renewable Energy Forum*. 2012.

77. Bo, R. and F. Li. *Impact of load forecast uncertainty on LMP*. in *Power Systems Conference and Exposition, 2009. PSCE'09. IEEE/PES*. 2009. IEEE.

78. Wu, H., et al., *Chance-constrained day-ahead scheduling in stochastic power system operation.* Power Systems, IEEE Transactions on, 2014. **29**(4): p. 1583-1591.

79. Khodayar, M.E., M. Shahidehpour, and L. Wu, *Enhancing the dispatchability of variable wind generation by coordination with pumped-storage hydro units in stochastic power systems.* Power Systems, IEEE Transactions on, 2013. **28**(3): p. 2808-2818.

80. *Wind farm power output data from Transparency in power market*. Available from: http://www.eex-transparency.com/.

81. Dupačová, J., N. Gröwe-Kuska, and W. Römisch, *Scenario reduction in stochastic programming.* Mathematical programming, 2003. **95**(3): p. 493-511.

82. Heitsch, H. and W. Römisch, *Scenario reduction algorithms in stochastic programming.* Computational optimization and applications, 2003. **24**(2-3): p. 187-206.

83. Rolim, J.G. and L.J.B. Machado, *A study of the use of corrective switching in transmission systems.* Power Systems, IEEE Transactions on, 1999. **14**(1): p. 336-341.

84. Bacher, R. and H. Glavitsch, *Network topology optimization with security constraints.* Power Systems, IEEE Transactions on, 1986. **1**(4): p. 103-111.

85. Mazi, A.A., B.F. Wollenberg, and M.H. Hesse, *Corrective Control of Power System Flows by Line and Bus-Bar Switching.* IEEE Transactions on Power Systems, 1986. **1**(3): p. 258-264.

86. Bakirtzis, A.G. and A.P.S. Meliopoulos, *Incorporation of Switching Operations in Power System Corrective Control Computations.* IEEE Transactions on Power Systems, 1987. **2**(3): p. 669-675.

87. Quintana, V.H., et al., *Overload and voltage control of power systems by line switching and generation rescheduling.* Canadian Journal of Electrical and Computer Engineering, 1990. **15**(4): p. 167-173.

88. O'Neill, R.P., et al., *Dispatchable transmission in RTO markets.* IEEE Transactions on Power Systems, 2005. **20**(1): p. 171-179.

89. Fisher, E.B., R.P. Neill, and M.C. Ferris, *Optimal transmission switching.* Power Systems, IEEE Transactions on, 2008. **23**(3): p. 1346-1355.

90. Khanabadi, M. and H. Ghasemi. *Transmission congestion management through optimal transmission switching*. in *2011 IEEE Power and Energy Society General Meeting*. 2011.

91. Nasrolahpour, E., H. Ghasemi, and M. Khanabadi. *Optimal transmission congestion management by means of substation reconfiguration*. in *20th Iranian Conference on Electrical Engineering (ICEE2012)*. 2012.

92. Ahmadi, H., M. Khanabadi, and H. Ghasemi. *Transmission system reconfiguration for congestion management ensuring transient and voltage stability*. in *Environment and Electrical Engineering (EEEIC), 2013 13th International Conference on*. 2013.

93. Khanabadi, M., H. Ghasemi, and M. Doostizadeh, *Optimal transmission switching considering voltage security and N-1 contingency analysis.* Power Systems, IEEE Transactions on, 2013. **28**(1): p. 542-550.

94. Khodaei, A. and M. Shahidehpour, *Transmission switching in security-constrained unit commitment.* Power Systems, IEEE Transactions on, 2010. **25**(4): p. 1937-1945.

95. Doostizadeh, M., et al. *Optimal energy management of a retailer with smart metering and Plug-in Hybrid Electric Vehicle*. in *Environment and Electrical Engineering (EEEIC), 2011 10th International Conference on*. 2011.

APPENDIX A

AUXILIARY PROBLEM PRINCIPLE APPLICATIONS

In this appendix, the selection and the derivation of the auxiliary problem principle of “Fully Parallel Stochastic Security-Constrained Unit Commitment” and “Parallel Co-Optimization of Generation Unit Commitment and Transmission Switching with Post-Contingency Corrective” will be discussed

A.1 Auxiliary problem principle applications in “fully parallel stochastic security-constrained unit commitment”

The Auxiliary Problem Principle (APP) allows us to substitute the augmentation terms in the augmented Lagrangian function (3.24) with decomposed terms. According to the APP theory, a master problem could be replaced by its alternative problem. Without loss of generalization, the augmented Lagrangian function (3.24) can be represented as:

$$Min \quad J(u)+J_1(u) \tag{A.1}$$

$$\begin{aligned} J(u) &= \frac{c_{uc}^{0}}{2}\left\|y_{uc}^{0}-y_{brdg}^{0}\right\|^2+\frac{c_{opf}^{0}}{2}\left\|y_{opf}^{0}-y_{brdg}^{0}\right\|^2 \\ &+\sum_s\left(\frac{c_{uc}^{0,s}}{2}\left\|y_{uc}^{0,s}-y_{brdg}^{0}\right\|^2+\frac{c_{uc}^{s}}{2}\left\|y_{uc}^{s}-y_{brdg}^{s}\right\|^2+\frac{c_{opf}^{s}}{2}\left\|y_{opf}^{s}-y_{brdg}^{s}\right\|^2\right) \end{aligned} \tag{A.2}$$

$$\begin{aligned} J_1(u) &= cx^0+\rho^0 dy_{uc}^0+\sum_s \rho^s d y_{uc}^s \\ &+\lambda_{uc}^0\left(y_{uc}^0-y_{brdg}^0\right)+\lambda_{opf}^0\left(y_{opf}^0-y_{brdg}^0\right) \\ &+\sum_s\left(\lambda_{uc}^{0,s}\left(y_{uc}^{0,s}-y_{brdg}^0\right)+\lambda_{uc}^s\left(y_{uc}^s-y_{brdg}^s\right)+\lambda_{opf}^s\left(y_{opf}^s-y_{brdg}^s\right)\right) \end{aligned} \tag{A.3}$$

where, $J(u)$ is a convex, and differentiable function, $J_1(u)$ is a non-convex mixed-integer function. Then, its auxiliary problem is defined as:

$$Min \quad G^v(u)=K(u)+\left[\varepsilon J'(v)-K'(v)\right]^T \times u+\varepsilon J_1(u) \tag{A.4}$$

where, $K(u)$ is a selected convex differentiable function, ε is a selected positive number, v is the optimal solution of G^v, $J'(v)$, $K'(v)$ are differential result of $J(v)$ and $K(v)$, respectively. Based on the variational inequality character [52], we can get:

$$J(v)+J_1(v)=Min \quad J(u)+J_1(u) \tag{A.5}$$

This means, if v happens to be a solution of the auxiliary problem of minimizing G^v (A.4), then it is also a solution of its master problem (A.1). Based on the theory above, the equivalent function G^v depends on choice of ε and $K(u)$. With different choices of ε and $K(u)$, and we can get a different equivalent function (A.4) to its original function (A.1). In this study, ε is set as 1, $K(u)$ is selected as below:

$$\begin{aligned} K(u) &= c_{uc}^{0}\left((y_{uc}^{0})^2-(y_{brdg}^{0})^2\right)+c_{opf}^{0}\left((y_{opf}^{0})^2-(y_{brdg}^{0})^2\right) \\ &+\sum_{c}\left[c_{uc}^{0,s}\left((y_{uc}^{0,s})^2-(y_{brdg}^{0})^2\right)+c_{uc}^{s}\left((y_{uc}^{s})^2-(y_{brdg}^{s})^2\right)+c_{opf}^{s}\left((y_{opf}^{s})^2-(y_{brdg}^{s})^2\right)\right] \end{aligned} \tag{A.6}$$

As a result, based on the equation (A.4), we can obtain its auxiliary problem (A.7).

$$
\begin{aligned}
G^{v}(u) &= c_{uc}^{0}\left((y_{uc}^{0})^{2}-(y_{brdg}^{0})^{2}\right)+c_{opf}^{0}\left((y_{opf}^{0})^{2}-(y_{brdg}^{0})^{2}\right)\\
&+\sum_{c}\left[c_{uc}^{0,s}\left((y_{uc}^{0,s})^{2}-(y_{brdg}^{0})^{2}\right)+c_{uc}^{s}\left((y_{uc}^{s})^{2}-(y_{brdg}^{s})^{2}\right)+c_{opf}^{s}\left((y_{opf}^{s})^{2}-(y_{brdg}^{s})^{2}\right)\right]\\
&+\left(\begin{bmatrix}
c_{uc}^{0}(y_{uc}^{0})^{(\mathrm{k}-1)}-c_{uc}^{0}(y_{brdg}^{0})^{(\mathrm{k}-1)}\\
c_{opf}^{0}(y_{opf}^{0})^{(\mathrm{k}-1)}-c_{opf}^{0}(y_{brdg}^{0})^{(\mathrm{k}-1)}\\
\begin{pmatrix}-c_{uc}^{0}(y_{uc}^{0})^{(\mathrm{k}-1)}+c_{uc}^{0}(y_{brdg}^{0})^{(\mathrm{k}-1)}-c_{opf}^{0}(y_{opf}^{0})^{(\mathrm{k}-1)}\\
+c_{opf}^{0}(y_{opf}^{0})^{(\mathrm{k}-1)}-\sum_{c}c_{uc}^{0,s}(y_{uc}^{0,s})^{(\mathrm{k}-1)}+\sum_{c}c_{uc}^{0,s}(y_{brdg}^{0})^{(\mathrm{k}-1)}\end{pmatrix}\\
c_{uc}^{c}(y_{uc}^{c})^{(\mathrm{k}-1)}-c_{uc}^{c}(y_{brdg}^{c})^{(\mathrm{k}-1)}\\
c_{opf}^{c}(y_{opf}^{c})^{(\mathrm{k}-1)}-c_{opf}^{c}(y_{brdg}^{c})^{(\mathrm{k}-1)}\\
c_{uc}^{0,s}(y_{uc}^{0,s})^{(\mathrm{k}-1)}-c_{uc}^{0,s}(y_{brdg}^{0})^{(\mathrm{k}-1)}\\
-c_{uc}^{c}(y_{uc}^{c})^{(\mathrm{k}-1)}+c_{uc}^{c}(y_{brdg}^{c})^{(\mathrm{k}-1)}-c_{opf}^{c}(y_{opf}^{c})^{(\mathrm{k}-1)}+c_{opf}^{c}(y_{brdg}^{c})^{(\mathrm{k}-1)}
\end{bmatrix}^{T}
-\begin{bmatrix}
2c_{uc}^{0}y_{uc}^{0}\\
2c_{opf}^{0}y_{opf}^{0}\\
\left(2c_{uc}^{0}+2c_{opf}^{0}+\sum_{c}2c_{uc}^{0,s}\right)y_{brdg}^{0}\\
2c_{uc}^{s}y_{uc}^{s}\\
2c_{opf}^{s}y_{opf}^{s}\\
2c_{uc}^{0,s}y_{uc}^{0,s}\\
\left(2c_{uc}^{s}+2c_{opf}^{s}\right)y_{brdg}^{s}
\end{bmatrix}^{T}\right)
\begin{bmatrix}
y_{uc}^{0}\\ y_{opf}^{0}\\ y_{brdg}^{0}\\ y_{uc}^{s}\\ y_{opf}^{s}\\ y_{uc}^{0,s}\\ y_{brdg}^{s}
\end{bmatrix}\\
&+F(I,P_{0}^{uc})+\lambda_{0}^{P}(P_{0}^{uc}-P_{0}^{opf})+\lambda_{0}^{PL}(PL_{0,S}^{opf}-PL_{0,S}^{ts})+\lambda_{0}^{\overline{PL}}(\overline{PL}_{0,S}^{opf}-\overline{PL}_{0,S}^{ts})\\
&+\sum_{c}\left(\lambda_{c}^{P}(P_{c}^{uc}-P_{c}^{opf})+\lambda_{c}^{PL}(PL_{c,S}^{opf}-PL_{c,S}^{ts})+\lambda_{c}^{\overline{PL}}(\overline{PL}_{c,S}^{opf}-\overline{PL}_{c,S}^{ts})\right)
\end{aligned}
\tag{A.7}
$$

A.2 Auxiliary problem principle applications in "parallel co-optimization of generation unit commitment and transmission switching with post-contingency corrective"

The Auxiliary Problem Principle (APP) allows us to substitute the augmentation terms in the augmented Lagrangian function (4.29) with decomposed terms. According to the APP theory, a master problem could be replaced by its alternative problem. Without loss of generalization, the augmented Lagrangian function (4.29) can be represented as:

$$Min \quad J(u)+J_1(u) \tag{A.8}$$

$$\begin{aligned} J(u) &= \frac{c_0^P}{2}\left\|P_0^{uc}-P_0^{opf}\right\|^2+\frac{c_0^{PL}}{2}\left\|PL_{0,S}^{opf}-PL_{0,S}^{ts}\right\|^2 \\ &+\frac{c_0^{\overline{PL}}}{2}\left\|\overline{PL}_{0,S}^{opf}-\overline{PL}_{0,S}^{ts}\right\|^2+\sum_c\left(\frac{c_c^P}{2}\left\|P_c^{uc}-P_c^{opf}\right\|^2\right) \\ &+\sum_c\left(\frac{c_c^{PL}}{2}\left\|PL_{c,S}^{opf}-PL_{c,S}^{ts}\right\|^2\right)+\sum_c\left(\frac{c_c^{\overline{PL}}}{2}\left\|\overline{PL}_{c,S}^{opf}-\overline{PL}_{c,S}^{ts}\right\|^2\right) \end{aligned} \tag{A.9}$$

$$\begin{aligned} J_1(u) &= F(I,P_0^{uc})+\lambda_0^P(P_0^{uc}-P_0^{opf})+\lambda_0^{PL}(PL_{0,S}^{opf}-PL_{0,S}^{ts}) \\ &+\lambda_0^{\overline{PL}}(\overline{PL}_{0,S}^{opf}-\overline{PL}_{0,S}^{ts})+\sum_c\left(\lambda_c^P(P_c^{uc}-P_c^{opf})\right) \\ &+\sum_c\left(\lambda_c^{PL}(PL_{c,S}^{opf}-PL_{c,S}^{ts})\right)+\sum_c\left(\lambda_c^{\overline{PL}}(\overline{PL}_{c,S}^{opf}-\overline{PL}_{c,S}^{ts})\right) \end{aligned} \tag{A.10}$$

where, $J(u)$ is a convex, and differentiable function, $J_1(u)$ is a non-convex mixed-integer function. Then, its auxiliary problem is defined as:

$$Min \quad G^v(u)=K(u)+\left[\varepsilon J'(v)-K'(v)\right]^T\times u+\varepsilon J_1(u) \tag{A.11}$$

where, $K(u)$ is a selected convex differentiable function, ε is a selected positive number, v is the optimal solution of G^v, $J'(v)$, $K'(v)$ are differential result of $J(v)$ and $K(v)$, respectively. Based on the variational inequality character [52], we can get:

$$J(v)+J_1(v)=Min \quad J(u)+J_1(u) \tag{A.12}$$

This means, if v v happens to be a solution of the auxiliary problem of minimizing G^v (A.11), then it is also a solution of its master problem (A.8). Based on the theory above, the equivalent function G^v depends on choice of ε and $K(u)$. With different choices of ε and $K(u)$, and we can get a different equivalent function (A.11) to its original function (A.8). In this study, ε is set as 1, $K(u)$ is selected as below:

$$\begin{aligned} K(u) &= c_0^P\left((P_0^{uc})^2-(P_0^{opf})^2\right)+c_0^{PL}\left((PL_{0,S}^{opf})^2-(PL_{0,S}^{ts})^2\right) \\ &+c_0^{\overline{PL}}\left((\overline{PL}_{0,S}^{opf})^2-(\overline{PL}_{0,S}^{ts})^2\right)+\sum_c c_c^P\left((P_c^{uc})^2-(P_c^{opf})^2\right) \\ &+\sum_c c_c^{PL}\left((PL_{c,S}^{opf})^2-(PL_{c,S}^{ts})^2\right)+\sum_c c_c^{\overline{PL}}\left((\overline{PL}_{c,S}^{opf})^2-(\overline{PL}_{c,S}^{ts})^2\right) \end{aligned} \tag{A.13}$$

As a result, based on the equation (A.11), we can obtain its auxiliary problem (A.14).

$$
\begin{aligned}
G^{v}(u) &= c_0^{P}\left((P_0^{uc})^2-(P_0^{opf})^2\right)+c_0^{PL}\left((PL_{0,S}^{opf})^2-(PL_{0,S}^{ts})^2\right)+c_0^{\overline{PL}}\left((\overline{PL}_{0,S}^{opf})^2-(\overline{PL}_{0,S}^{ts})^2\right)\\
&+\sum_c\left[c_c^{P}\left((P_c^{uc})^2-(P_c^{opf})^2\right)+c_c^{PL}\left((PL_{c,S}^{opf})^2-(PL_{c,S}^{ts})^2\right)+c_c^{\overline{PL}}\left((\overline{PL}_{c,S}^{opf})^2-(\overline{PL}_{c,S}^{ts})^2\right)\right]\\
&+\left(\begin{bmatrix}
-c_0^{P}(P_0^{uc})^{(k-1)}+c_0^{P}(P_0^{opf})^{(k-1)}\\
-c_0^{PL}(PL_{0,S}^{opf})^{(k-1)}+c_0^{PL}(PL_{0,S}^{ts})^{(k-1)}\\
-c_0^{\overline{PL}}(\overline{PL}_{0,S}^{opf})^{(k-1)}+c_0^{\overline{PL}}(\overline{PL}_{0,S}^{ts})^{(k-1)}\\
-c_c^{P}(P_c^{uc})^{(k-1)}+c_c^{P}(P_c^{opf})^{(k-1)}\\
-c_c^{PL}(PL_{c,S}^{opf})^{(k-1)}+c_c^{PL}(PL_{c,S}^{ts})^{(k-1)}\\
-c_c^{\overline{PL}}(\overline{PL}_{c,S}^{opf})^{(k-1)}+c_c^{\overline{PL}}(\overline{PL}_{c,S}^{ts})^{(k-1)}\\
c_0^{P}(P_0^{uc})^{(k-1)}-c_0^{P}(P_0^{opf})^{(k-1)}\\
c_0^{PL}(PL_{0,S}^{opf})^{(k-1)}-c_0^{PL}(PL_{0,S}^{ts})^{(k-1)}\\
c_0^{\overline{PL}}(\overline{PL}_{0,S}^{opf})^{(k-1)}-c_0^{\overline{PL}}(\overline{PL}_{0,S}^{ts})^{(k-1)}\\
c_c^{P}(P_c^{uc})^{(k-1)}-c_c^{P}(P_c^{opf})^{(k-1)}\\
c_c^{PL}(PL_{c,S}^{opf})^{(k-1)}-c_c^{PL}(PL_{c,S}^{ts})^{(k-1)}\\
c_c^{\overline{PL}}(\overline{PL}_{c,S}^{opf})^{(k-1)}-c_c^{\overline{PL}}(\overline{PL}_{c,S}^{ts})^{(k-1)}
\end{bmatrix}^{T}
-\begin{bmatrix}
2c_0^{P}(P_0^{opf})^{(k-1)}\\
2c_0^{PL}(PL_{0,S}^{ts})^{(k-1)}\\
2c_0^{\overline{PL}}(\overline{PL}_{0,S}^{ts})^{(k-1)}\\
2c_c^{P}(P_c^{opf})^{(k-1)}\\
2c_c^{PL}(PL_{c,S}^{ts})^{(k-1)}\\
2c_c^{\overline{PL}}(\overline{PL}_{c,S}^{ts})^{(k-1)}\\
2c_0^{P}(P_0^{uc})^{(k-1)}\\
2c_0^{PL}(PL_{0,S}^{opf})^{(k-1)}\\
2c_0^{\overline{PL}}(\overline{PL}_{0,S}^{opf})^{(k-1)}\\
2c_c^{P}(P_c^{uc})^{(k-1)}\\
2c_c^{PL}(PL_{c,S}^{opf})^{(k-1)}\\
2c_c^{\overline{PL}}(\overline{PL}_{c,S}^{opf})^{(k-1)}
\end{bmatrix}^{T}\right)
\begin{bmatrix}
P_0^{opf}\\ PL_{0,S}^{ts}\\ \overline{PL}_{0,S}^{ts}\\ P_c^{opf}\\ PL_{c,S}^{ts}\\ \overline{PL}_{c,S}^{ts}\\ P_0^{uc}\\ PL_{0,S}^{opf}\\ \overline{PL}_{0,S}^{opf}\\ P_c^{uc}\\ PL_{c,S}^{opf}\\ \overline{PL}_{c,S}^{opf}
\end{bmatrix} \qquad \text{(A.14)}\\
&+F(I,P_0^{uc})+\lambda_0^{P}(P_0^{uc}-P_0^{opf})+\lambda_0^{PL}(PL_{0,S}^{opf}-PL_{0,S}^{ts})+\lambda_0^{\overline{PL}}(\overline{PL}_{0,S}^{opf}-\overline{PL}_{0,S}^{ts})\\
&+\sum_c\left(\lambda_c^{P}(P_c^{uc}-P_c^{opf})+\lambda_c^{PL}(PL_{c,S}^{opf}-PL_{c,S}^{ts})+\lambda_c^{\overline{PL}}(\overline{PL}_{c,S}^{opf}-\overline{PL}_{c,S}^{ts})\right)
\end{aligned}
$$

APPENDIX B

SETUP OF THE MATLAB DISTRIBUTED COMPUTING SERVICE CLUSTER

The proposed framework is tested by MATLAB Distributed Computing Service (MDCS), which is employed to cooperate the parallel computing cluster with 16 computing nodes. In Appendix B, the setup procedure of the MDCS is presented, which would be helpful for the setup of the MDCS cluster.

B.1 Start mdce service

Turn on mdce service on all the nodes in the parallel computing clustering (including both the head node and the computing nodes).

a) in the “command window”, get into the path of “your MATLAB location”\toolbox\distcomp\bin.
b) input “mdce install” to install mdce service
c) input “mdce start” to start mdce service

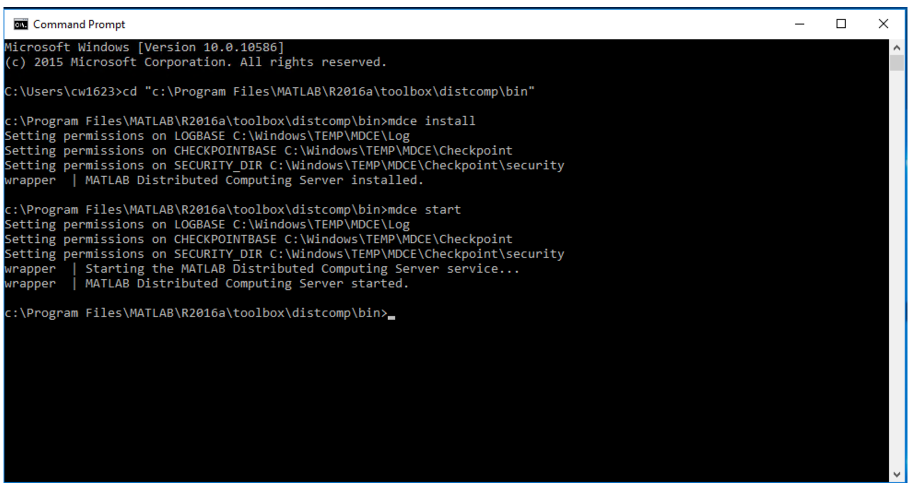

B.2 Create and configure job manager

Open the “admincenter.bat” in the “your MATLAB location”\toolbox\distcomp\bin

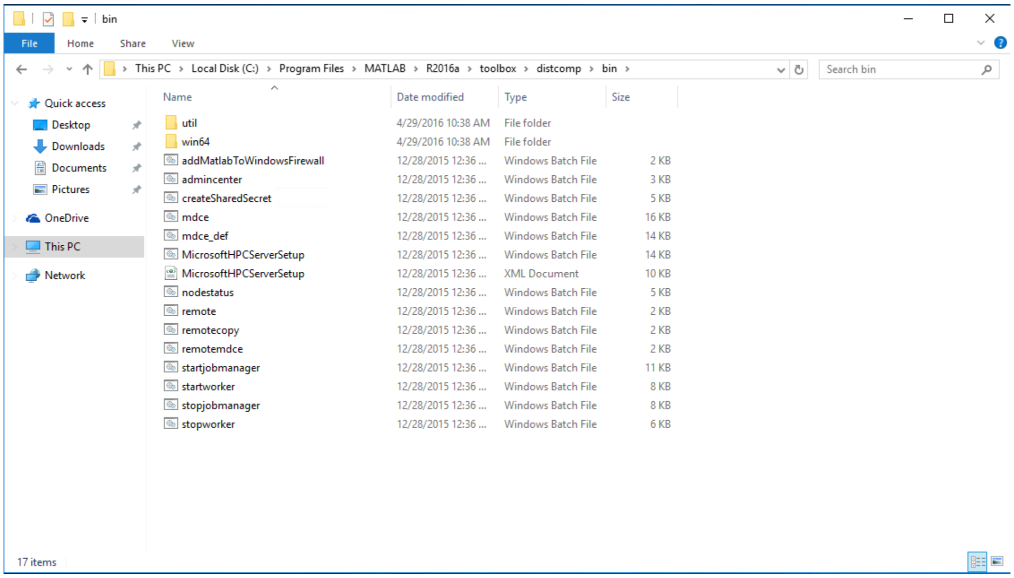

Under the "Hosts" tab, click "Add or Find" to add nodes by Hostnames or IP address

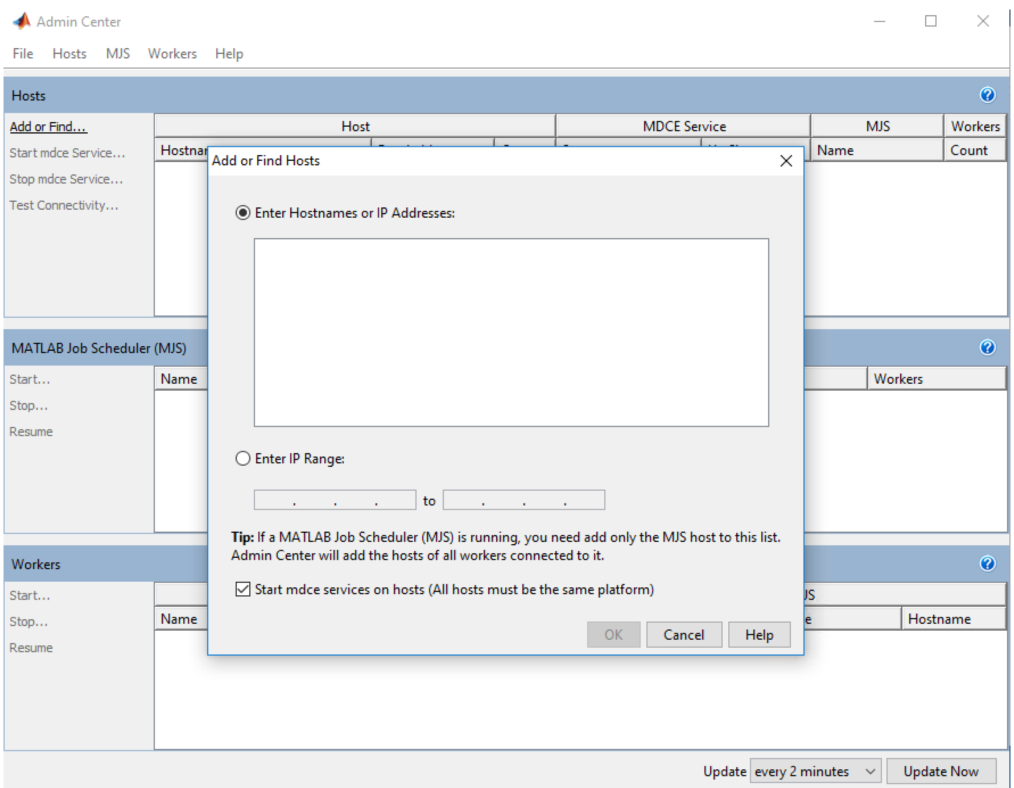

Under "Job Manager" tab, click "start" to create job manager, and select the location of this MJS

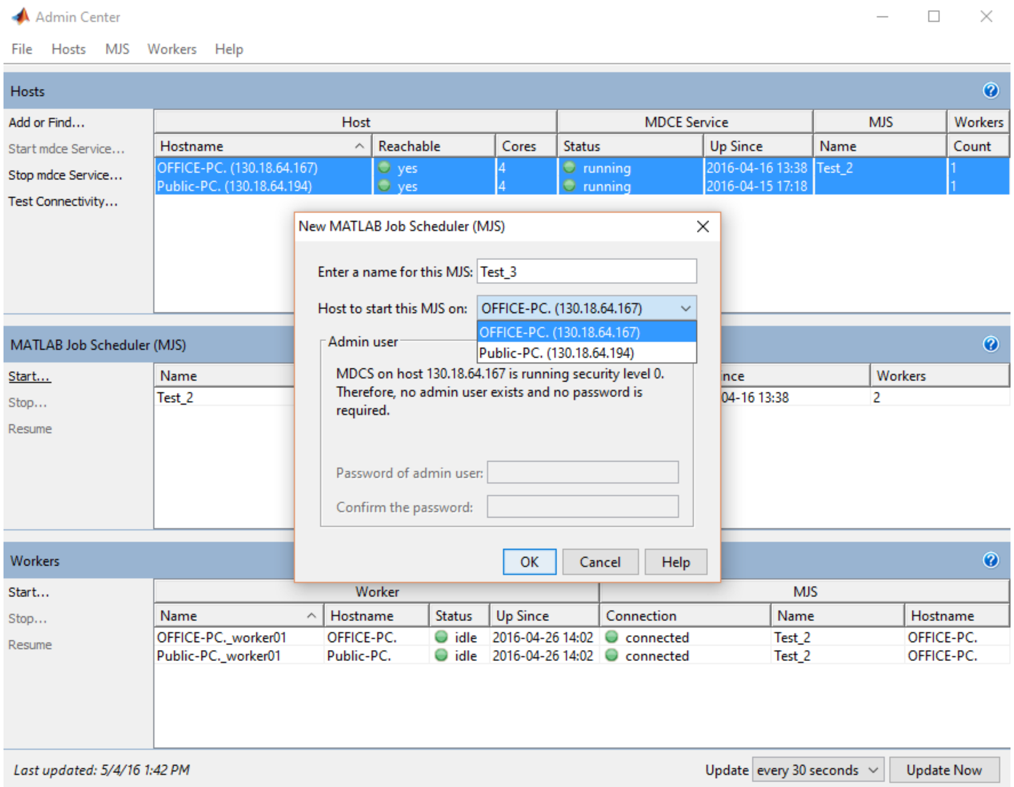

Under “Worker” tab, click “start” to create worker. In which, you can select your computing nodes and the number of workers in each computing node.

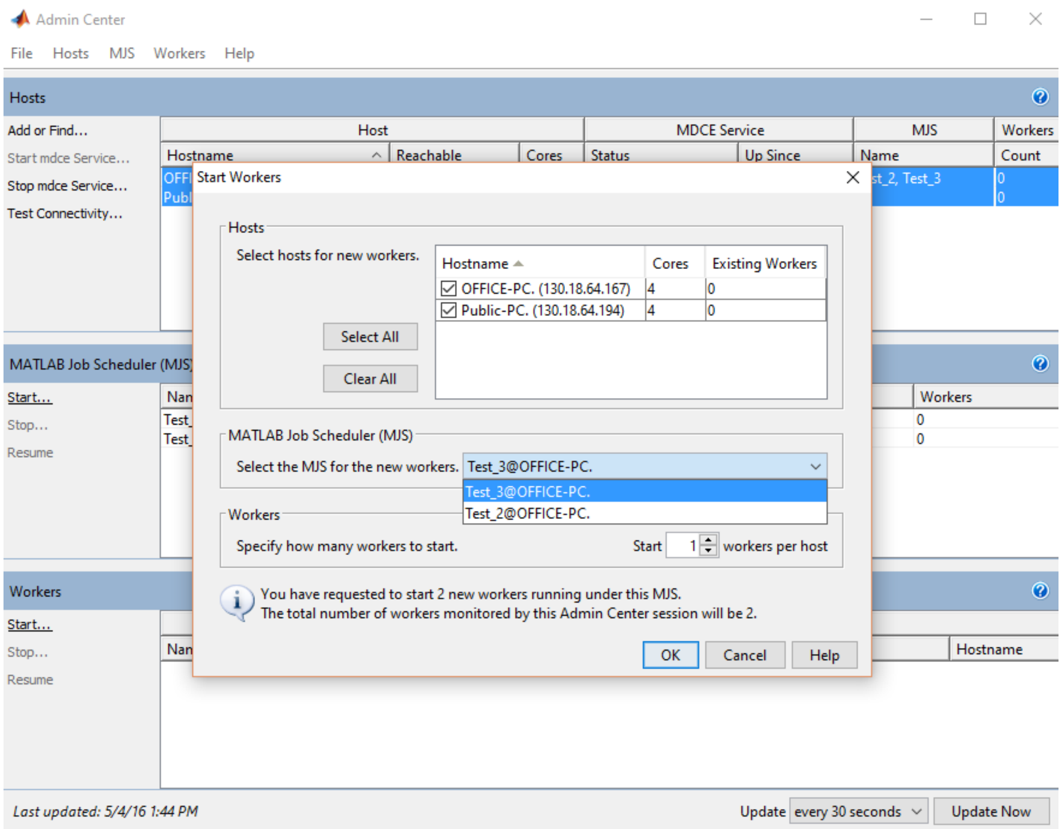

B.3 Add job manager in MATLAB

In the MATLAB interface, select job manager in the head node, by selecting "Discover Clusters…" under "Parallel" Tab, and check the check box of "On your network".

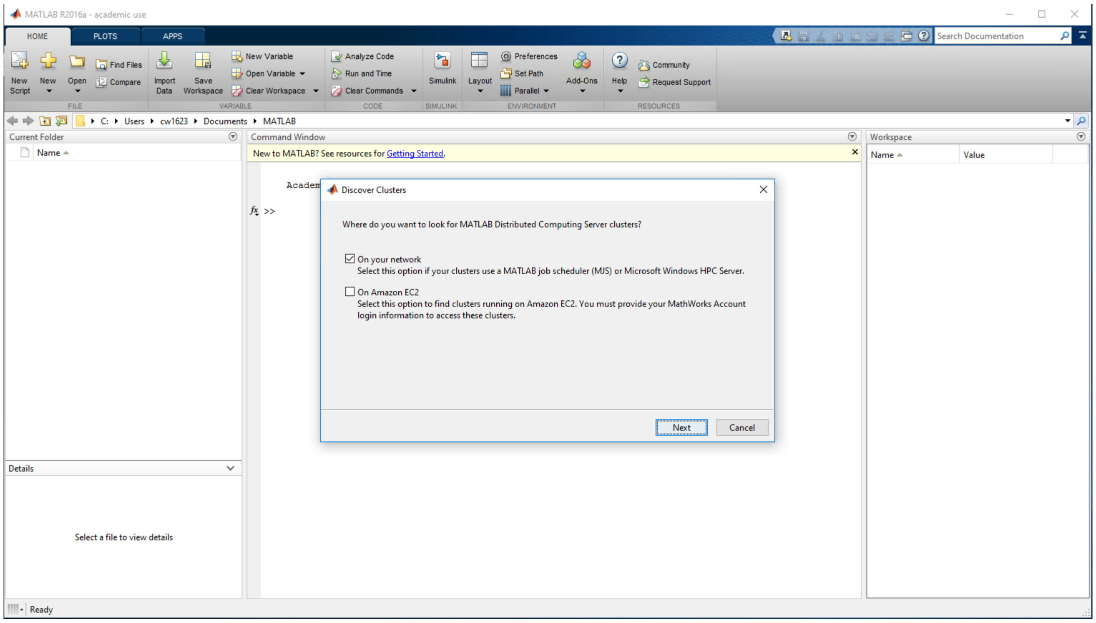

Select the desired “job manager”, and set it as your default cluster

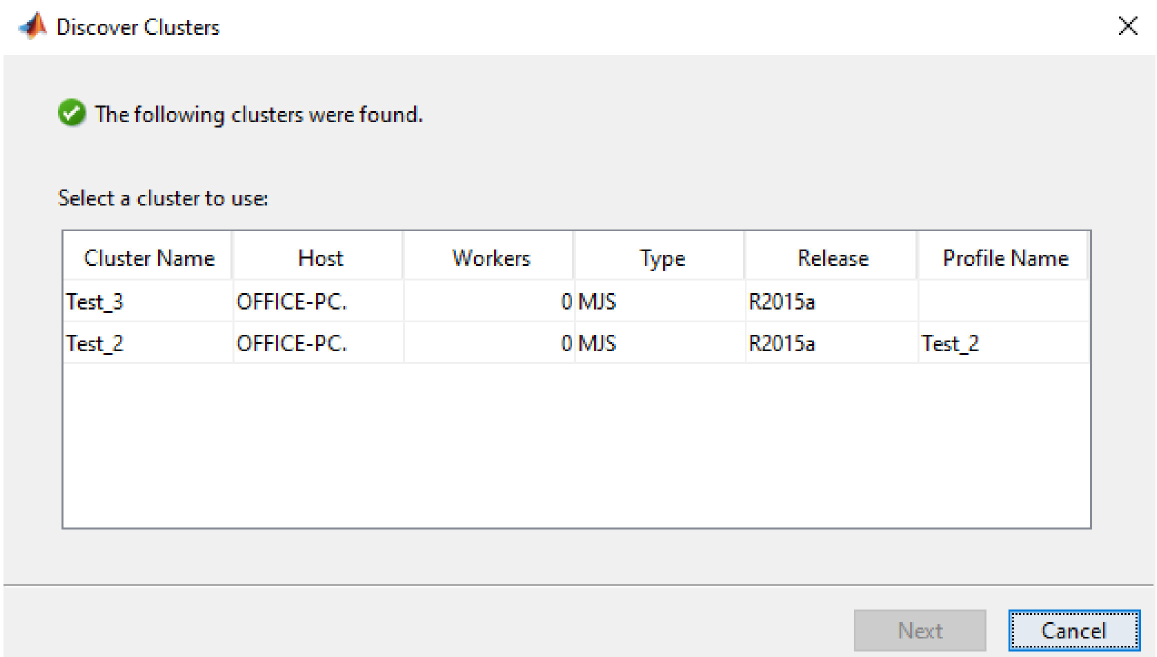

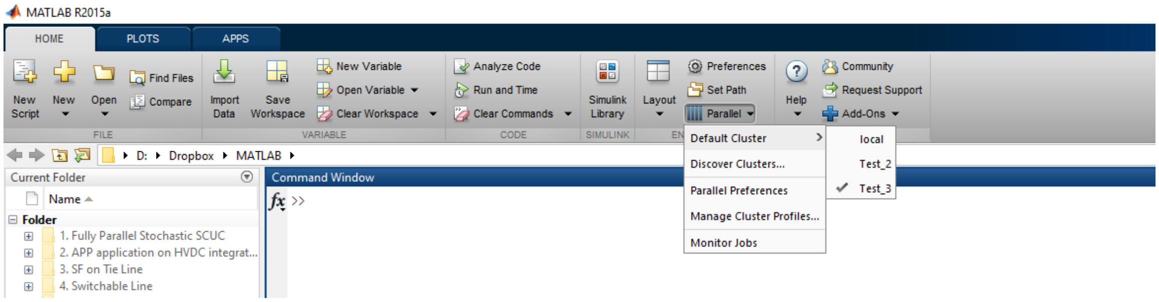

Finally, you can run your MDCS code on your head node.